UNIVERSITY OF CALIFORNIA

Santa Barbara

Modeling the Interconnected Effects of Fuel Treatments on Forests, Water, and Fire

A dissertation submitted in partial satisfaction of the

requirements for the degree Doctor of Philosophy

in Environmental Science and Management

by

William Douglas Burke

Committee in charge:

Professor Naomi Tague, Chair

Professor Max Moritz

Professor James Frew

Professor Scott Jasechko

June 2022

The dissertation of William Douglas Burke is approved.

_____

Max Moritz

_____

James Frew

_____

Scott Jasechko

_____

Naomi Tague, Committee Chair

June 2022

VITA OF WILLIAM DOUGLAS BURKE
June 2022

EDUCATION

Bachelor of Science (B.S.) in Environmental Science, Santa Clara University, Santa Clara, CA, December 2013
Master of Science (M.S.) in Geography, Indiana University, Bloomington, IN, June 2016
Doctor of Philosophy in Environmental Science and Management, University of California Santa Barbara, CA, June 2022 (expected)

PUBLICATIONS

Burke, W., Tague, C.N., Kennedy, M., Moritz, M., 2020. Understanding fuel treatments: how treatments interact with climate and biophysical setting to affect fire, water, and forest health. Frontiers in Forests and Global Change 3, 143. https://doi.org/10.3389/ffgc.2020.591162

Burke, W.D., Ficklin, D.L., 2017. Future projections of streamflow magnitude and timing differ across coastal watersheds of the western United States. International Journal of Climatology 37, 4493–4508. https://doi.org/10/gcj2qz

Stewart, I.T., Bacon, C.M., Burke, W.D., 2014. The uneven distribution of environmental burdens and benefits in Silicon Valley's backyard. Applied Geography 55, 266–277. https://doi.org/10.1016/j.apgeog.2014.09.016

RESEARCH INTERESTS

Ecohydrology, hydrologic modeling, ecoinformatics, computational methods, hydroclimate, water resources, GIS

TEACHING

University of California Santa Barbara
Spring 2019 Teaching Assistant – ESM 232: Environmental Modeling
Winter 2018 Teaching Assistant – ESM 263: Geographic Information Systems
Spring 2017 Teaching Assistant – ESM 232: Environmental Modeling
Winter 2017 Teaching Assistant – ESM 215: Landscape Ecology

Indiana University
Spring 2016 Assistant Instructor – GEOG 109: Weather and Climate
Fall 2015 Assistant Instructor – GEOG 109: Weather and Climate

Santa Clara University
Fall 2012 Teaching Assistant – ENVS 115: GIS in Environmental Science

ABSTRACT

Modeling the Interconnected Effects of Fuel Treatments on Forests, Water, and Fire

by

William Douglas Burke

Fuel treatments, the reduction of forest biomass through mechanical removal or burning, are a flexible forest management tool used to address a variety of human and environmental concerns. Treatments can be used to reduce high severity fire, improve forest productivity and drought resilience, and increase streamflow. However, the effects of fuel treatments can be inconsistent and uncertain and are sensitive to both the treatment and the biophysical environment in which the treatment is done, and these uncertainties may be exacerbated by climate change. Climate change is already increasing wildfire size and frequency, drought, and strain on water supply in much of the Western US. Given that fuel treatments are likely to play a key role in current and future forest management, it is critical that we understand the full range of fuel treatment interactions with climate and effects on forests, water, and fire. Existing ecohydrologic models are limited in their ability to model fuel treatment effects because they do not account for both the within forest stand ecohydrologic effects of changes in forest structure and the watershed scale variation in radiation, water availability, and other factors. The ability to simulate heterogenous vegetation at fine scales is key to implementing fuel treatments like forest thinning. To address this lack I adapted the Regional Hydro-

Ecological Simulation System (RHESSYs) to include a new multiscale routing (MSR) approach, RHESSys-MSR. In addition to allowing modeling of within forest stand heterogeneity, MSR enables an additional layer of hydrologic routing, on top of existing topographic hillslope routing. The first chapter of this thesis describes the implementation of RHESSys-MSR and the second two apply this model to investigate fuel treatment effects in a changing climate. In the first application of these methods, I simulate a large set (13,500) of model scenarios varying treatment type, biophysical and climatic conditions for a Central California Sierra forest stand. Results show that plant accessible water storage capacity and vegetation type are dominant environmental controls on the effects of fuel treatments. More broadly I find that estimating the effect of fuel treatments based on only a single biophysical variable fails to capture the extent of possible treatment effects. In the second application, I investigate the interactions between projected climate change and fuel treatment area on the effects of treatments on forest health, fire risk, and streamflow at the watershed scale. Results show that projected climate change, has a nontrivial influence on net treatment effects, even compared to a maximized area treated. Fuel treatments and their effects are complex, spanning the environmental domains of forests, water, fire, and climate. Treatments are further complicated by the wide variety in the treatment itself, varying in how forest structure is affected, where it's implemented, and how often. Model applications like RHESSys-MSR are critical to reducing this uncertainty and developing place-based estimates of fuel treatment effects that can support forest managers. The persistent challenges in understanding fuel treatments and their effects make any progress all the more essential, and as this research and more contributes to this understanding, we can make better and more informed forest management decisions into the future.

TABLE OF CONTENTS

Introduction....1
Chapter 1: Multiscale Routing: Integrating Tree-scale Water Exchanges into the Regional HydroEcologic Simulation System (RHESSys)....3
1. Introduction....3
2. Methods....8
3. Results....16
4. Discussion....20
5. Conclusions....26
6. Figures....27
7. Equations....34
Chapter 2: Understanding How Fuel Treatments Interact with Climate and Biophysical Setting to Affect Fire, Water, and Forest Health: a Process-Based Modeling Approach36
1. Introduction....36
2. Methods....42
3. Results....53
4. Discussion....58
5. Conclusions....67
6. Figures....68
7. Tables....75
Chapter 3: How Climate Change and Treatment Size Impact Fuel Treatment Effects76
1. Introduction....76
2. Methods....80
3. Results....86
4. Discussion....91
5. Conclusions....96
6. Figures....98
Conclusions....106
References....108

Introduction

Fuel treatments are an important forest management tool used to modify forest biomass for a range of purposes. Though fuel treatments can refer to a host of actions, most noteworthy are forest thinning and prescribed fire. Fuel treatments are varied in their implementation. Different types of thinning can be used to reduce fuels and modify forest structure in different ways. Fuel treatments of commonly used with the goal to reduce high severity fire risk, increase forest health and productivity, or increase streamflow (Agee and Skinner, 2005; Stephens et al., 2012). The magnitude, spatial, and temporal extent of fuel treatment effects varies widely and reflects variation in how fuel treatments are implemented and the environments where they are performed. The uncertainty surrounding fuel treatment effects is exacerbated by climate change which both increases the challenge in predicting treatment effects and worsens many of the very problems fuel treatments are used to address. As a result, there exists substantial uncertainty in predicting the full effects of a fuel treatment. This research aims to improve our understanding of fuel treatment effects on forests, water, and fire. Modeling methods, specifically process-based ecohydrologic modeling, is the means by which the following chapters investigate fuel treatment effects. Chapter 1, "Multiscale Routing: Integrating Tree-scale Water Exchanges into the Regional HydroEcologic Simulation System (RHESSys)" develops novel model methods needed to adequately simulate the implementation of fuel treatments and their effects on forests, water, and fire. Chapter 2, "Understanding how fuel treatments interact with climate and biophysical setting to affect fire, water, and forest health: a process-based modeling approach" leverages these novel modeling methods to investigate a wide range of fuel treatment scenarios. This research takes a broad approach to understanding how differences

in treatment and environment combine to alter treatment effects. Finally, Chapter 3, “How Climate Change and Treatment Size Impact Fuel Treatment Effects” further studies the effects of fuel treatments, with particular interest towards the role of treatment area and projected climate change. Together these chapters drive better understanding of how fuel treatments effect our environment. Each chapter attempts to answer in some form the following question: if fuel treatments are going to be a part of how we manage forests and fire in the future, what are the complete extent of fuel treatment interactions and effects on climate, forests, water, and fire?

Chapter 1: Multiscale Routing: Integrating Tree-scale Water Exchanges into the Regional HydroEcologic Simulation System (RHESSys)

1. Introduction

As the questions we ask of models become more complex and integrate across multiple spatial scales, simulating neighborhood-scale, non-topographic routing processes, which are not traditionally accounted for in watershed-scale ecohydrologic models, becomes more important (Blöschl and Sivapalan, 1995; Fan et al., 2019; Tague and Moritz, 2019). Models that simulate hillslope hydrology typically move water among model units based on the topographic gradients. However, a variety of natural or artificial processes can lead to water being 'routed' or distributed non-topographically, such as in urban areas where many small features route water among each other. In this study we highlight the role of non-topographic routing associated with lateral root access of shared soil water stores. Tree roots have the potential to reach laterally, far enough that they access the same water stores as neighboring vegetation (Schenk and Jackson, 2002). Answers to societally relevant questions related to land and climate change may depend on whether these exchanges occur. For example, how forest management impacts forest water stress and water yield may depend on the extent of lateral water exchange between cleared areas and remaining vegetation (Tague and Moritz, 2019; Tsamir et al., 2019). The role of lateral roots in affecting access to water stores is difficult to capture in current models due to both the fine scale (<30m) of root exchanges, and the fact that the movement of water is not based on the same topographic routing logic that would normally be used when moving water among model units. In this paper we present a new modeling approach that combines non-topographic routing with existing

topographic hillslope routing within a single model. This dual routing system combines traditional ecohydrologic hillslope dynamics with additional exchanges of water at scales smaller than are typically modeled with explicit spatial units in distributed watershed-scale hydrologic models.

The motivating case for non-topographic routing used in this paper is assessing the hydrologic impacts of forest thinning. Forest thinning (short of a complete clear cut) often results in spatially heterogeneous reductions in biomass, with some trees and shrubs cut down, and others untouched. This selection of trees can be based on size, age, or species to meet specific forest structure goals and the often limited resources available to accomplish forest thinning (Agee and Skinner, 2005). For example, thinning to reduce high severity fire risk can result in stands with increased gap spaces and reductions in certain types of vegetation like shrubs or small trees, while leaving other vegetation untouched (Stephens et al., 2012). The change in forest structure following thinning becomes problematic for estimating ecohydrologic variables (evaporation, transpiration, net primary productivity) using big leaf watershed ecohydrologic models where those fine-scale changes in vegetation structure are represented as averaged reductions in biomass across a single model unit. This failure to capture the fine-scale subgrid variability that emerges due to disturbance is an established challenge in hydrologic modeling (Blöschl and Sivapalan, 1995). The added hurdle we highlight here is the need to account for water being routed among these subgrid units.

Lateral root access plays an important role in the dynamics of plant water relations and is of relevance here when considering tree access to shared water stores (Saksa et al., 2017; Tague and Moritz, 2019). Substantial variation in both vertical and lateral root length can be

explained by plant size (Schenk & Jackson, 2002). A common assumption is that lateral root spread is commensurate with canopy extent. Though this serves as a useful first-order approximation, actual lateral root spread depends on species along with the availability of water, nutrients, and incoming radiation (Klein et al., 2016). Lateral root spreads (one-sided) of trees average 11 meters with the 25^{th} to 75^{th} percentile range spanning 4 to 15 meters (Schenk and Jackson, 2002). These spreads create a tree 'neighborhood', within which there is the potential for competition for shared stores of water. Given that forest thinning is often a process spread across and within forests, and lateral exchanges based on root spread are most likely to occur across distances less than 30 meters, a non-spatial approach becomes needed to capture such distinctions at neighborhood scales (Schenk and Jackson, 2002).Lateral root spread is challenging to measure, moreover, root length and access is varied across and within species and impacted by a range of environmental conditions (Fan et al., 2017). The uncertainty and variability in lateral root spread makes it a process well suited to exploration through modeling. Forest thinning, at neighborhood-scales among trees that compete for shared water stores, presents a prime case for the importance of lateral root access, and the need to include this non-topographic routing in models. To explore the implications of lateral root-based transfers on aggregate watershed fluxes, it becomes important to represent distinct unthinned and thinned areas within our models.

The broader challenge of characterizing and routing between heterogeneous units in earth systems and hydrologic modeling is not new (Blöschl and Sivapalan, 1995). Sub-grid heterogeneity can present a problem across earth systems as well as land surface modeling, and there are a range of approaches to modeling it, notably aggregation, analytical, and mosaic approaches (Giorgi and Avissar, 1997). More recently work by Clark et al. (2015)

has reviewed and reframed some of these same issues, highlighting methods from simply increasing the resolution of the model (using a smaller cell size), to the use of effective parameters which aim to reflect the upscaled effect of the sub-grid heterogeneity. “Mosaic” approaches, in which grid cells are built up of multiple homogenous sub-units or tiles, are frequently used as middle grounds between the accuracy of process characterization and the computational feasibility of running those simulations (Giorgi and Avissar, 1997). There is often a tension between the discretization of the landscape for the purposes of topographic routing and segmentation based on other factors like vegetation or the lack or presence of thinning (Clark et al., 2015). This is complicated further when the exchanges or ‘routing’ of interest is not driven by easily observable gradients (such as topographic or moisture gradients). In the case of processes like forest thinning, we are interested in the water exchanges that follow disturbance both within and among thinned and unthinned units. Within-unit routing occurs between remaining trees and gaps. At hillslope scales, however, topographic routing remains important – for example, downslope riparian areas may benefit from water released from upslope thinned units. The effects of these two types of routing can be in competition or compounding – topographic hillslope routing may reduce the effects of any non-topographic sub-grid routing by virtue of moving large amounts of water such that no vegetation is water limited. The inclusion of both routing approaches and their interactions is needed for a more complete understanding at hillslope to watershed scales.

With the goal of incorporating non-topographic exchanges of water while still accounting for the topographic hillslope routing, here we propose a method termed multiscale routing (MSR). Two forms of routing occur in MSR – first hillslope routing moves water topographically among explicit spatial model units, followed by neighborhood routing which

moves water among co-located non-spatially explicit model subunits. The MSR method is designed to be both lightweight and flexible. It does not require further spatial data at greater resolutions beyond what is already being used for topographic routing between spatial units. By representing sub-grid scale heterogeneity as non-spatial areas, MSR also limits the added computational load. Using RHESSys and MSR we present a modeling test case to compare the standard and MSR versions of the model. We use a hillslope located within Providence creek in the southern Sierra Nevada to compare routing methods as well as the effects of varying parameterizations of the MSR method. We examine how the inclusion of MSR impacts model estimates of a range of ecophysiological variables including forest health, plant accessible soil water storage capacity (PAWSC), and streamflow across different temporal scales.

We ask the following questions:

Research Questions

1. How does sub-grid vegetation characterization and the inclusion of non-topographic routing affect undisturbed (pre-treatment) forest health, productivity, and water use as compared to a traditional lumped approach?
2. How does the routing method and parameterization directly affect the water transferred, stored, and subsequently the availability of that water for evapotranspiration and productivity?
3. In comparing pre-treatment and post-treatment thinning impacts, what the effect of the routing method and parameterization on forest health, productivity, and water

use? In what contexts are these effects noteworthy and in which are they mild or difficult to distinguish?

2. Methods

2.1. *Development and testing of the multiscale routing method*

The new MSR method incorporates neighborhood scale heterogeneity and non-topographic routing into RHESSys. RHESSys is a process-based ecohydrologic model, which in addition to traditional hydrologic modeling, dynamically models plant growth, carbon, and nitrogen cycling, and has successfully been applied to simulate the effects of thinning and similar applications (Grant et al., 2013; Hanan et al., 2018; Saksa et al., 2017; Tague, 2009; Tsamir et al., 2019). RHESSys can run at variable resolutions, dependent on input data, and can be run across and aggregated up to watershed scopes where management decisions are made. RHESSys is a distributed model, and as such, routes subsurface water explicitly based on topographic gradients using a precomputed routing table, based on methods originally from the Distributed Hydrology Soil Vegetation Model (DHSVM; Tague and Band, 2004; Wigmosta et al., 1994). This explicit topographic routing has been used in many RHESSys applications across a range of conditions, including Son et al. (2016a) which includes the P301 site used in this research.

2.2. *Multiscale Routing General Architecture*

Standard RHESSys uses patches as the smallest spatial unit. RHESSys with multiscale routing, RHESSys-MSR, leverages the existing spatial units in RHESSys by placing multiple patches in the same location. These co-located patches are then treated as aspatial units,

occupying the same spatial extent. Together these co-located patches are termed a “patch family” and the constituent units are still referred to as “patches” (or more specifically as “aspatial patches”). Each patch is assigned an area, based on its percent cover of the total patch family area. The subdivision of the patch family area is tied to one of the key assumptions of the RHESSys-MSR architecture – that patch areas are well mixed within each patch family. Thus, while patches still have physically accurate total areas, those areas not spatially explicit within the patch family, Instead, we assume the area of each patch is distributed and mixed with other patches throughout the spatial extent of the patch family.

Using the MSR method, we consider two categories of routing: “Local routing” is the fine-scale routing that occurs within the patch family and between the co-located aspatial patches. “Hillslope routing”, or topographic routing, is the standard routing in RHESSys which functions as expected based on topography and gradients in water height. Where previously topographic hillslope routing moved water between single patches, now it moves water between patch families. Hillslope routing is adapted to MSR based on the relative coverages of patches within the patch family e.g., a patch covering 50% of the family would receive 50% of the incoming water from upslope patch families.

This general architecture is useful for a few reasons, patch families are a lightweight addition to RHESSys and are not true spatial units but rather a structure used to group the existing unit, patches. Because of this, the numerous existing ecological and hydrologic process sub-models are not changed. The second major advantage of the MSR architecture is its flexibility – the division of patch families into “aspatial” patches and the parameterization of transfers between them can be adapted to represent a wide range of scenarios. For example, water and nutrient transfers between hummocks and small-scale depressions in

many low relief settings or between vegetated patches and impervious areas within urban settings. Alternatively, transfers between patches within patch families may be “turned off” to allow simulation of spatially separate land cover heterogeneity (i.e., A patch family that is 40% forest, 40% grass and 20% bare soil) as a means of increasing computational efficiency. Though this work will use multiscale routing to simulate the root access dynamics of neighboring vegetation, future work may use it as a means of accounting for roofs and sidewalks when routing urban water at small scales, or upscaling high-resolution remote sensing. While novel applications will require careful consideration about parameterization and logic of routing within a patch family, they will benefit from the foundation laid as a part of the MSR method in RHESSys.

Multiscale routing features some key differences in the watershed setup, which are accounted for by use of the R-based RHESSysPreprocessing package. The setup also requires a new input file called a “rules file”, which contains the rules for the setup and composition of the patches within each patch family. This rules file describes the different types of patch families present in the watershed. Characterizing a patch family at minimum includes specifying the number of patches and the percent coverage for each patch. Each patch can be further differentiated by any number of variables normally defined by a RHESSys template file, including number of canopy strata, vegetation types, soils type, landscape characteristics, and changes to any patch or strata-level parameters. There can be as many rules, and thus patch family compositions as needed.

2.2.1. Multiscale Routing – Root Access-Based Routing

Local routing, the transfer of water among co-located patches, for this research aims to simulate the root access of neighboring trees to shared storage. Here we build on the concept

of the tree neighborhood and use ‘neighborhood’ as a defining scale at which we consider lateral root access to shared stores of water. We present a simulation of the role of lateral root access that aims to be both simple and straightforward, the central logic of which is described by Equation 1.

Water movement between patches is governed by the water content of each patch relative to a mean patch family water content. All routing of water between patches is modulated by one of the two sharing coefficients, either sh_g (gaining) or sh_l (losing) and is normalized by area. Sharing coefficients are static through a simulation and can be set to reflect species differences in root spread and distribution or gap size distributions (determined by the preexisting forest structure, thinning method, and thinning intensity). Though in many cases a patch will gain and lose water equally, there are two sharing coefficients for cases where the water routing is unidirectional. Water in the rooting zone and unsaturated zone is transferred among patches within each patch family. When gaining water, only water up to field capacity is available to the root zone, with excess going to the unsaturated zone. Water is lost from the root zone down to the wilting point, with any additional remainder coming from the unsaturated zone. Water in the saturated zone can be included though is not in this work. If included, saturated water is routed separately and is redistributed based on the difference from the mean, and modified by conductivity, to prevent overly large amounts of water moving between patches. Nitrate and dissolved organic carbon (DOC) are transferred along with water following existing approaches in RHESSys for linking water and nutrient transport.

2.2.2. Multiscale Routing – Shading

Shading between patches within a patch family is another addition introduced as a part of multiscale routing (Eq 2). Shading already exists within RHESSys in two primary places: (1) attenuation of the radiation as it filters through canopy layers (understory canopies are shaded by overstory canopies), and (2) as an effect of the horizon angle due to topographic shading on the duration and amount of incoming radiation. MSR adds an additional shading routing to account for shading by different patches within a patch family. This shading aims to model how large height differences among neighboring trees reduce the radiation for shorter trees. Shading is implemented by an adjustment to the existing east/west horizon for each patch, that is used to determine total daily incoming shortwave radiation. This change is based on the relative height of each patch compared to the remaining patch family. Shading is adjusted if the shading angle is greater than the existing horizon angle. Shading for a patch is based on the angle between ¾ overstory vegetation height and ¾ mean overstory vegetation height of the patch family without the patch of interest. The ¾ height is used to estimate the location of the bulk of the canopy where shading will be present. The distance used to estimate the shading angle is an average for the patch family (since each patch is not explicitly located), defined by the square root of the patch area divided by the square root of the tree density plus one. This method assumes an even distribution of trees across a patch and that we know the tree density in the patch. See the graphics below for greater detail.

2.3. *Setup and Initialization of P301 Test Case*

P301 is a small part subbasin of the Providence Creek Headwater Catchments, part of the Kings River Experimental Watersheds (KREW) and Southern Sierra Critical Zone Observatory (Hunsaker et al., 2012; O'Geen et al., 2018). The basin covers ~ 0.9 km^2, and

importantly includes the Grant Grove meteorological station (Grant Grove, National Climate Data Center Station, Lat: 36.73603ºN, Lon: 118.96122ºW, elevation 2,005m. Mean annual temperature is 8ºC and mean annual precipitation is 1037 mm (highly variable from 635 mm to 2172 mm) (Bart et al., 2021). The watershed elevation spans from 1781m to 2104m and gets seasonal snowpack. The vegetation is largely mixed conifer (76-99%), with some chaparral and bare ground. Conifers include white fir, ponderosa pine, Jeffery pine, California black oak, sugar pine, and incense cedar (O'Geen et al., 2018; Safeeq and Hunsaker, 2016). Soils include Gerle-Cagwin and Shaver at depths of 76 to 203 cm (Bales et al., 2011) The P301 watershed has been used and run previously with RHESSys, which is both useful and necessary to benchmark the performance of the MSR method (Bart et al., 2021; Son et al., 2016a).

For our test case we set up a hillslope of the P301 basin for use with both standard RHESSys and RHESSys-MSR. While the model implementations are similar, they also reflect the inherent differences between a 'lumped' approach (standard RHESSys) and the RHESSys-MSR approach which distinguishes within-stand differences in vegetation. For RHESSys-MSR we use a single patch family rule for the entire hillslope, with four patches, the conceptual diagram of which is shown by Figure 1. The MSR patch family is composed of four total patches, two patches with a conifer overstory and a shrub understory (combined 64% coverage), an uncovered shrub only patch (26% cover), and a bare earth patch (10% cover). The conifer coverage (64%) is based on canopy cover data from the California Forest Observatory ("California Forest Observatory," 2019). The lumped standard RHESSys implementation uses the same percent cover data to set the patch level "canopy cover" parameter. Though this canopy cover parameterization is useful, in standard RHESSys this is

the extent to which that vegetation can be varied at the patch scale. By contrast the MSR patch family composition leverages the ability of RHESSys-MSR to characterize more than one type of vegetation cover in the same area. In this case in addition to the conifer overstory and shrub understory patches (of which there are two to implement thinning more accurately) there is a patch of uncovered shrub, which would otherwise not be possible to account for in standard RHESSys. This addition of vegetation types is one of the fundamental differences between the lumped standard RHESSys approach and the RHESSys-MSR approach, specifically in regards to how vegetation is represented within the model.

RHESSys uses parameters to affect soil and vegetation behavior. Vegetation parameters control plant species characteristics, while soil parameters control the hydrologic properties of the soils. Parameters can be found via the RHESSys parameter database (https://github.com/RHESSys/ParamDB), directly from existing literature, or from previous RHESSys implementations. For the P301 watershed soil parameters have been calibrated previously by Son et al. (2016a) and so only required minor additional sensitivity analysis due to the addition of the MSR method. Vegetation parameters have also been previously established but changes due to the addition of multiscale routing warranted further sensitivity analysis. Sensitivity analysis of vegetation parameters was done specifically to achieve stable overstory and understory canopies that reflect reasonable total carbon estimates. A single set of vegetation parameters was found and used across all standard RHESSys and RHESSys-MSR scenarios to ensure the model runs were similar. In addition to finding vegetation parameters, setting up RHESSys also involves “spinning up” the initial soil carbon and nitrogen stores. RHESSys was run initially for 200 years, until soil carbon and nitrogen reached steady states, and then after clearing, run for an additional 60 years for vegetation to

grow to appropriate ages/sizes. While all soil and vegetation parameters were used consistently across standard and MSR runs, all runs were spun up separately, allowing for divergence due to baseline differences in the watershed setups before the simulation period.

2.4. *Simulation & Analysis of P301 Test Case*

We compare standard RHESSys and RHESSys-MSR estimates of ecohydrologic variables under undisturbed and thinned scenarios. RHESSys was run for a single hillslope of P301 for using both the RHESSys and RHESSys-MSR versions. All runs were done using 30-meter patch families, 17 in the case of standard RHESSys, 68 (4 patches for each patch family) in the case of RHESSys-MSR. To test the sensitivity of MSR runs to sharing coefficients an initial sensitivity analysis was done by varying coefficients from 0-1 by 0.1. The parameter space was found to be skewed with much greater sensitivity towards 0, and with the range from 0.3 to 1 being highly unsensitive. The final range of runs chosen based on this initial analysis include: 0, 0.1, 0.2, 0.3, 1, and the standard RHESSys comparison (shortened to MSR0, MSR01, MSR02, MSR03, MSR1, and STD). For simplicity and clarity both sharing coefficients (sh_g, sh_l) were varied simultaneously, and the sharing coefficient was changed for all patches in the simulation. Though this research doesn't aim to specify what values of the sharing coefficients are "realistic", we do want to highlight the sensitivity of ecohydrologic outputs to changes in sharing coefficients, and hopefully give a starting place for any further analysis.

Using available climate data from the Grant Grove station, a simulation period from 1975 to 2015 was run. Thinning was initiated in all simulations 5 years into the simulation (1980), allowing for comparison of pre and post thinning, as well as observing the full length of potential regrowth period. For both models (MSR and standard) the implementation of

thinning was structured to simulate a 40% reduction in overstory biomass. In standard RHESSys, a 40% reduction in carbon was done by a reduction in all aboveground carbon stores (leaves, stems), leaving effectively smaller trees. This is the same approach that would be used in big leaf models where types of carbon (e.g., leaves) are lumped below the grid scale. With RHESSys-MSR, the first of the two conifer and shrub patches (covering 38% of patch family area) was thinned completely. When considering only the patches with vegetation (see Figure 1) this constitutes 40% of the total coverage of the patch family. In both cases only the conifer overstory was thinned.

Stand carbon, leaf area index, evapotranspiration, and gross primary productivity are the output variables selected to cover a broad range of ecohydrologic processes and reflect both the structure and behavior of vegetation. Stand carbon here refers to the combined carbon (in kg per m^2) from roots, stems, and leaves. Output was done at a daily time step, but both daily and seasonal timescales were assessed. Analyses also include the multiscale transfers, the quantity of water transferred daily due to multiscale routing. Additional hydrologic-focused metrics include root and unsaturated zone storage, streamflow, snowpack, and total water in. Together these variables are used to paint a more complete picture of the hydrologic effects of multiscale transfers and the repercussions of those effects.

3. Results

Initialization and spinup of RHESSys with the MSR method led to substantial differences in starting carbon, LAI, evapotranspiration, and NPP, as compared to the standard version of RHESSys (Figure 3). There are noteworthy differences between standard and MSR methods across all four variables. Stand carbon (A) is noteworthy, both due to the median value from the standard RHESSys scenario falling in the middle of the MSR runs, and because it's the

only case where the MSR0 scenario diverges noticeably from the other MSR scenarios. Stand carbon is also the only variable where the 25th to 75th percentiles are narrow enough to distinguish not only median values but also the ranges between the different MSR and standard simulations. For the remaining three variables – LAI, ET, and NPP – standard RHESSys leads to higher values, and the MSR runs are clustered closely with a slight gradient across the sharing coefficient values. This gradient is most visible in the case of LAI (B) where MSR1 has the lowest median LAI and as the sharing coefficient decreases, LAI increases.

Central to this research is an understanding of the water transfers involved in multiscale routing. Figure 4 gives an in-depth view of these multiscale transfers, showing the total transfers for all patch families within the hillslope, for varied sharing coefficients, over a period of two years. The transfers metric shown here is a sum of the absolute values of all transfers, both gains and losses. The magnitude of the transfers is particularly noteworthy here, resulting in daily transfers regularly over 0.5 mm and peaking over 2 mm. These values, while slightly lower, are on the same order of magnitude as daily evapotranspiration (Figure 6c). The narrow time window here is to better see both the transfers occurring at a daily time-step, and the variation between sharing coefficients. The need for such a narrow time window is driven largely by the very high day-to-day variability multiscale transfers in the MSR1 scenario which regularly exceeds the range of all other sharing coefficients combined. Despite the difference in daily variability, MSR1 follows the same seasonal trends shown by both MSR03 and MSR02. MSR01 on the other hand routinely diverges from the larger trends of the other sharing coefficients. For both years shown, the MSR01 run is delayed by nearly a month in reaching the late summer/early fall peak compared to all other

runs. A small response is shown immediately following the implementation of thinning (marked by the vertical line). At the scale and scope shown, a two-year time window showing daily data for patch families across a single hillslope, the effect of varied sharing coefficients is notably larger than the effect of the thinning.

The role of the sharing coefficients is clearly demonstrated when considering average daily transfers across the entire simulation period, shown in Figure 5. With sharing coefficients of 1, the trend in average daily transfers shows two clear peaks, the first falling in late spring around April, and coinciding with falling snowpack. The second peak occurs at the end of the water year in late summer around August. Though the second peak doesn't align with a direct hydrologic driver, it does occur only slightly delayed from peak transpiration, the same point where water stress would be increasing as well. While all of the runs show some degree of peak in August, the April peak is reduced or even nonexistent with reductions in the sharing coefficients. An inflection point occurs between sharing coefficient values near or just above the 0.1 value, marking noteworthy behavioral differences. While there are variations between the larger coefficient values the result is largely a difference of degrees, with shifts in the magnitude of the April peak, and the timing of the August peak, the MSR01 run demonstrates substantially different behavior. In the MSR01 scenario the April peak is nonexistent, with the entire years trend building only to a single peak in September, and with a notably reduced magnitude. Conversely, the tail from the peak in the fall is longer with the lower sharing coefficient those transfers longer into the winter. The last major distinction between sharing coefficients shown by the average daily transfers is the increased variability shown in the snowmelt driven period but only in the MSR1 scenario, while any reduction in coefficient seems to mute that effect.

Figure 6 includes a broader view of ecohydrologic processes to better contextualize the relative behavior of the standard RHESSys and RHESSys-MSR scenarios, and the sensitivity of ecohydrologic estimates to variation in sharing coefficients. Storage, combined root zone and unsaturated zone, is one of the more notable areas of divergence between MSR and standard RHESSys runs. The standard scenario features a peak not found in the MSR runs, and conversely the standard runs have otherwise markedly lower storage, particularly in the post-thinning period. By comparison, though there is variation across MSR scenarios, with greater coefficient values having larger storage, the differences are generally small relative to difference between MSR and standard scenarios. Both ET and GPP feature minimal variation both between standard and MSR scenarios, and among MSR scenarios. In both cases the seasonal variation dwarfs any differences among scenarios, with the only noteworthy divergence among scenarios occurring at the summer peaks. In the case of ET, the standard and MSR0 scenarios peak higher than the other scenarios. Though the same behavior is present in GPP, at least in the first summer peak shown, the difference is marginal.

The effects of thinning are assessed in the broader context comparison between standard RHESSys and MSR as well as sensitivity to variation in sharing coefficients (Figure 7). It's important to note that pre- and post-thinning periods are taken from continuous model runs, and so reflect different climatic periods. This makes direct comparison of pre- to post-thinning effects challenging, but the more important analysis remains the comparison between standard RHESSys and RHESSys-MSR. This difference in climate is shown with total water in (F). Only the MSR1 and MSR01 scenarios are included, to represent the extent of ecohydrologic responses to variations in MSR coefficients. Total transfers (A), as previously shown in Figure 4, indicate a clear divergence between MSR1 and MSR01, and

while thinning does shift the MSR1 peaks earlier somewhat, the variation between coefficients remains the dominant feature. GPP (B) is exceptional only in how similar the outputs across all scenarios are, with the only visible trend being a slight reduction in peak GPP in the post treatment period, though even that is a marginal difference. More substantial and dynamic differences are present in ET (C). There we see the standard scenario has a notably higher summer peak but also is the only scenario where there is a clear difference in the pre- and post-thinning trends, with the post-thinning ET peaking slightly higher and a month later. Streamflow (D) shows greater pre and post thinning differences, though given the changing water inputs (F), a substantial portion of these thinning impacts may be attributed to the influence of different climatic periods. Standard and MSR scenarios diverge in how streamflow shifts due to thinning, with the standard runs featuring a higher summer peak, but with no meaningful timing shift. The MSR scenarios by contrast show a decrease in peak summer streamflow following thinning but a shift ~1 month later. Snowpack (E) is unchanged in magnitude in the standard RHESSys scenario, and only shifts earlier due to thinning. By contrast, the MSR runs shift slightly earlier, but increase noticeably in magnitude. In all cases, the post-thinning period has snowpack both onset and decline earlier by a month or more.

4. Discussion

Understanding the ecohydrologic implications of fuel treatments is key for any future of forest management. This is especially true in the context of climate change which not only challenges our ability to anticipate vegetation behavior but brings to the fore sometimes competing demands on our forests. Management desires include increasing resilience of forests to fire and drought to limit the effects of climate change and wildfire, increasing

streamflow to aid water supply, and increasing carbon sequestration to mitigate the causes of climate change (Hanan et al., 2020; Stephens et al., 2013). To better account for not only the uncertainty of a changing climate, but also the varied effects that fuels treatments have on fire, water, and forests, we need modeling tools that adequately characterize those complex variables. These new tools need to not only be able to account for fuel treatment-driven within-stand changes to forest structure and the ecohydrologic effects that follow, but also be aggregated up to watershed scales where forest management decisions are made (Clark et al., 2015; Fan et al., 2019). Multiscale routing serves to meet this need and works with the existing RHESSys model to simulate the neighborhood-scale non-topographic routing that occurs due to lateral root access, while still accounting for topographic hillslope routing and the range of hydrologic and ecophysiological processes RHESSys normally models.

Multiscale routing is of potential use in a variety of scenarios, both including and beyond the use-case highlighted in this paper. RHESSys applications aiming to simulate within-stand scale (<30m), non-uniform disturbance are particularly suited to the use of MSR. In these cases, MSR is key to appropriately characterizing the disturbance, and accounting for the subsequent effects of that disturbance. Our initial application in this work focuses on thinning and the role of lateral root access to shared storage following that thinning. In addition to the inclusion of the within-stand routing between heterogeneous vegetation cover, the added ability to characterize disturbance at scales that would normally involve lumping and aggregation is valuable. In cases where improved characterization of vegetation types and structure is of importance, such as modeling with a focus on canopy structure and changes to those canopies, MSR adds valuable utility and precision. Simulation of fire effects is a salient

example of such a use, and MSR has been integrated into the RHESSys fire spread and effects models for exactly this purpose (Bart et al., 2020a; Kennedy et al., 2017).

The need for more accurate characterization of heterogeneous vegetation at within-stand or neighborhood-scales, and the non-topographic routing that can occur among that vegetation, is not needed in all modeling contexts. RHESSys is particularly suited to the addition of the MSR architecture, while models that simulate a single stands or individuals will typically already explicitly capture the heterogeneity in vegetation cover and variable water access we highlight here. Conversely, models that simulate across large regions (e.g., 100's to 1000's of square kilometers) will usually use spatial units that already encompass so much variability in vegetation that the additional distinction between thinned and unthinned vegetation and their subsequent exchanges of water is unlikely to be a meaningful source of uncertainty in context. The resulting models where MSR is both useful and applicable can be classified as 'intermediate complexity stand models' which simulate distributed ecohydrology across a watershed (10's to 100's of square kilometers). For the models where MSR is most appropriate, broadly classified as 'intermediate complexity watershed models', the addition of non-topographic routing to the existing distributed topographic hillslope routing can be critical – as is the case when considering neighborhood routing between thinned and unthinned spatial units demonstrated in this paper. For models of this scope and scale workloads are frequently in tension with computing capacity, and as such, added functionality such as addressing non-topographic routing necessitates an approach like MSR that minimizes the added computational burden.

Our example application of MSR shows that the addition of MSR to RHESSys can have impacts on specific model outputs (e.g., carbon stores, water, and carbon fluxes) in different

ways that vary over time. The full extent of changes when comparing standard RHESSys to RHESSys-MSR are numerous and varied, but there are also key areas in which RHESSys-MSR demonstrates improvements over standard RHESSys. The impact of MSR can be seen in post-spinup differences in initial stores and fluxes (Figure 3), which are driven by the differences in how the distribution of vegetation within a stand is characterized. By moving from one patch to a patch family containing many patches (Figure 1), variables like total carbon reach different equilibriums with spinup. These changes in initial state go on to influence subsequent analyses of thinning effects. The RHESSys-MSR runs characterize the landscape in a way standard RHESSys is fundamentally unable to replicate due to the limitations of a lumped view of vegetation cover. The RHESSys-MSR characterization is more realistic not only in the ability to represent the more varied types of vegetation cover we know often exist on the ground, but also because it facilitates more realistic modifications to forest structure from actions like thinning.

Specific model applications, such as assessing the impacts of a fuel treatment, further highlight the utility of RHESSys-MSR as compared to standard RHESSys. Overall, while MSR is unlikely to dramatically change ecohydrologic function in all or even most scenarios, it will likely impact hydrologic and plant water use variables in a variety of circumstances that are relevant to assessing the impact of disturbance. Following treatment, while standard RHESSys shows substantial increases to peak summer ET, MSR scenarios instead lead to decreases in ET for the same period (Figure 7C). This effect on ecohydrologic dynamics is nontrivial – the RHESSys-MSR simulation matches the expected (short term, 5-year) effects of forest thinning in the Sierra Nevada (Roche et al., 2018). Streamflow (Figure 7D) and snowpack (Figure 7E) both feature shifts from pre- to post-thinning dependent on standard or

multiscale RHESSys, with minimal differentiation among the sharing coefficients. Using standard RHESSys leads to an increase in peak streamflow from treatment while the MSR scenarios result in minimal change, indicating a greater degree of adaptability in water use as the excess water following the treatment must then be used elsewhere before becoming streamflow. Snowpack has the opposite trend, with an increase in peak post-thinning snowpack in the MSR scenarios, which aligns with the expected effects of a treatment on peak snow accumulation (Krogh et al., 2020). This is likely a product of the MSR characterization, which results in greater uncovered area in the post-thinning period.

The sharing coefficients are a central feature of MSR. They serve to demonstrate the sensitivity of ecohydrologic processes to assumptions about rooting distributions and behavior. Following a thinning, or another type of disturbance, the remaining vegetation, in particular trees, may have roots with enough lateral reach to access soil water storages previously used by the now thinned vegetation. The exact extent of that root access is very difficult to predict, both due to the nature of roots being underground, but also due to the variation in how different plants grow roots and allocate resources to root growth. MSR allows users to explore the effects of this highly uncertain plant behavior – root access to storages of neighboring vegetation by using the sharing coefficients to parameterize that behavior. Figure 4, showing total multiscale transfers at a daily time-step over two years, gives the most direct insight into the role of the sharing coefficients. Distinct trends in daily transfers arising from sensitivity to sharing coefficients can be seen, particularly in the leading slopes of the two late summer seasonal peaks. This variation in transfer behavior due to sharing coefficients indicates that each scenario reaches a slightly different saturation point, where water is being transferred as fast as possible. MSR scenarios with sharing

coefficients of 1, 0.3, and 0.2 all follow similar trends, and though small differences in transfers exist among them, runs reach similar peaks, and have very similar timing. At a sharing coefficient of 0.1 however, the leading slopes are shifted, pointing towards slower transfers of water. Although the sharing coefficients directly influence transfers, the other key control here is spatial variation in water demand due to patch heterogeneity within a patch family. Climatic conditions may also influence how spatially variable water demand will be within a patch family, with the potential for disturbance like drought induced mortality to affect some but not all patches within a patch family.

In some cases, MSR with different sharing coefficients produces substantial differences in the timing and magnitude of water fluxes as in seen in Figure 5, showing the day of year averages over the simulation period. MSR with a coefficient of 0.1 displays only a single annual peak in transfers unlike the two peaks present in runs with all other coefficients. These differences in the timing of water transfer do not substantially alter timing of ET or GPP, which behave similarly across MSR coefficients (Figure 7). This indicates that the differences in water transfers among MSR runs with varied sharing coefficients is either showing up in other ecohydrologic variables we aren't tracking or being attenuated. This has the potential to lead to similar circumstances to the dynamics with ET across thinning scenarios (Figure 7C), where the differences from modeling method only emerge in the context of forest thinning. Total transfers when split into pre- and post-treatment periods (A) shows further evidence of the diverging behavior between the sharing coefficients of 1 and 0.1. In this instance the MSR01 scenario shows little variation across pre- and post-thinning periods, compared to the greater variability in the MSR1 scenario, indicating the lower sharing coefficient serves to attenuate the impacts of the thinning on transfers.

5. Conclusions

Multiscale routing is both a versatile architectural addition to RHESSys, and moreover, enables modeling of fine-scale processes and interactions such as forest thinning and the subsequent impacts on lateral root access to storage. This advancement to RHESSys enables new research avenues, incorporating scales and processes previously not feasible or practical. Beyond the application investigated here, MSR has great potential for use in urban applications, routing water between discrete areas such as roofs, gutters, and sidewalks, and in upscaling high-resolution input data while retaining the input precision. Though MSR can benefit from greater input data and observed parameters, it is designed with scarcity of both input data and parameters in mind and is well suited to exploring uncertain subgrid processes. We demonstrate this here in our simulations of potential root access. This work is then well situated to be built upon and coordinate with field work aiming to improve understanding and narrow parameterization of root access into the storage of neighboring vegetation (Klos et al., 2018). We hope MSR can serve as a foundation for a wide range of future research, leveraging not only the root access-focused application included here, but both the architecture implemented within RHESSys, and the broader approach towards accounting for fine-scale processes which is potentially relevant in a range of similar models.

6. Figures

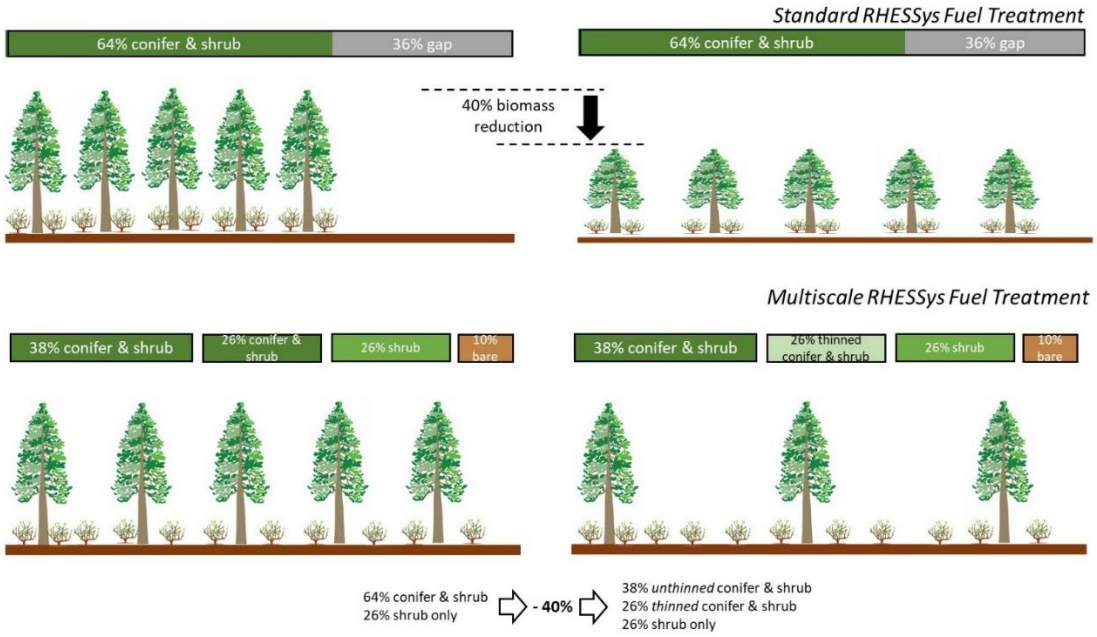

Figure 1. Conceptual figure of patches and vegetation in both standard and multiscale RHESSys and showing the effects of a forest thinning. Bars above each scenario indicate percent coverages, and continuous bars indicate a single patch (standard RHESSys has only a single patch, while MSR has 4 in the scenario shown).

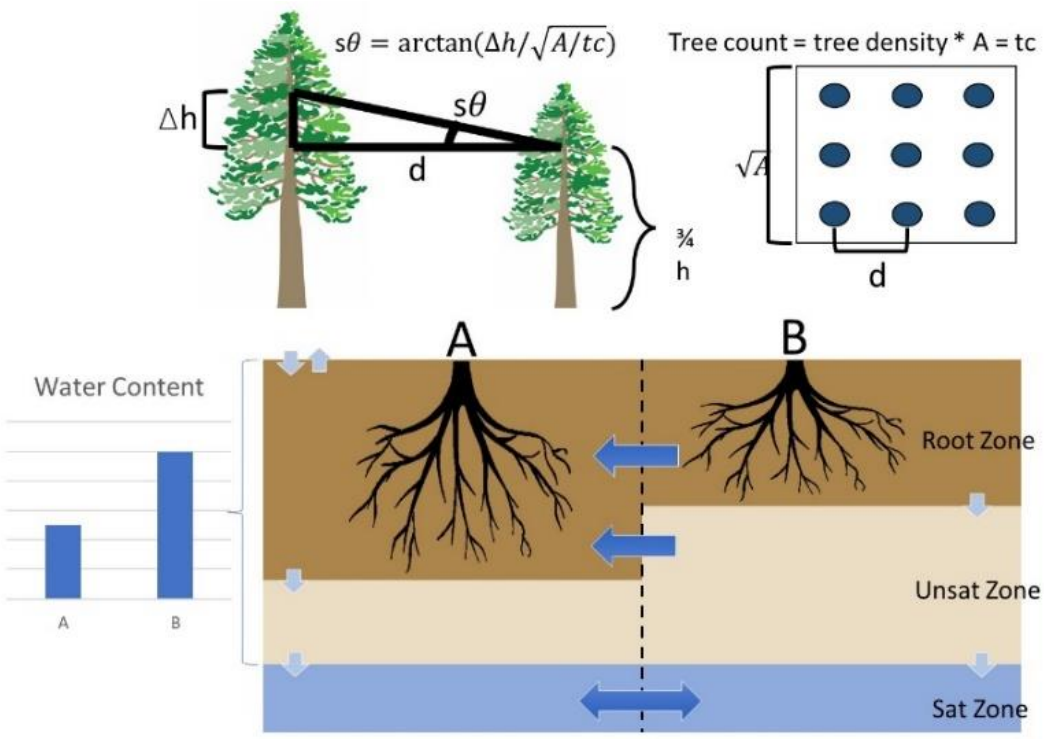

Figure 2. Conceptual diagram of the multiscale routing method, specifically the underlying logic behind the routing of subsurface water and shading of vegetation within the patch family.

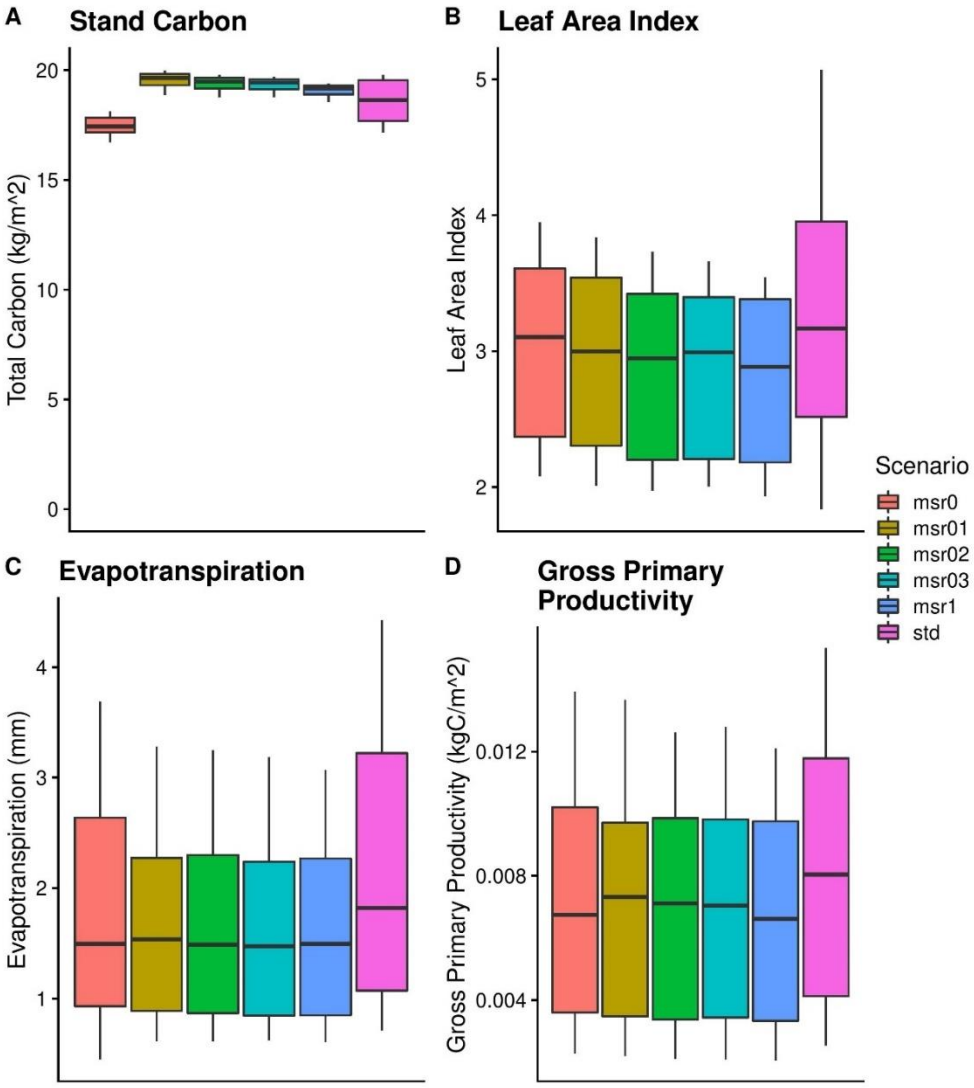

Figure 3. Distributions of initial variable states, before thinning is implemented. Stand carbon (A), leaf area index(B), evapotranspiration(C), and gross primary productivity (D) are shown, each with scenarios for standard RHESSys and MSR RHESSys using sharing coefficients 0, 0.1, 0.2, 0.3, and 1.

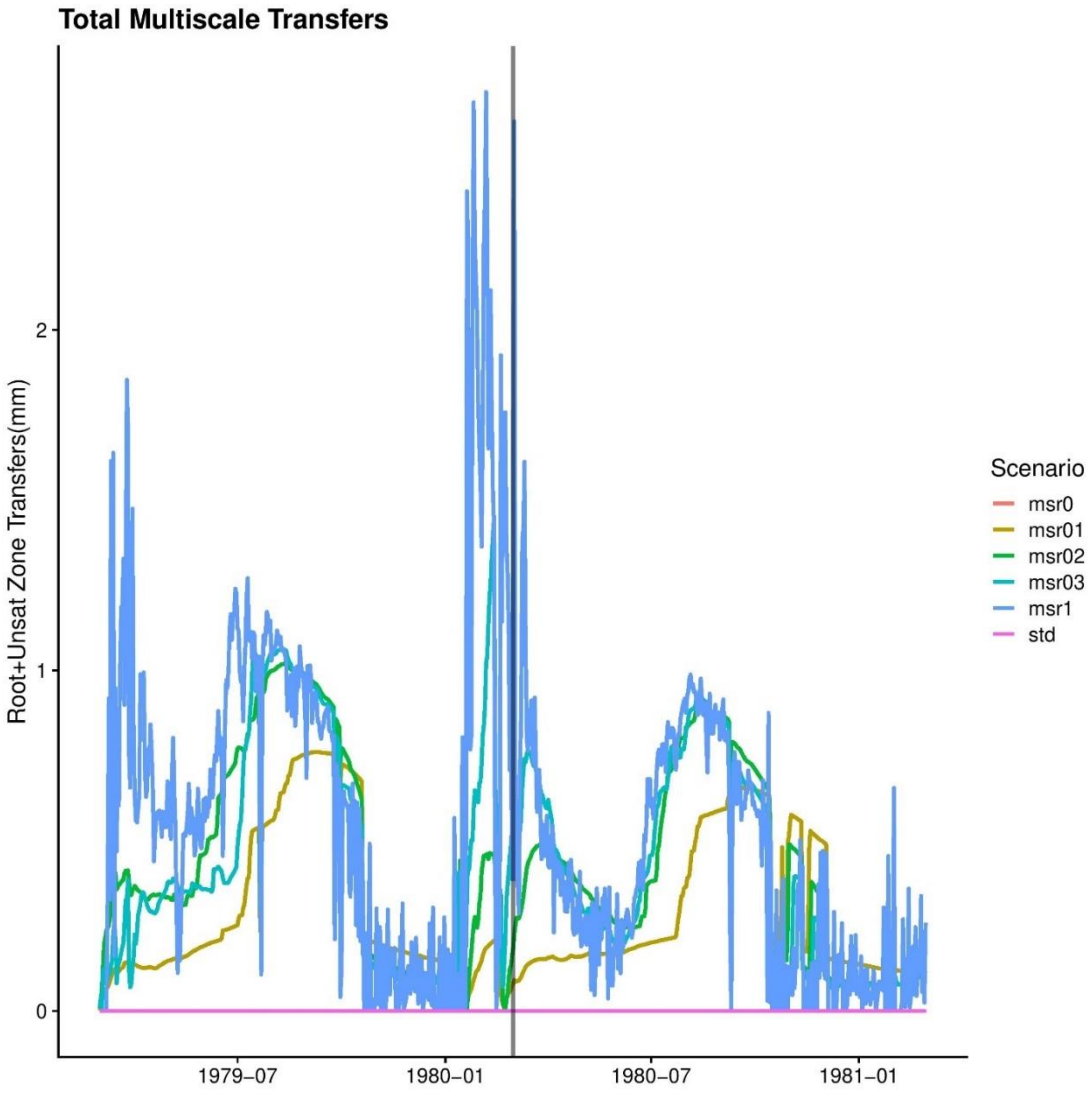

Figure 4. Combined root and unsaturated zone transfers owing to multiscale routing, e.g., among patches within a patch family. Transfer value is in mm, and is the absolute value of all transfers, both loses and gains. Focused on a two-year period to make day-scale effects visible. Shows scenarios for standard RHESSys and MSR RHESSys using sharing coefficients 0, 0.1, 0.2, 0.3, and 1.

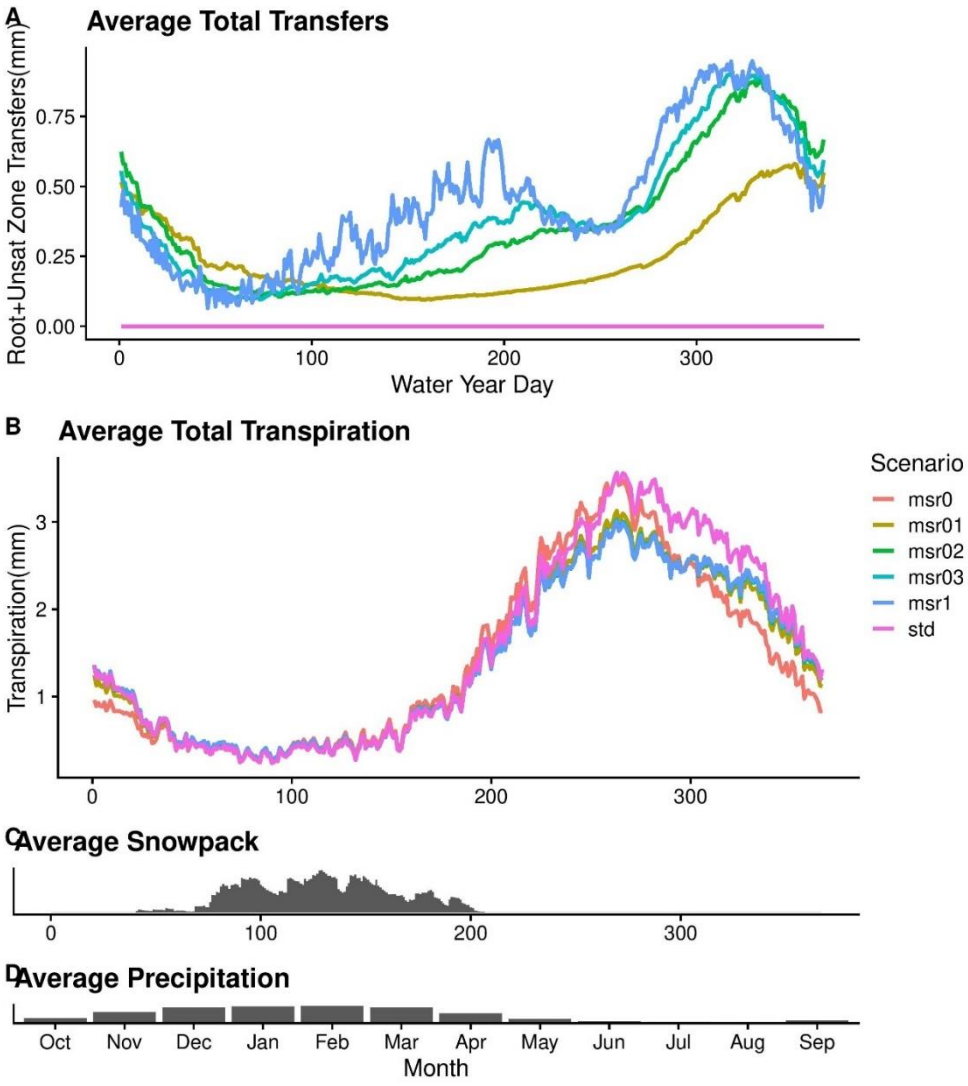

Figure 5. Line and column plots showing the annual distribution of average transfers, transpiration, snowpack, and precipitation, all averaged across by day-of-year over the complete simulation. Total transfers and transpiration each include scenarios for standard RHESSys and MSR RHESSys using sharing coefficients 0, 0.1, 0.2, 0.3, and 1.

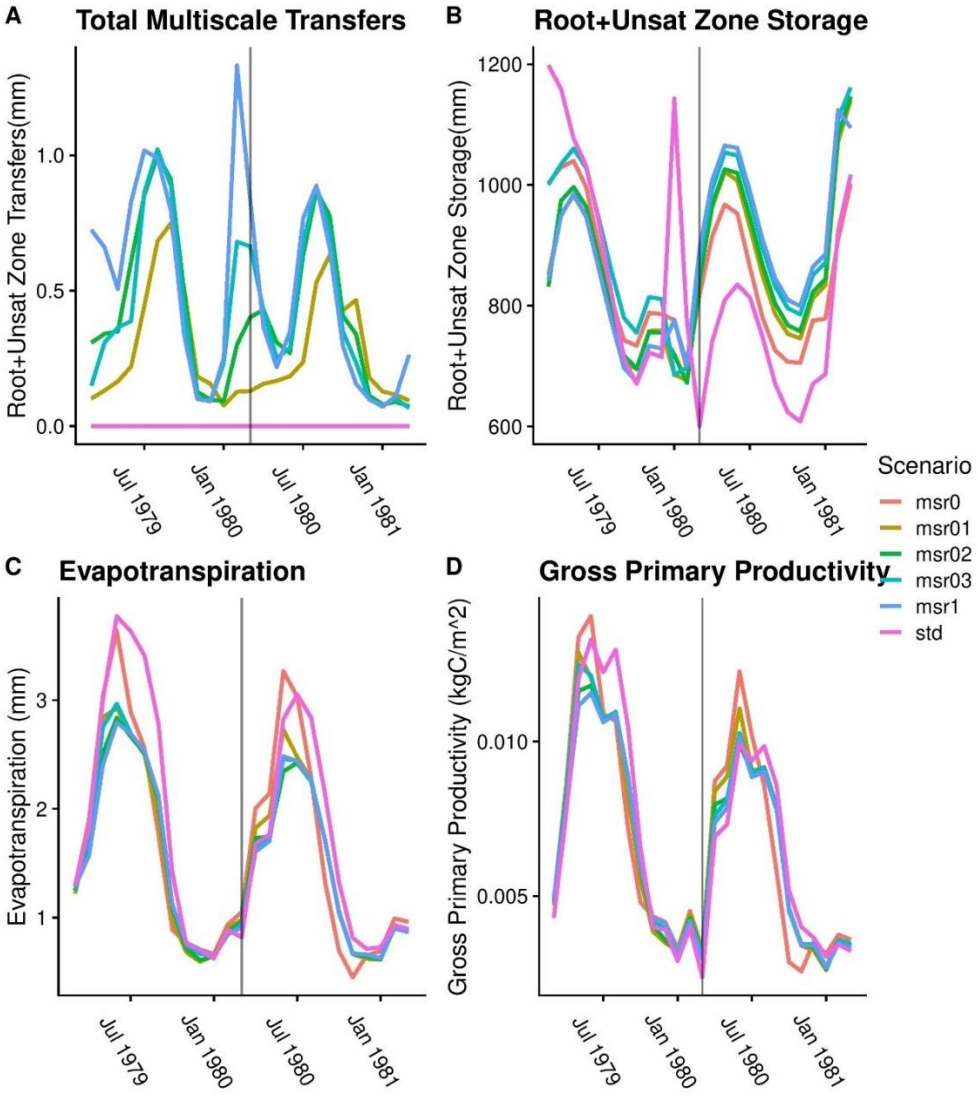

Figure 6. Time series comparison of total transfer, root zone and unsaturated zone storage, evapotranspiration, and gross primary productivity show across standard RHESSys and MSR RHESSys using sharing coefficients 0, 0.1, 0.2, 0.3, and 1.

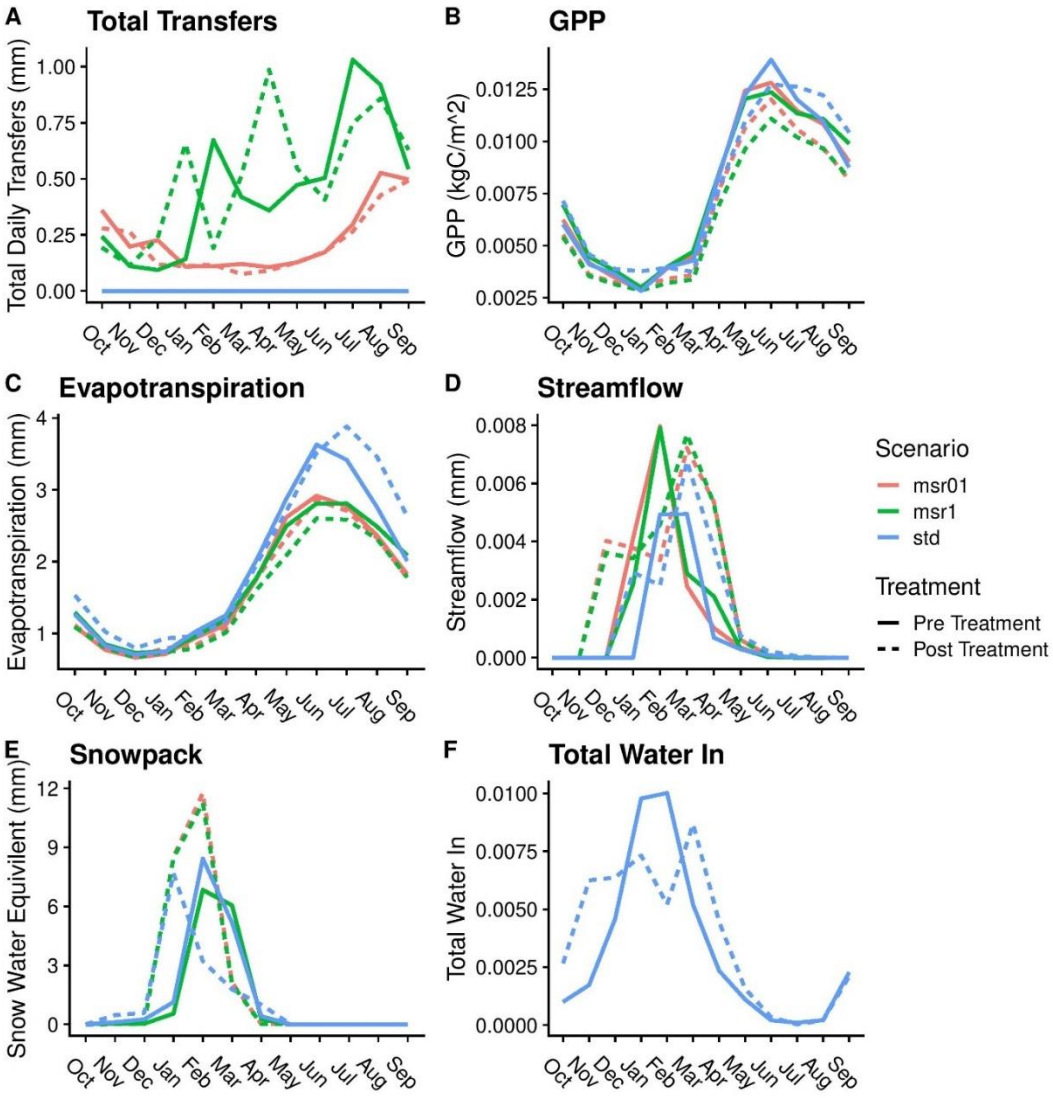

Figure 7. Monthly averages for pre- and post-treatment periods, for a subset of sharing coefficients (0.1 & 1) and standard RHESSys. Includes total transfers, gross primary productivity, evapotranspiration, streamflow, snowpack, and total water in (input precipitation).

7. Equations

Equation 1. Set of equations describing local routing within a patch family in multi-scale routing

Change in storage = ⊿

For patch X = p (subscript)

Root zone = rz

Unsaturated zone = unsat

Storage = str (subscript)

Saturated deficit = sat_def

Field capacity = fcap

Sharing coefficient (gaining, losing) = sh_g , sh_l

Loss ratio (total estimated loses/potential loses) = lr

Root zone depth percent = rz_z

Wilting point = wp

Patch water content:

$$wc_p = (rz_{str} + unsat_{str})/sat\_def$$

Mean water content:

$$wc_{avg} = \frac{\sum wc_p * area_p}{total\_area}$$

Losing transfer estimate:

$$\Delta L_{est} = (wc_p - wc_{avg}) * area_p * sh_l * sat\_def$$

Gaining transfer total:

$$\Delta G_p = (wc_p - wc_{avg}) * area_p * sh_g * sat\_def * lr * rz\_z$$

Gained transfer to root zone, unsaturated zone:

$$\Delta G\_rz_p = \min\left(\left(\frac{\Delta G_p}{area_p}\right), (fcap - rz_{str})\right)$$

$$\Delta G\_unsat_p = \max\left(min\left(\left(\frac{\Delta G_p}{area_p}\right) - \Delta G_{rz_p}, (fcap - unsat_{str})\right), 0\right)$$

Losing transfer total:

$$\Delta L_p = \Delta L_{est} - (\Delta L_{total} - \Delta G_{total}) * (\frac{\Delta L_{est}}{\Delta L_{total}})$$

Loses from root zone and unsaturated zone:

$$\Delta L\_rz_p = -1 * \min(\Delta L_p/area\ , rz\_str - wp\ )$$

$$\Delta L\_unsat_p = -1 * \max\left(\left(\frac{\Delta L_p}{area}\right) + \Delta L\_rz_p, 0\right)$$

Equation 2. Equation describing shading among patches within a patch family

Patch horizon adjustment:

$$horizon_p = \text{atan}\left(\frac{height_{avg} - 0.75 * height_p}{\frac{\sqrt{area}}{\sqrt{density * area}}}\right)$$

Chapter 2: Understanding How Fuel Treatments Interact with Climate and Biophysical Setting to Affect Fire, Water, and Forest Health: a Process-Based Modeling Approach

This is a pre-publication version of a manuscript which has been published:

Burke, W., Tague, C.N., Kennedy, M., Moritz, M., 2020. Understanding fuel treatments: how treatments interact with climate and biophysical setting to affect fire, water, and forest health. Frontiers in Forests and Global Change 3, 143. https://doi.org/10.3389/ffgc.2020.591162

1. Introduction

Informed forest and vegetation management is progressively more important as both severe drought and wildfire activity are predicted to increase in the Western US (Clark et al., 2016; Moritz et al., 2012). In many Mediterranean fire-prone ecosystems drought is already shaping stand-scale dynamics, shifting habitats, and altering the severity and frequency of disturbances including fire and insects (Clark et al., 2016). Recent droughts, like the 2012-2015 California event and subsequent water stress and mortality (Asner et al., 2016), highlight the magnitude of potential impacts of droughts on forest structure and water resources. At the same time, increasing fire severity in many of these regions has led to unprecedented social and economic costs (Moritz et al., 2014). Given these ecologic and socio-economic costs, fuel treatments are increasingly proposed as a way to reduce risks associated with both droughts and fires. Fuel treatments modify forest structure typically by removing understory and small diameter trees, either through mechanical harvest or

controlled burns (Agee and Skinner, 2005). Fuel treatments have a variety of purposes, from timber harvest-oriented practices to increase productivity, to the restoration of historic forest structures and associated habitat. Key among these purposes is the role that fuel treatments can play in reducing wildfire severity (Hessburg et al., 2016; Barros et al., 2019) and mitigating drought impacts on vegetation (Tague et al., 2019). We need to understand more broadly how those treatments are altering our landscapes and affecting resources we care about, both directly and indirectly.

Heterogeneity in forest species and stand structures, along with different goals and available resources for forest management, leads to a wide range of actions that fall under the broad category of fuel treatments. Mechanical thinning is frequently used to reduce fire severity and limit canopy fires by reducing surface fuels, increasing the height to live canopy, and decreasing the density of the canopy (Agee and Skinner, 2005; Evans et al., 2011). Prescribed fire is often paired with mechanical thinning, and in this same context aims to increase forest resilience through reductions in surface fuels and scorching (killing) lower branches of trees, increasing the height to live canopy (Evans et al., 2011; Fernandes, 2015). The size and placement of fuel treatments, however, varies. Treatments, particularly thinning, are expensive and are typically focused on areas where fire threatens residences and communities, or where abnormally high severity fire is expected (Anderson et al., 2018; Wibbenmeyer et al., 2016). Fuel treatments can be effective in reducing fire severity or altering fire regimes, but effectiveness varies with forest type and treatment implementation. Treatments can also have adverse and unintended effects (Agee and Skinner, 2005; Omi and Martinson, 2002; Safford et al., 2012). For instance – the stems removed during thinning, called slash, if left on the forest floor can result in greater surface fuels which then increase

fire intensity (Stephens et al., 2012). The long-term efficacy and effects of treatments are linked to regrowth and the presence or absence of new and competing species, leading to uncertainty in the net effects on fire severity (Moritz et al., 2014). The uncertainty in these long-term effects, combined with the (often large) expense of each treatment, make long-term planning for, and prediction of, the effectiveness of fuel treatments for reducing fire severity challenging.

In addition to reducing fire severity, fuel treatments, specifically forest density reductions through thinning, have been used to increase forest productivity and growth as part of silviculture, and more recently, as a forest management tool to reduce drought vulnerability and forest mortality (Cabon et al., 2018; McDowell et al., 2007; Spittlehouse and Stewart, 2003). While there is general agreement on the short-term effectiveness of treatments to reduce drought vulnerability and forest mortality, there is still noteworthy uncertainty in the long-term net effects of treatments. In fact, there is potential for post-treatment scenarios to instead increase vulnerability to future drought (Clark et al., 2016; Tague et al., 2019). Typically, density reduction increases the productivity of remaining trees, and reduces overall water stress, largely by a reduction in tree-scale competition for water (Clark et al., 2016; Sohn et al., 2016). However, in semi-arid regions, increases to productivity may be diminished during dry periods (Sohn et al., 2016). Increased leaf-to-sapwood area ratios and type conversion can also both lead to greater drought vulnerability (Clark et al., 2016). Treatment effects on productivity are further affected by the access of remaining trees to shared subsurface storage and changes to the tree scale radiation environment (Tague et al., 2019; Tsamir et al., 2019). Density reductions both directly and indirectly affect carbon sequestration, and while the short-term effect is straightforward, long term sequestration

depends on post-disturbance regrowth (North et al., 2009). The interactions between treatments and forest health are also expected to evolve with climate change, making a priori predictions of treatment success uncertain (Allen et al., 2010).

Fuel treatments can also be used to alter water yield (surface and subsurface water leaving an area). Though paired catchment clear cutting studies show consistent increases in water yield; thinning, particularly in Mediterranean forests, shows variability in the magnitude and direction of effects on water yield (Brown et al., 2005; Hewlett and Hibbert, 1967; Saksa et al., 2017). Thinning effects on water yield are dependent on a range of factors, including regrowth, access to storage, species changes, and the resulting forest structure, and there remains persistent debate on the dominant controls on the forest cover-water yield relationship (Brown et al., 2005; Ellison et al., 2012; Filoso et al., 2017; Tsamir et al., 2019; Kirchner et al., 2020, Tague and Moritz, 2019).

The wide range of covarying factors that both affect and are affected by fuel treatments combine to make predicting the net effects of a given treatment difficult. Much of this difficulty is associated with the multiple sources of variation including fuel treatment options, species characteristics, landscape, topographic position, climate, and the possible interactions among them. Understanding and ultimately predicting the total impacts of fuel treatments requires considering the interplay between these factors and thinning objectives, such as carbon sequestration, fire management, forest health. Models are key tools that can be used to explore variable interactions and identify particularly important sources of variation even within the same watershed (Fatichi et al., 2016). By identifying which factors matter and when, these tools provide uncertainty bounds on expected outcomes and can guide strategic fuel treatment placement.

Here we use a mechanistic coupled ecohydrologic model to explore the range of fuel treatment scenarios through time and across biophysical sources of variation. We focus on a mid-elevation forest stand within the California Sierra as a representative example of a region where fuel treatments are both likely to occur and may be focused on multiple benefits (Gould, 2019a, 2019b). In the context of existing uncertainty around the effects of treatments, the goals of this work are twofold:

1. To characterize the expected distribution of fuel treatment effects on key response variables (covering the domains of forests, water, and fire), across likely variability in biophysical contexts that would occur within a management unit (e.g., a forest stand within a particular bioclimatic region).

2. To understand how variability in fuel treatment effects is explained by different biophysical, climatic, or fuel treatment parameters. We demonstrate a novel approach, combining modeling and statistical methods, to understand this parameter-driven variability in fuel treatment effects.

In our analysis, we highlight fuel treatment effects on fire severity, carbon sequestration, water yield and forest productivity and examine whether estimates of these effects are similar to commonly held assumptions of treatment outcomes. We typically expect that over short to medium time periods (5-30 years) fuel treatments:

H1. Reduce fire severity – fuel treatments remove fuel and alter canopy structure, limiting the ability of fire to reach the canopy and thus reducing risk of high severity fires (Agee and Skinner, 2005).

H2. Reduce carbon sequestration – fuel treatments are a direct removal of carbon from the landscape, and so lead to lower carbon sequestration, in the short term and in the absence of future fires (North et al., 2009).

H3. Increase water yield – removal of vegetation directly reduces total transpiration. Though more soil is exposed, increasing ET, those increases are typically smaller than decreases to transpiration, and so water yield (or streamflow) is expected to increase overall (Brown et al., 2005).

H4. Increase productivity – remaining vegetation after a fuel treatment will tend to have less competition and greater access to resources (light, water, nutrients) following a treatment, increasing net primary productivity (Cabon et al., 2018; Clark et al., 2016).

Through sensitivity analysis, we assess how biophysical and treatment variation within a given watershed impact these expected outcomes. While the goal of precise prediction of the total long-term effects of fuel treatments on a specific landscape is still in the future, this work demonstrates a watershed scale approach for mapping the fuel treatment-ecohydrologic parameter space. Our approach can be leveraged to assess fuel treatment effects not only at the stand to watershed scale, but regionally. Moreover, understanding the linkages between biophysical parameters and fuel treatment effects can serve to inform future modeling and forest management in similar watersheds.

2. Methods

2.1. *Model Framework*

We use the Regional Hydro-Ecological Simulation System (RHESSys) to simulate the effects of thinning (RHESSys 7.1.1). RHESSys captures the relevant range of processes, at scales that support analysis of the hydrologic and vegetation carbon cycling impacts of density reduction. RHESSys is a process-based ecohydrologic model, which in addition to traditional hydrologic modeling, dynamically models plant growth, carbon, and nitrogen cycling, and has successfully been applied to simulate the effects of thinning and climate change impacts on forest growth, carbon cycling and hydrologic fluxes (Tague et al., 2009; Grant et al., 2013; Saksa et al., 2017; Tague and Moritz, 2019, Tsamir et al., 2019). In particular, Saksa et al. (2017) demonstrated the use of RHESSys to estimate post-thinning water fluxes and vegetation responses. The model has also been used to estimate hydrologic impacts of the restoration of natural fire regimes, including the removal of understory vegetation in Yosemite National Park (Boisramé et al., 2019). RHESSys has recently been coupled with fire spread and fire effects models and coupled model evaluation shows the model can capture spatial and temporal variation in fire regimes (e.g., variation in fire return interval) (Kennedy et al., 2017) and expected relationships in pre- and post-fire forest structure (Bart et al., 2020b). Previous work has also evaluated the ability of RHESSys to capture hydrologic and carbon cycling in semi-arid mountain systems (Garcia et al., 2016; Son et al., 2016b).

RHESSys accounts for both understory and overstory vegetation. Vegetation ecophysiology parameters can be adjusted to simulate a different plant species. These parameters are set via the RHESSys parameter database

(https://github.com/RHESSys/ParamDB), literature derived values, previous RHESSys implementations, or a combination of these methods. Precipitation, wind, and radiation are attenuated through overstory and then understory canopies. All vegetation grows stems, leaves, and roots dynamically. Downwelling radiation is adjusted by topography following MT-CLIM (Running et al., 1987) and landscape scale topographic shading through horizon angles. Radiation interactions with the ecosystem are modelled separately for direct and diffuse radiation, as radiation is attenuated through the canopy. Leaf scale fluxes differentiate between sunlit and shaded leaves. Gross photosynthesis is estimated using the Farquhar Photosynthesis model (Farquhar et al., 1980), which is driven primarily by the availability of light, water, and nitrogen, as well as growth and maintenance respiration models adapted from Ryan (1991). Net photosynthesis is allocated using the method from Dickinson et al. (1998) as also described in Garcia et al. (2016), and carbon and nitrogen both cycle vertically and can transfer laterally. Water input to RHESSys is driven by precipitation, and the model features vertical and horizonal water fluxes, both above and below-ground. Above-ground there is canopy, litter, and soil evaporation and transpiration (using Penman-Monteith (Monteith, 1965)), as well as overland flow (either Hortonian or saturation) and infiltration. Snow accumulation and melt, and the impact of forest shading on these processes is also simulated. Below-ground water (and nutrient) stores are separated into the root zone, which is dynamically defined by the depth of vegetation roots, the unsaturated zone, and the saturated zone. A groundwater store can also be used both as a sink from the saturated zone and contribution to the stream, and water fluxes occur vertically between these below-ground stores as well as laterally, driven by elevation gradients derived from above ground elevation.

A stochastic fire spread module has been recently added to RHESSys (Kennedy et al., 2017). In the module, spread is iteratively tested against a spread probability that is calculated from the litter load, relative deficit (1-ET/PET), topographic slope, and wind direction relative to the direction of spread. RHESSys also calculates fire effects on forest stand and litter variables for those burned cells (Bart et al., 2020b) by using the spread probability as a proxy for surface fire intensity. This, in combination with biomass and the relative heights of the understory and overstory, is used to calculate fire-related changes to the surface, understory, and overstory carbon stores. We use a subset of this functionality for our purposes, not running the full fire spread and effects models but instead components derived from them, which is detailed more in section 2.3.2.

Previously in RHESSys the patch was the smallest modeling unit both spatially and with respect to nutrient and water routing. Here, we include the use of a new 'multiscale routing' method (Burke and Tague, 2019; Tsamir et al., 2019). This approach creates a 'patch family' as the smallest spatially explicit model unit and use 'aspatial patches' within the patch family to account for within patch heterogeneity (e.g., areas within a spatial stand that comprise thinned, open areas, and remaining trees) without requiring very fine scale (meter) spatially explicit representation that would require computational complexity beyond currently available tools. In this context, the aspatial patch is then the smallest modeling unit for vertical water, energy, and nutrient dynamics. In previous RHESSys applications, RHESSys used only hillslope routing, routing subsurface water between spatially explicit model units (patch families) based only on topography. Within patch family routing or "local" routing occurs not because of topography but rather root access, and at scales smaller than are typically modeled. Crucially for the purposes of this work, we have added RHESSys

functionality to capture finer scale density reduction impacts on water availability and growth. These advances account for between vegetation (aspatial patch) exchanges (among gaps, thinned, and unthinned vegetated areas) as well as shading by neighboring trees within a stand (patch family). Thus, RHESSys now supports 'multiscale routing' with two scales of water (and nutrient) routing: a) routing due to topography between patch families within a hillslope or watershed and b) a new "local routing" that allows exchanges between aspatial patches and their associated vegetation types, that are typically at scales too small (<30-meter) to characterize as spatially explicit units within a watershed scale model such as RHESSys. Sensitivity of ecophysiological fluxes to the addition of multiscale routing methods is demonstrated by Tsamir et al. and presented by Burke and Tague (2019; 2019).

Previous work has shown that this "local" routing between gaps, thinned areas and remaining trees can have a substantial impact on post disturbance (fire or density reduction) hydrology and regrowth (Tague and Moritz, 2020). In this study, local routing (shown conceptually in Figure 2.), moves water between patches, with the water content of each patch approaching the mean of the patch family, mediated by the sharing coefficient. Water in the rooting zone and unsaturated zone is transferred among aspatial patches in each patch family. A sharing coefficient is defined to modulate the transfer of water between patches. When gaining water, only water up to field capacity is available to the root zone, with excess going to the unsaturated zone. When losing water, only water down to the wilting point is available from the root zone, with the remainder coming from the unsaturated zone. Sharing coefficients will vary primarily with species (which controls root spread and distribution) and gap size distributions (determined by the preexisting forest structure, thinning method, and thinning intensity) (Clark et al., 2016; Schenk and Jackson, 2002). Nitrate and dissolved

organic carbon (DOC) are transferred along with water following existing approaches in RHESSys for linking water and nutrient transport.

Shading within the patch family is also accounted for as a part of multi-scale routing. Though the multi-scale routing method does not model individual trees explicitly, by modeling thinned and unthinned areas separately, we approximate the effects of shading between neighboring thinned, unthinned and open area patches. Shading is modified by an adjustment to the east/west horizon, which is used to determine total daily incoming shortwave radiation, based on the relative height of the patch compared to the patch family. Shading is adjusted if the shading angle is greater than the existing horizon angle. Note that for each patch, vertical shading or attenuation of radiation through vertical canopy layers remains as in earlier versions of RHESSys (Tague and Band, 2004). Figure 2 shows our implementation of shading and how it evolves with changing conifer height.

2.2. *Site*

Our study site is a typical mid-elevation conifer forest in the Southern California Sierra, an area that has been previously identified as a high priority area for fuel treatment (Thompson et al., 2016). For model set up and parameterization we use data from the Kings River Experimental Watersheds (KREW) and the Southern Sierra Nevada Critical Zone Observatory (CZO). Higher elevations at this site maintain a seasonal snowpack but transition to rain dominated at lower elevations (Son et al. 2016). Vegetation cover is mainly mixed-conifer forest, consisting of white fir (*Abies concolor*), ponderosa pine (*Pinus ponderosa*), Jeffery pine (*Pinus jeffreyi*), California black oak (*Quercus kelloggii*), sugar pine (*Pinus lambertiana*), and incense cedar (*Calocedrus*), that transition to sclerophyll shrubs (greenleaf manzanita (*Arctostaphylos patula*), mountain whitehorn (*Ceanothus cordulatus*))

at lower elevations (Bart et al., 2016; Safeeq and Hunsaker, 2016). Soils are coarse sand and sandy loam (Gerle-Cagwin) with high infiltration capacities, and relatively deep storage (Bales et al., 2011). For this study, we build on previous watershed scale RHESSys simulations at this site (Bart et al., 2016; Son et al., 2016b). Here we sample forest stand characteristics by selecting from aspect, elevation, subsurface water storage capacity, and vegetation types within the watershed. For our model scenarios, described in more detail in section 2.3, we use data from a local meteorology station (Grant Grove, National Climate Data Center Station, Lat: 36.73603°N, Lon: 118.96122°W, elevation 2,005m). Historic records (1943 - 2015) for this station have a mean annual temperature of 8ºC and mean annual precipitation of 1037 mm.

2.3. *Scenarios*

Model simulation scenarios were designed to cover a reasonable range of possible physical conditions and fuel treatment types for mid-elevations in the Southern Sierra Nevada. A synopsis of these scenarios is included in Table 1. Given the high computational cost of simultaneous parameter variation with continuous sampling of the parameter space, we use a factorial approach and choose 2-3 end member parameter values encompassing high, medium, and low ranges, that define the expected extremes and, in some cases, mid points for each parameter. All simulations are done for a single location (patch family).

2.3.1. Biophysical Parameters and Climate Scenarios

Three vegetation covers were simulated: shrub, conifer overstory with a shrub understory, and a 50/50 mix of uncovered shrub and conifer over shrub (also referred to subsequently as shrub, conifer+shrub, and conifer+shrub/shrub). For aspect we used north

and south. For plant (root) accessible subsurface water storage capacity (PAWSC, included at 'low', 'medium', and 'high' intervals), we used parameters from Tague and Moritz (2019). These parameters span the range of PAWSC for vegetated locations in mid-elevation Sierras. We note that "high" PAWSC is greater than typical soil depth for this site, and acknowledge that plants often access water well below organic soil depths (Klos et al., 2018). We use root sharing coefficients of {0, 0.25, 0.5, 0.75, 1}, where 0 indicates no root sharing (all aspatial patches are isolated) and 1 indicates complete sharing by all vegetation. Climate in each scenario is varied in two ways: the aridity and the presence or lack of climate warming. 'Aridity' is defined by the subset of the observed climate record at Grant Grove station over which the simulation is run, with 'wet', 'variable', and 'dry' periods being the maximum, median, and minimum of 30-year moving averages of annual precipitation. The 'wet' period is (water years)1953-1983 (1103 mm mean annual precipitation), 'variable' is 1942-1972 (1057 mm), and the 'dry' period is 1985-2015 (967 mm). Though there is overlap in these periods, importantly the wet and dry periods are mutually exclusive, and the dry period captures the recent Californian droughts which is of particular interest here. Climate warming is included through a uniform shift in the observed climate record, increasing temperature by 2°C, and increasing CO_2 to 450 ppm. Climate warming is applied to the wet, dry, and variable periods to extend the range of climate conditions (e.g., to include the possibility of warmer droughts). We acknowledge that future climate may include a wider range of conditions (such as longer duration or more frequent droughts). However, climate model estimates of precipitation change for this region remain uncertain (Hayhoe et al., 2018). To limit computational and model complexity we focus on our simple set of scenarios that have a high likelihood of occurring in the short-term (next decade).

Model estimates require initial conditions that may vary with the biophysical parameters listed above. To account for this, spin-up to initial conditions was done separately for each vegetation, PAWSC, root sharing coefficient, and aspect, as each of these factors could alter the long-term soil nutrient and above ground biomass supported by the plot. Each instance was initialized with known soil nutrient values for the mid-elevation Southern Sierra site, and then each was run for an additional 140 years (looping the observed climate record) to further initialize the soil nutrients and allow vegetation to grow and reach maturity. Our analysis focuses on mature forest/shrubs, assuming no recent fires as these are likely to be the conditions targeted by fuel treatments.

2.3.2. Fuel Treatment Scenarios

Fuel treatment scenarios were selected to explore the range of possible thinning methods, intensities, and frequencies, while being limited and guided based on reasonable real-world (financial and physical) constraints on area treated and treatment frequency (Calkin and Gebert, 2006; North et al., 2015). Three main categories of treatment were selected: understory thinning (paired with prescribed fire), overstory thinning, and prescribed fire alone. In RHESSys, fuel removal is implemented as removal of a combination of litter and vegetation understory or overstory carbon and nitrogen stores (including stores in leaf, stems, and roots). RHESSys does not currently track individual stems, thus all thinning scenarios remove a given percentage of litter, overstory and/or understory pools, based on the type and intensity of thinning. Understory thinning is meant to approximate a thinning from below strategy, though we limit fuels removed to only the shrub understory. All understory treatments were coupled with a lagged (by 1 month) prescribed fire. Understory thinning was simulated in RHESSys through removal of both carbon and nitrogen from the shrub

understory. Prescribed fire following thinning removes litter carbon and nitrogen stores. Overstory thinning is meant to approximate a selection thinning strategy and is limited to removal of overstory vegetation carbon and nitrogen pools. Overstory thinning was combined with two slash (vegetation removed during thinning) management scenarios. One where slash remains and becomes part of litter pools (potentially increasing future fire spread and severity) and a second where slash is removed. Prescribed fire, both when it follows an understory thinning and when used alone, is simulated by removal of both litter and coarse woody debris.

Understory and overstory treatments were performed at 3 intensities, implemented in RHESSys through application of the treatment (e.g., removal of vegetation) at fractional area coverages of 0.1, 0.25, and 0.4. For example, a 0.1 intensity understory treatment removes all understory carbon and nitrogen for an aspatial patch with 10% coverage, which for the encompassing patch family, translates to removal of 10% of the total understory (and a smaller reduction in total stand carbon). A treatment of only prescribed fire was also run where 100% of litter and coarse woody debris pools were removed for all aspatial patches. For scenarios with only shrub vegetation cover, where there is no understory, we omit the overstory thinning scenarios (as the single shrub canopy ‘overstory’ is already thinned equivalently by the understory thinning scenarios).

Each of the treatment method and intensity combinations was run at three different temporal frequencies over the 30-year simulation. All treatment scenarios start with a treatment at the simulation start. We then have three different temporal treatment frequencies over the 30-year simulations: no further treatments, treatments every 5 years, and treatments every 10 years. Each of these treatment scenarios were repeated for all combinations of

biophysical parameters. A no treatment scenario was also run for each biophysical scenario. A total of 31 treatment scenarios, and 540 biophysical and climatic scenarios were run yielding a total of 13500 scenarios (with incompatible vegetation type + treatment method scenarios removed). All scenarios were run at a daily timestep for 30 years. For each scenario we output three key biophysical variables: stand carbon, net primary productivity (NPP), and evapotranspiration (ET), and three fire-related variables: fire spread probability (FSP), shrub fuel height (shrub only scenarios), and conifer canopy fuel gap (conifer+shrub scenarios). The three biophysical variables broadly serve as metrics for key functions in the domains included in Figure 1. Stand carbon is included as a means of tracking carbon sequestration, NPP is used as a metric of forest health and is further useful as a measure of drought resilience, and ET shows direct effects on the water balance and indirect effects of treatments on water yield.

The fire-related variables: FSP, shrub fuel height, and conifer canopy fuel gap, are indicators of how fire regimes might vary across scenarios and parameters. FSP denotes the likelihood that a location would burn, given ignition (or fire in a neighboring patch), and is broadly an indicator of surface fire occurrence and fire spread. This metric however does not reflect the fire severity or the impact of a fire on stand structure and biomass. We note that for the single patch family implementation used here (without neighboring patch families), we cannot run the full RHESSys-Fire model (Bart et al., 2020b; Kennedy et al., 2017) directly. RHESSys, however, does provide fire-related outputs at the patch scale, from which we calculate the metrics included here. Shrub fuel height and conifer canopy fuel gap are direct indicators of stand structure/biomass, and indirectly serve as proxies for potential fire severity. In the shrub only case we use mean annual maximum shrub height (over the

simulation period), as it is indicative of available fuels. In conifer+shrub scenarios we use the difference in understory and overstory fuel heights. We use the canopy height gap here as an indicator of the likelihood that ladder fuels (understory shrubs) would facilitate a crown fire if fire were to spread into this patch. The mixed 50/50 vegetation runs (conifer overstory with shrub understory combined with uncovered shrub alone) were excluded in these analyses as the severity metrics are not comparable. Together the 6 variables, stand carbon, ET, NPP, FSP, shrub fuel height, and conifer canopy fuel gap, span the range of domains encompassed in Figure 1.

2.4. *Analysis*

The number and breadth of simulation outputs presents a challenge in analyzing the simulation results. Each scenario produces a time series of responses to the fuel treatments, that reflects the impact of daily to inter-annual variation in meteorological forcing. Figure 3 highlights an example of this, illustrating the roles of fuel treatment timing, vegetation regrowth, and seasonally driven trends in stand carbon. There are complex interactions that arise from the layered effects of baseline seasonal trends (in stand carbon) and post-treatment regrowth – Figure 3 shows just one example of this that illustrates differences between treatments and the baseline 'no treatment' case at a monthly time scale. Though these finer-time scale regrowth dynamics certainly merit greater investigation, this work is focused on a broader synthetic perspective. Our goal is to assess the differential role of biophysical and climatic parameters and treatment scenarios on the long-term aggregate effects of fuel treatments. For all response variables, our analyses look at changes in treated scenarios relative to otherwise equivalent untreated scenarios, computed as the percent change of the simulation-long (30-year) annual averages, between each treated scenario and untreated

equivalent scenario. Because we average over the 30-year simulation, we provide a longer-term perspective of fuel treatment effects, with less emphasis on the ephemeral and more immediate fuel treatment responses.

As the goal of this research is both to characterize the broader scope of outcomes, while also interrogating specific parameter interactions, we include analyses to facilitate both goals. Histograms are used to capture the range and distribution of fuel treatment effects on each response variable. To illustrate parameter interactions, we also use a series of boxplots, showing response variable distributions subset by parameters. Showing all possible parameter interactions in this way is not feasible, thus we select several particularly salient examples. We also use Random Forests (with the R packages RandomForest and randomForestExplainer; (Liaw and Wiener, 2002; Paluszynska et al., 2019)) to identify the relative importance of biophysical and climatic parameters in predicting the treatment effects. Random forests use a bootstrap of the regression tree combined with random sampling of predictors at each node in the tree. We generated the random forests each with 500 trees (bootstrap runs) and with local importance set to TRUE. We use minimum depth to rank the parameters by importance. The depth in a tree indicates the order in which a parameter is selected. A smaller value for depth indicates higher importance, with typical low values (for our purposes) of ~1, and high values >3.

3. Results

The 13,500 scenarios produced by the varied input parameters result in noteworthy range and variability in effects on forests (stand carbon and NPP), water (ET), and fire (FSP, shrub fuel height, and conifer canopy fuel gap). The distribution of effect sizes of the biophysical and fire variables of interest, across expected variability in biophysical, climatic, and fuel

treatment parameters, is shown in Figure 4. Effect sizes highlight the long-term mean changes in each response variable to a fuel treatment, relative to untreated equivalents. Distributions shown for each response variable are grouped (colored) only by treatment type, and thus results for each treatment type include variation in not only biophysical parameters but also fuel treatment intensities and timing. All four of the expected fuel treatment outcomes (H1 – H4) are confirmed to varying degrees by means of simulation distributions, although for NPP mean is not significantly different from 0 (no change). Fire severity (as indicated by shrub fuel height and conifer canopy fuel gap) is reduced, carbon sequestration goes down, and water yield increases. However, for all effects there is substantial variation in the magnitude, and for some scenarios, direction of the outcomes. Most treatment effect distributions are roughly normally distributed, although some variables including ET, shrub fuel height, and conifer canopy fuel gap (Figure 4C, 4E, 4F) show left tailed skews. The result of this is that, despite fuel treatment effects broadly conforming to expected outcomes (H1 – H4), some subset of scenarios will diverge from those expectations. Stand carbon and ET (Figure 4A, 4C) adhere to expected treatment effects (H2, H3) in most cases, with only 23.4% and 22.4% of scenarios showing increases in stand carbon and ET respectively, and those increasing scenarios are weighted towards 0% change. NPP features a large range of treatment effects (-150% to 50%), with 42% of scenarios leading to decreases, departing from expected treatment effects (H4). FSP has a narrow range, spanning only -13% to 8%, which is an expected outcome given that fuel treatments are not typically expected to have a strong effect on fire spread rates. Potential fire severity, on the other hand, is expected to be affected by fuel treatments. Shrub fuel height and conifer canopy fuel gap show a substantial range of outcomes, -62% to 1% for shrubs, and -170% to 48% for conifer. Treatment effects

on shrub fuel height consistently align with expected reductions in fire severity (H1) whereas changes in conifer canopy fuel gap are strongly dependent on treatment type with overstory treatments leading to increases in potential fire severity, diverging from expected effects.

Interactions between fuel treatment and biophysical parameters, and the subsequent impact on fuel treatment effects, are of specific interest in this research. Interactions between treatment type and PAWSC alter fuel treatment effects on NPP, ET, conifer canopy fuel gap, and fire spread probability (subset for only conifer+shrub vegetation scenarios; Figure 5). Treatments, of all types, performed on high PAWSC, largely lead to increasing NPP (Figure 5A), In contrast, in low PAWSC, overstory thinning produces substantial decreases in NPP (median of -24%), while understory thinning and prescribed fire both have a positive median change of 4%. These varied treatment effects show that for some sites with lower PAWSC (shallow soils), NPP declines may occur and are more likely, while for other sites with high PAWSC, differences in treatment can lead to substantially larger or smaller increases. Treatment effects on ET (Figure 5B), by comparison to NPP, tend to be smaller and have less variation, both across PAWSC and treatment type. At medium and low PAWSC, thinning leads to expected reductions in ET, while at high PAWSC and for all prescribed fire scenarios ET increases, deviating from expectations (H3). Conifer canopy fuel gap (Figure 5C) shows a more notable difference in treatment effects across treatment type as opposed to PAWSC. Overstory treatment effects on conifer canopy fuel gap are nearly all negative (median -32% to -38%), indicating increasing fire severity contrary to expected reductions (H1), while understory treatments and prescribed fire have more moderate, and typically positive effects on conifer canopy fuel gap (median ~ 0% to 32%). Fire spread probability (Figure 5D) has much smaller magnitude of effects overall than any of the other responses,

and shows increasingly negative changes with lower PAWSC, though across all treatments and PAWSC, median changes still only range from 0% (prescribed fire on high PAWSC) to -3% (understory thinning on low PAWSC).

For a subset of parameters, assessed across treatment type, treatment effects on conifer canopy fuel gap vary consistently with fuel treatment type, and inconsistently with the other varied parameters (Figure 6). Across all parameters, fuel treatment effects on conifer canopy fuel gap are split, with consistent negligible to moderate increases from understory treatments and prescribed fire, and reductions from overstory treatments. Though treatment type is the strongest determinant of whether treatment effects will lead to expected reductions in potential fire severity (through increases in conifer canopy fuel gap), the other varied parameters alter the magnitude of those changes. Climate warming (Figure 6A) and aridity (Figure 6B) lead to marginal differences in conifer canopy fuel gap. Increased warming and dry aridity scenarios reduce variability of understory treatments and prescribed fire, though median effects are consistent regardless warming at 9% and 2%, respectively (for both parameters). Treatment intensity (Figure 6C) results in progressively larger changes in conifer canopy fuel gap with greater treatment intensities. For intensities of 0.1 to 0.4, overstory treatments lead to reductions of -12% to -77%, while understory treatments produce the expected increases (H1) from 5% to 11% (prescribed fire does not have an associated intensity). Treatment interval (Figure 6D) mirrors treatment intensity somewhat, though with greater variability and smaller median shifts. The shortest treatment interval (most frequent) leads to the largest magnitude changes in conifer canopy fuel gap, increases coming from understory treatments and prescribed fire, and reductions from overstory treatments.

To summarize the influences of all parameters, accounting for their potential interactions we use random forests. Minimum depth distributions, generated from the random forest decision trees for stand carbon, NPP, ET, FSP, shrub fuel height, and conifer canopy fuel gap are shown in Figure 7. Climate, treatment scenarios and biophysical parameters (collectively 'parameters') are ordered by mean minimal depth. In all cases the predicted metric is the difference between the treated and untreated paired simulation. The rank order of simulation parameters differs across effects – a parameter is ranked higher (has a lower mean minimum depth) when it has a greater ability to reduce variability in subsets of the variable of interest, with the mean value indicating the mean decision tree level at which that occurs. However, lower ranked parameters may still contribute to explaining variability in effect size, particularly if there are a substantial number of trees (cases) where this parameter is ranked highly (ex. minimal depth <= 3). This variable importance occurs for all parameters to some degree apart from aspect.

Fuel treatment method and intensity rank either first or second for all response variables while treatment interval shows more variation in its contribution to treatment effects and tends to rank lower, ranging from second to fourth. Nonetheless fuel treatment interval is a higher-order control, often ranking higher than biophysical or climate parameters. The most consistent parameter across variables, and least influential is aspect, ranking last for all parameters and with a particularly high mean minimal depth of 3.1-3.4. Both PAWSC and vegetation type are moderately important with a consistently high degree of influence. PAWSC matches or exceeds the mean minimal depth of the treatment parameters for stand carbon and NPP effects.

Aridity and climate warming tend to rank relatively low but still contribute to variation in effect. For stand carbon (Figure 7A) these climate parameters have influence that is nearly equal to that of treatment interval. Climate warming, compared to aridity, has a slightly more pronounced effect on NPP and ET (Figure 7B, 7C), and has less influence in the case of FSP (Figure 7D), but both the ranking and magnitude of the mean minimal depths (~2 – 2.7) of climate warming and aridity are very similar. The root sharing coefficient, which determines fine-scale within-stand interaction, ranks low, second to last in general, but both the mean minimal depth values (2.39 – 2.58) and the distributions of minimal depth are similar to that of climate parameters.

Minimum depths of shrub fuel height (Figure 7E) and conifer canopy fuel gap (Figure 7F) feature fewer parameters due to already being subset by vegetation type. The mean minimal depth values and distributions for shrub fuel height follow both the form and general order of the mean minimal depths and distributions of the other response variables. The minimal depth distributions for conifer canopy fuel gap have a somewhat different form, with four parameters grouped tightly at mean minimum depths of 1.98 to 2.08. Root sharing coefficient also stands out in the conifer case, ranking 3rd with a mean minimal depth of 1.98 (ranked 5th at 2.06 for shrub fuel height), indicating a greater influence of this parameter on the effect of thinning on conifer canopy fuel gap, relative to the role of root sharing coefficient for the other response variables.

4. Discussion

This analysis has improved our understanding of the effects of fuel treatments across a range of biophysical and climate settings with varied fuel treatment practices. Through the simulations and subsequent analysis done here we provide insight towards two goals: 1)

understanding the scope and magnitude of expected fuel treatments effects on forests, water, and fire for a mid-elevation Southern Sierra site and 2) understanding how fuel treatments, biophysical parameters, and climate interact and serve to explain responses in fuel treatment effects on forests, water, and fire.

4.1. *Distribution of Fuel Treatment Effects on Water, Carbon, and Fire*

The distributions of fuel treatment effect sizes characterize the range of outcomes across expected biophysical conditions and varying treatments at the Southern Sierra site (Figure 4). While simulations reflect results for a particular site, these distributions have broader use in a few main ways: 1) By varying topographic and climate parameter sets used in our simulations, results are likely to be representative of much of the Southern Sierra Nevada region. Thus, these results can support regional-scale questions and goals or be upscaled into multi-region analyses. 2) The distributions of effect sizes serve as a starting point, highlighting potential sources of variation in fuel treatment effects that should be explored by more focused simulations for watershed-specific fuel treatment impact assessments. 3) Our approach demonstrates a method that could be readily applied in other locations.

Our sensitivity analysis found non-trivial differences in fuel treatment impacts on mean annual stand carbon, NPP, ET, FSP, shrub fuel height, and conifer canopy fuel gap across fuel treatment type, biophysical, and climate parameters. This is evident both through the varying parameter relationships, such as effects on NPP resulting from varied fuel treatment type and PAWSC (Figure 5A), or effects on conifer canopy fuel gap across fuel treatment type and treatment intensity (Figure 6C), and the differences in parameter influence across response variables shown via the random forest analysis (Figure 7). These parameter relationships are complex, context dependent, and vary by response variable, but together

they emphasize that fuel treatment effects are likely to be highly variable even within the same watershed. Variation is not only in magnitude, but often also in direction with some conditions leading to increases and others decreases in the response variable of interest. We find key instances where fuel treatment effects deviate from expected outcomes (H1-H4), such as increases in carbon sequestration or reductions in water yield. This variation across fuel treatment practices, biophysical conditions, and climate parameters (that could all occur within the same management unit) underline the need for a more comprehensive understanding of the factors affecting fuel treatment effectiveness. Results here can extend to regional planning to meet forest management goals; attempting to balance key regional priorities like fire severity reduction and carbon sequestration will require accounting for the likely variation in fuel treatment effects.

Our results serve as a first-order approximation of possible outcomes resulting from a fuel treatment, as well as distributions indicating likely outcomes. Stand carbon (Figure 4A) and ET (Figure 4C; showing changes in water yield), are noteworthy here. Both response variables have relatively few scenarios resulting in increases (percent change > 0%), which is indicative both of how often treatments lead to increases in water yield (reduce ET) and the challenge in increasing carbon sequestration through fuel treatments. These results are generally consistent with our expectations (H2, H3) from other modeling and field-based studies. While these results suggest that fuel treatments alone will generally lead to a decline in sequestered carbon, other studies have shown that if fuel treatments effectively reduce fire severity, this could lead to a long term net gain in carbon storage in the Sierra (Liang et al., 2018). In this study, where wildfire is not explicitly included, the scenarios that do show modest increases in carbon (up to 30%), reflect cases where thinning effectively stimulates

growth of remaining vegetation (potentially by reducing competition for water or reducing understory shading). These cases are particularly noteworthy given the baseline assumption of decreasing sequestration (H2). While large scale biomass removal generally leads to increases in streamflow due to declines in transpiration (Brown et al., 2005), the smaller biomass removal associated with thinning is often compensated for by increases in evaporation, and transpiration of remaining trees (Saksa et al., 2017; Tague and Moritz, 2019). We find similar outcomes in this study where some scenarios have a net decrease in water availability (a net increase in ET), diverging from the typically expected water yield increases (H3). The magnitude of changes resulting from treatment are modest – a positive skew from 0% up to 14% increase in ET. For both stand carbon and ET, understanding the limited, but still present, scenarios that depart from typically expected outcomes (H2 & H3), will be key to forest management planning, but also useful as a basis for further, more focused modeling and analysis.

In considering the distribution of fuel treatment effects on fire related variables we see a dichotomy between the small range of effects on FSP (Figure 4D) and the more noteworthy range of effects on shrub fuel height and conifer canopy fuel gap (Figure 4E, 4F). The difference between the fire metrics shown in Figure 4 underscores the often-small magnitude of effects a fuel treatment is likely to have on fire spread. However, treatments do produce a large range of effects on fire severity, shown in our study particularly when considering the conifer canopy fuel gap, which broadly aligns with expected treatment effects (H1). It should be noted that despite generating metrics assessing potential fire spread and severity, we do not run these simulations dynamically with fires affecting the landscape. Our results emphasize that fuel treatments mostly contribute to reducing potential fire severity, rather

than fire spread. We note, however, that our spread indicator does not consider active fire suppression and it is likely that the fire suppression will be more effective at reducing spread when fires are less extreme. Our results also highlight that reductions in potential fire severity also differ both with biophysical/climatic conditions and the type of fuel treatment. Critically, even when only considering understory treatment followed by prescribed fire, a treatment option supported by the literature in regards to its efficacy in reducing fire severity (Agee and Skinner, 2005), there is still a nontrivial range of effects, with many at or near 0% change. This range of effects is in contrast with the (often assumed) expectation of consistent treatment effects on fire severity (H1), and in turn emphasizes the challenge simply in consistently altering fire severity through fuel treatments. Though more specificity and detail on a fuel treatment scenario may lead to greater certainty on the efficacy of that treatment, the baseline assumption should account for this distribution of outcomes, or at the very least should emphasize the uncertainty inherent in these estimates.

4.2. *Parameter Interactions*

For all types of fuel treatment responses - carbon, water, and fire – our results demonstrate substantial interactions among biophysical, climatic, and fuel treatment parameters. Even when only viewing the influence of two parameters on fuel treatment effects (Figure 5), we find that treatment type and PAWSC can interact to produce varied effects across both dimensions. When comparing high and low PAWSC, changes in NPP (Figure 5A) are divergent across treatment type. ET (Figure 5B) and conifer canopy fuel gap (Figure 5C) show similar trends, though it is both the median effect as well as variability that varies across treatment type and PAWSC. This variability arising from parameter interactions is not present for all response variables – fire spread probability (Figure 5D) varies little

across PAWSC. Similarly, not all parameters interact and lead to variation in effects. Conifer canopy fuel gap (Figure 6) responds similarly across some parameter combinations and shows varying or diverging trends across others. Both climate warming and aridity (Figure 6A, 6B), subset by treatment type, show small median impacts on conifer canopy fuel gap, with the primary response being small effects on variability. Treatment intensity and interval (Figure 6C, 6D), on the other hand, show much less consistency, with conifer canopy fuel gap changing in median effect and variability across both parameters. A critical repercussion of the variable responses we demonstrate is that a treatment strategy, or expected outcome of a treatment (e.g., H1-H4), assessed solely across a single parameter, may miss key trends in how that treatment will more broadly affect forests, water, and fire.

When we look at the effects of all parameters simultaneously using the Regression Trees (Figure 7), we find that most of the parameters play a nontrivial role in explaining response variability. Some parameters, however, do appear to be consistently more important – treatment method and intensity, for example, more strongly control trends in treatment effects as compared to aspect. The high ranking of fuel treatment parameters (treatment method and intensity and treatment interval) is encouraging, suggesting that these actions (and changes in them) are likely to have an impact across a range of site and climate conditions. Nonetheless PAWSC and vegetation type also consistently rank high. Collectively this pattern underscores the importance of biophysical setting and its interaction with treatment strategies in determining how a treatment affects forests, water, and fire. Based on this, PAWSC and vegetation type should be considered in fuel treatment selection. This is not always actionable from a management perspective, as often specific locations in the wildland urban interface necessitate treatment to mitigate high severity fire risk – but in

modeling or planning possible treatments with a degree of flexibility, the cost-benefit of where to treat should consider PAWSC and vegetation type with weight similar to the type of fuel treatment itself. This is particularly true of treatments aimed at a broader range of forest and water-related goals – key among them are drought mitigation efforts like reduction in forest mortality or increasing water yield, while still aiming to reduce fire severity.

Climate is a less dominant control on fuel treatment effects as compared to the treatment method and intensity, treatment interval, vegetation type, and PAWSC. Though there is a consistent difference in rank order between the climate parameters (climate warming and aridity) and the above four parameters, the margin can be small, as with treatment effects on stand carbon (Figure 7A) or conifer canopy fuel gap (Figure 7F). Our results indicate that while climate is not a clear primary control on the outcome of a fuel treatment, neither can we ignore it given the often-marginal difference from other, higher ranked, parameters. As focus on fuel treatments used for climate change mitigation increases, the need for inclusion of climate in analyses of fuel treatment effects will also increase. This work serves to contextualize that inclusion of climate as a control on fuel treatments; in more expansive analyses, or those simulating long-term projections, climate (both climate warming and aridity) is a reasonable or even necessary control to include and vary, with the opposite being true in narrower, or shorter-term analyses. The role of climate here is also likely underestimated as we simulate climate warming only with a 2°C increase in temperature and our aridity scenarios do not account for the expected increased variability of precipitation (Hayhoe et al., 2018).

Our results are consistent with other research that has considered factors like treatment method, storage capacity, vegetation type, and climate as variables that can influence

treatment responses (Finney et al., 2007; Hurteau et al., 2014b). Tree-scale interactions between neighboring vegetation, specifically lateral transfers of water and shading, are not typically considered. In this study, the root sharing coefficient reflects variation in tree scale interactions. While the root sharing coefficient is not the dominant factor influencing fuel treatment effects, it is consistently comparable to the climate parameters, and has a particularly large influence on conifer canopy fuel gap. Our research underscores the importance of tree-scale lateral root access in facilitating emergent differences in vegetation heights. While more work is needed to fully understand tree-scale water transfers due to lateral root access, and how this varies with species and canopy structure, the role of tree-scale lateral transfers shown here is noteworthy. Finally, we note that aspect demonstrates a consistently weaker influence on all fuel treatment effects. Inevitably there will be specific cases in which aspect has a more noteworthy influence on treatment effects, but it nonetheless would be the first parameter to exclude when narrowing the scope of analysis.

4.3. *Model Limitations and Future Work*

Though our research makes meaningful strides to better characterize fuel treatments and fuel treatment effects, both through the incorporation of tree-scale lateral transfers, as well as other recent advances to RHESSys, our modeling approach (like any) remains an imperfect approximation of reality. Some limitations include the use of indicators of fire severity rather than natively including fires within the model, and the absences of lateral subsurface water inputs (see Methods). These are not limitations of RHESSys but rather are constraints due to modelling a single “patch family” rather than a hillslope. Focusing on a single patch allowed us to fully explore a complex parameter space. Practical computing would limit this exploration for a full watershed implementation, but future work will investigate watershed

scale behaviors for parameter scenarios selected from this study. In this study we did not account for heterogeneity in vegetation size classes nor species differences.

The relationships between scenarios and treatment effects in this research are based on assumptions and limitations specific to our mid-elevation Southern Sierra Nevada site. Despite this, little of the model or scenario parameterization is truly exclusive to our site. Parameter sets were selected specifically to be regionally representative. The results found here are then useful across regions where vegetation, climate, and PAWSC are comparable – Southern Sierra Nevada mid-elevation regions. Beyond the broader application of the results of this work, the methodology developed here, both the modeling methods (RHESSys and multiscale routing) and the general architecture of the scenarios, has merit for use elsewhere. Interest in fuel treatments for fire severity reduction, improved drought resilience, increased water yield, and myriad other purposes is not unique to the Southern Sierras. The methods demonstrated here can be replicated in other regions to build improved understanding of global effects of fuel treatments, which continues to be a key yet challenging goal (Evaristo and McDonnell, 2019; Kirchner et al., 2020). The methods shown in this work also present an opportunity for synthesis with empirical data on fuel treatment effects, and can serve as a foundational step, to preface either more focused modeling work, or to inform the planning of field work. Replication of this work is already planned across a series of sites in the Western United Sates, but with climate-driven increases to fire activity projected for many regions of the world (Moritz et al., 2012), additional locations merit further investigation of fuel treatment effects.

5. Conclusions

Interactions between biophysical setting, climate, and fuel treatments are complex and have non-linear effects on forests, water, and fire. As fuel treatments receive more interest, and more often with goals beyond fire severity reduction, it becomes increasingly important to understand and ultimately quantify the range and distribution of likely effects that a treatment may have. This presents a challenging task for modelers and field scientists alike given the intersecting scientific domains and complex interconnected processes. Our research works to address this problem and provide a blueprint for how to robustly identify both the range of expected treatment effects and which factors have the greatest influence on those treatment effects. Across our range of scenarios, we highlight cases where treatment effects deviate from expectations, such as instances of increasing carbon sequestration or decreasing water yields. Even when treatment effects conform to expected direction of change (e.g., increasing water yields), results show substantial variation in the magnitude of effects even within the same watershed. For our mid-elevation Southern Sierra site, fuel treatment parameters (i.e., treatment method and intensity, and treatment interval) along with biophysical parameters (i.e., vegetation type and PAWSC), are important controls on fuel treatment effects. Climate and root sharing coefficient are of lesser, albeit variable importance across fuel treatment effects, while aspect stands out with particularly little influence on fuel treatment effects for this site. Arising from these analyses, we underscore the difficulty in estimating fuel treatment effects over narrow ranges of biophysical and fuel treatment parameters, and the need for greater variation across the parameter space, particularly as treatments are used with multiple goals in mind concerning forests, water, and

fire. This approach allows for more focused analyses to further interrogate, at finer spatial and temporal scales, how fuel treatments affect our natural environment.

6. Figures

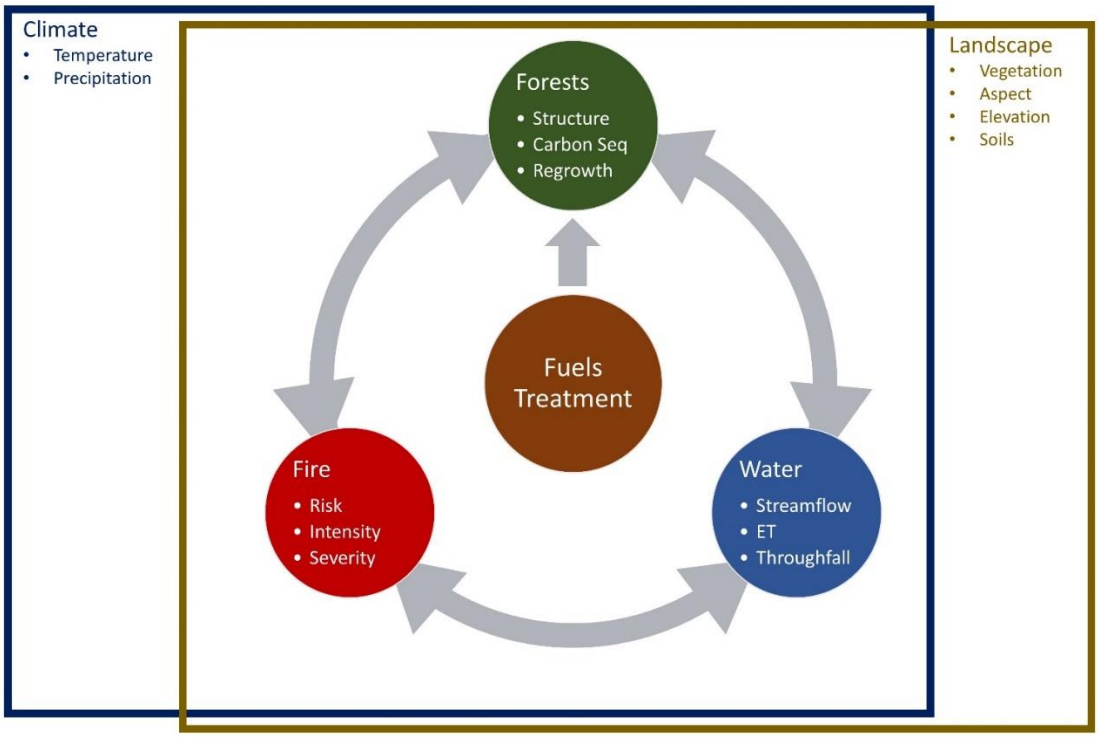

FIGURE 1. Conceptual model of the domains that underpin and are affected by fuel treatments.

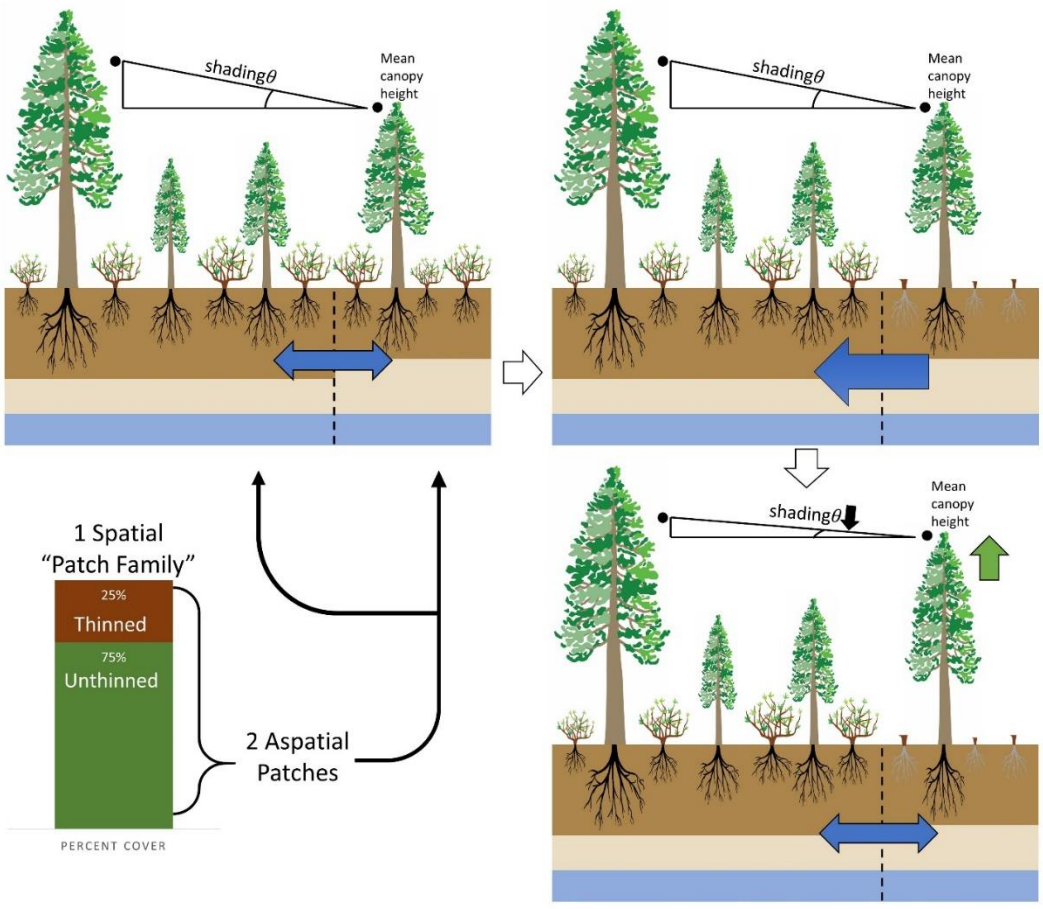

FIGURE 2. Conceptual model of the multiscale routing method, including the local routing of subsurface storage and shading that occurs between co-located aspatial patches. Shown are examples of pre-treatment, post-treatment, and post-regrowth dynamics, and possible associated changes in subsurface storage and shading.

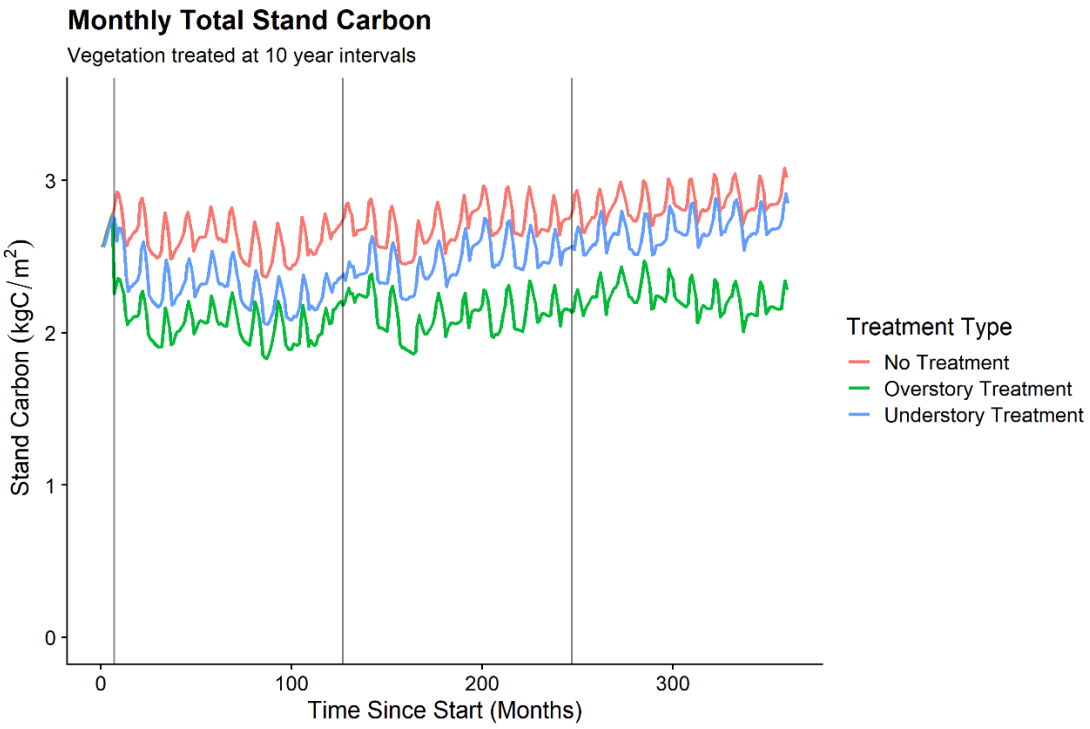

FIGURE 3. Monthly stand carbon for two treatment scenarios (40% understory removal with following prescribed fire and 40% overstory removal) and a no treatment scenario, performed on conifer overstory with shrub understory, implemented every 10 years (vertical lines), with otherwise identical biophysical and climatic parameters ('wet' aridity, no climate warming, 'low' PAWSC, 0.5 root sharing coefficient, North aspect)

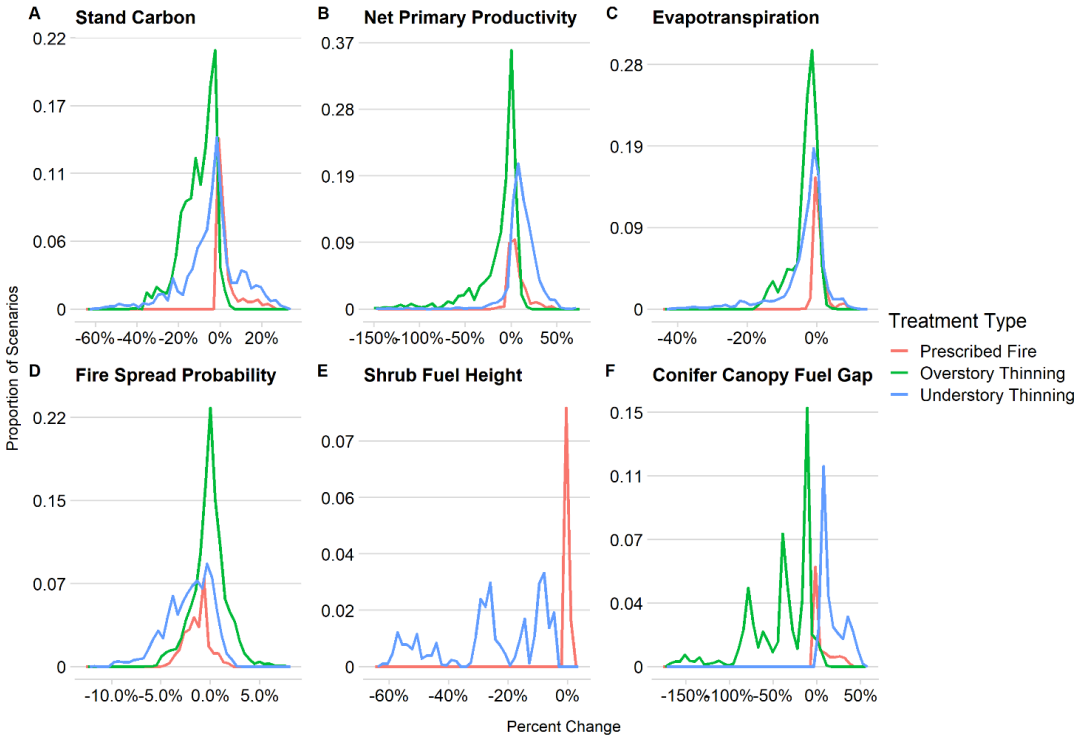

FIGURE 4. Histograms of fuel treatment effect sizes, in percent change of simulation long (30-year) means relative to untreated equivalent scenarios, for stand carbon (A), net primary productivity (B), evapotranspiration (C), fire spread probability (D), shrub fuel height (E), and conifer canopy fuel gap (F). Colored by treatment type.

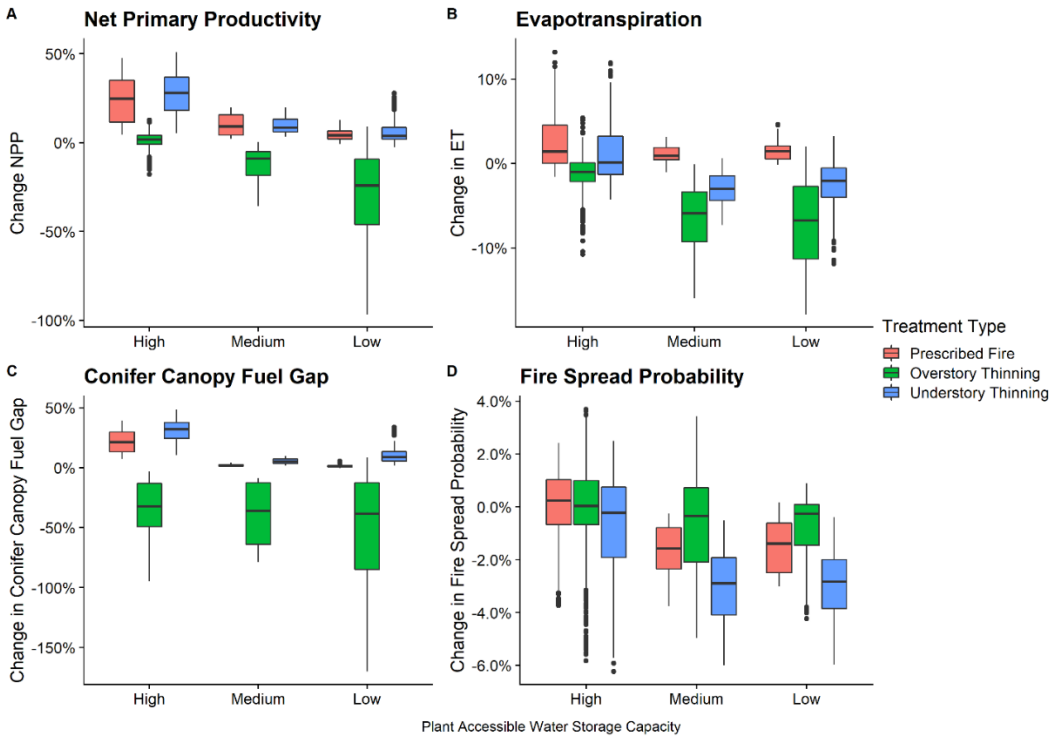

FIGURE 5. Boxplots of percent change of simulation long (30-year) means relative to untreated equivalent scenarios, for net primary productivity (A), evapotranspiration (B), conifer canopy fuel gap (C), and fire spread probability (D), for only conifer+shrub scenarios, subdivided by PAWSC on the x-axis and colored by treatment type. Upper and lower hinges indicate the 1st and 3rd quartiles (25th and 75th percentiles), and whiskers indicate the greatest/smallest value within the 1.5 times the inter-quartile range.

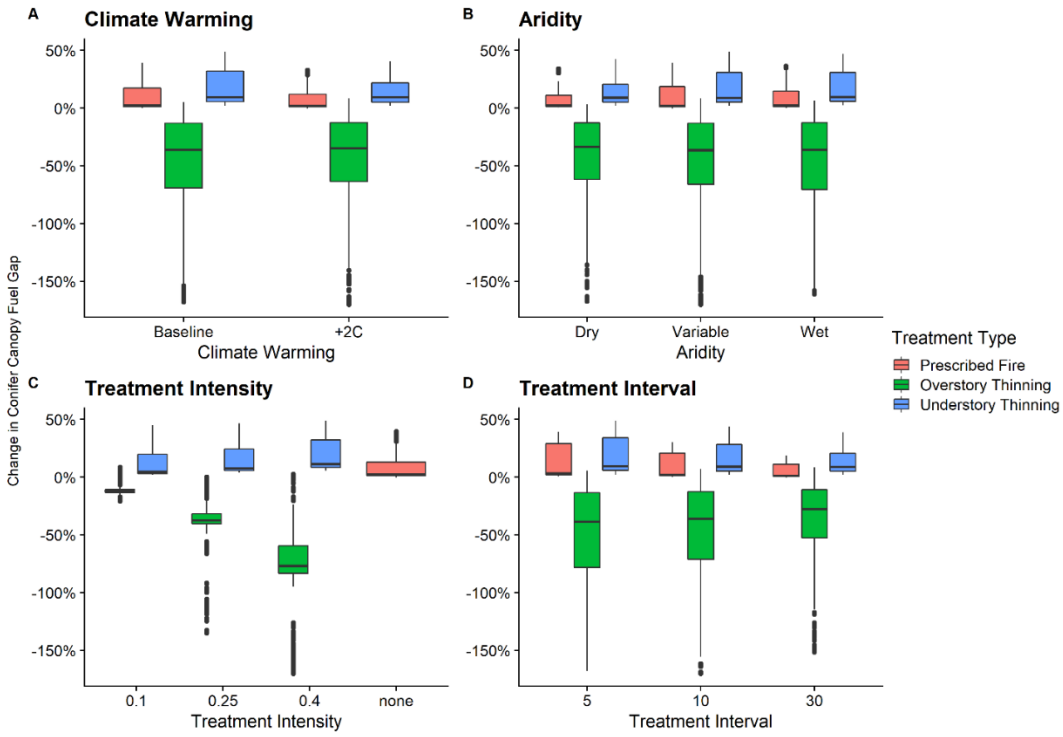

FIGURE 6. Boxplots of percent change of simulation long (30-year) mean conifer canopy fuel gap, relative to untreated equivalent scenarios, for only conifer+shrub scenarios, subdivided by climate warming (A), aridity (B), treatment intensity (C), and treatment interval (D) on the x-axes and colored by treatment type. Upper and lower hinges indicate the 1st and 3rd quartiles (25th and 75th percentiles), and whiskers indicate the greatest/smallest value within the 1.5 times the inter-quartile range.

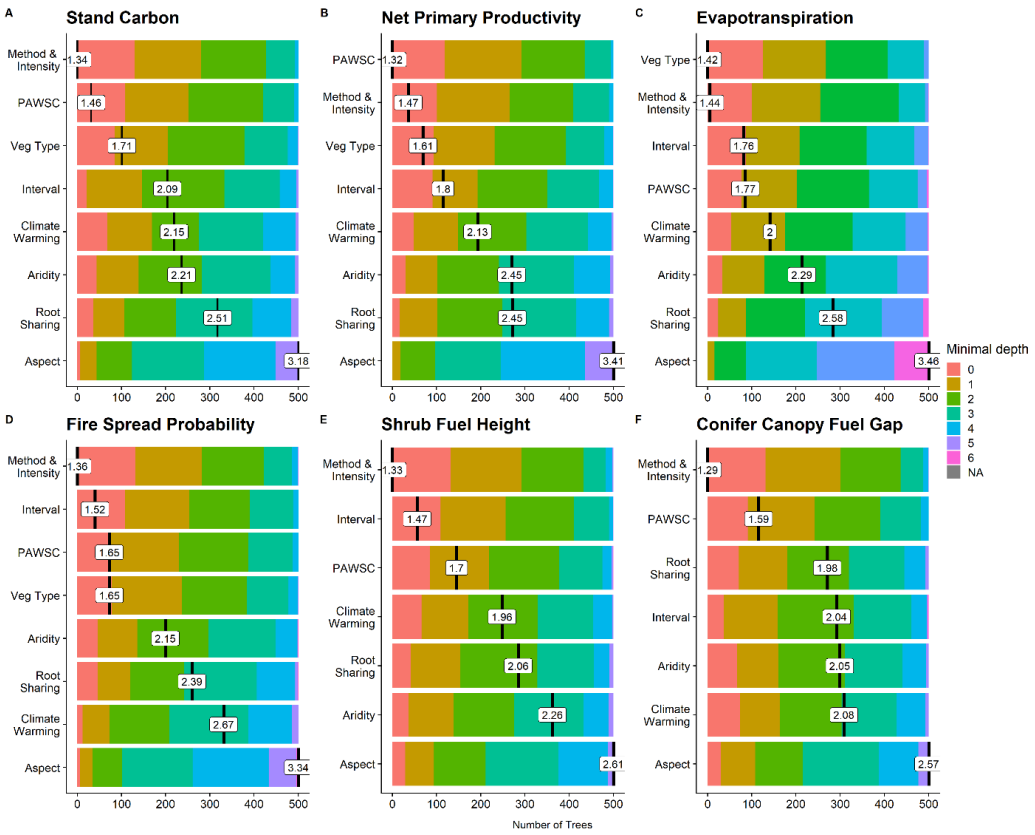

FIGURE 7. Means and distributions of minimal depths for the random forest decision trees of stand carbon (A), net primary productivity (B), evapotranspiration (C), fire spread probability (D), shrub fuel height (E), and conifer canopy fuel gap (F). Minimal depth indicates, for each random forest, the first decision tree node that a given parameter best grouped (minimized variance) for the output variable.

7. Tables

TABLE 1. Summary of fuel treatment scenario parameters

Fuel Treatment Scenarios	
Treatment Method & Intensity	**10**
Understory thinning + prescribed fire: *high, med, low*	3
Overstory thinning, with/without slash: *high, med, low*	6
Prescribed fire	1
Treatment Frequency: *5, 10, 30 years*	**3**
No Treatment	**1**
Site Characteristics	**540**
Vegetation: *shrub, conifer, shrub/conifer mix*	3
Aspect: *north, south*	2
Plant accessible water storage capacity: *low, med, high*	3
Aridity: *dry, variable, wet*	3
Climate warming: *baseline, + 2°C*	2
Root sharing coefficients: *0, 0.25, 0.5, 0.75, 1*	5
Total (incompatible combinations removed)	**13500**

Chapter 3: How Climate Change and Treatment Size Impact Fuel Treatment Effects

1. Introduction

Fuel treatments, the removal of vegetation through mechanical methods or controlled burns, have a wide range of uses including reducing high severity fire risk, promoting forest health, and increasing streamflow (Agee and Skinner, 2005; Ager et al., 2010; Tague et al., 2019). Depending on the type of treatment and the environment in which it is done, fuel treatments have the potential for positive and negative impacts on key areas of concern such as wildfire risk or water supply, areas of particular interest to forest and land managers (Burke et al., 2020). There is growing interest in the potential benefits of fuel treatments, not only as a method to reduce fire risk but also to manage streamflow and forest health. Climate change impacts on forests are substantial, mid elevation conifer forests in the Southwest U.S. experienced doubled tree death from 1955 to 2007, insect outbreaks killed more than 129 million trees in California from 2010 to 2017, and climate change led to double the area burned by wildfire from 1984 to 2015 in the western U.S (Garfin et al., 2018; Vose et al., 2018). How then, do the already complex interacting effects of fuel treatments change when we consider projected climate change? The effects of forest management decisions will change alongside climate, so it becomes necessary to consider how simultaneous changes in both the treatments themselves and climate will alter the effects of fuel treatments on the full range of biophysical processes we care about such as high severity fire, streamflow, and forest health.

Fuel treatments, specifically forest thinning, have the potential to affect not only the risk of high severity fire, but also a range of hydrologic and ecophysiological factors. Though not all landscapes are as well suited to the use of fuel treatments for reducing high severity fire, in many cases fuel treatments remain an effective forest management tool, such as in mixed conifer regions of the western U.S. (Barros et al., 2019). Longer term effectiveness is often dependent on regrowth dynamics and competition between new species (Moritz et al., 2014). Fuel treatments, as a means of reducing forest density, have also been long used to improve vegetation growth and increase silvicultural production (Cabon et al., 2018). In addition to increases in productivity, thinning can improve resiliency to drought, at least in the short term, while the longer term impact on drought resilience is more uncertain (Clark et al., 2016; Tague et al., 2019). Thinning can alter streamflow through changes to vegetation water use, with increases in evaporation typically being outweighed by reductions in transpiration (Brown et al., 2005; Tague et al., 2019). Though thinning most commonly leads to increases in streamflow, there remains cases to the contrary where thinning leads to little or no impact on water yield and streamflow (Brown et al., 2005; Ellison et al., 2012; Tague and Moritz, 2019).

Climate change is responsible for noteworthy changes in average annual temperatures at varied scales, but of note to this research are the impacts on the western U.S. and California. The Southwestern U.S. has already seen an increase in average annual temperatures of 0.9°C when comparing current temperatures (1986–2016) to those of the first half of the last century (1901–1960), with changes in minimum and maximum temperatures following the same shift (of 0.9°C) (Vose et al., 2017). Model ensembles for the Southwestern U.S. project increases of 4.8°C by 2100 under a ‘business as usual strategy’ (RCP 8.5) (Garfin et al.,

2018). California-specific estimates range from increases of 2-4°C under a medium emissions scenario (RCP 4.5) or 4-7°C under the more severe 'business as usual' scenario (RCP 8.5) (Pierce et al., 2018). Annual precipitation by contrast has no clear trend though time, either historically or in model projections, but instead is expected to increase in variability. Precipitation in California is projected to become less frequent but come in more extreme events, with estimates of increases in dry-to-wet precipitation events of 25% to 100% (Swain et al., 2018).

Climate change in the western U.S. is already transforming fire behavior and is likely to continue to have substantial effects on fire regimes. Climate-driven changes to wildfire, while related to changes in temperature, are also impacted by a broader range of variables including fuel loading and historic fire exclusion (Vose et al., 2018). Observed changes in the western U.S. show increases in area burned owing to longer and drier fire seasons, across a range of ecoregions (Parks and Abatzoglou, 2020). Climate has also been identified as increasing the frequency of large area wildfires, wildfire duration, and wildfire season (Westerling et al., 2006). Temperature is a key mechanism driving changes to fire – increased temperatures facilitate warmer drier weather ('fire weather') and lead to drier fuels, increasing the chances of fire spread (Kennedy et al., 2017). Warmer temperatures can also reduce vegetation productivity, which by limiting the available fuels can then reduce area burned (Hanan et al., 2020). Projections indicate that fire activity is likely to increase in already warm regions in the short term, with more variable impacts across other climatic conditions (Moritz et al., 2012). Projections for the end of the 21st century are less varied, with most regions estimating increases in fire probabilities. Given the existing and projected effects of climate change on fire, fire and forest management is continuously adapting,

though the specifics of that adaptation will be variable by site and circumstance, and evolving over time (Stephens et al., 2013).

The site conditions of a fuel treatment, such as soil and rooting depth, vegetation type, and topography, have been shown to influence both fire regimes and fuel treatment effectiveness (Burke et al., 2020; Tague and Moritz, 2019). In addition to location, fuel treatments have a wide range of implementations, notably including the treatment type and interval, and the treatment spatial design (Agee and Skinner, 2005; Finney, 2001; Prichard et al., 2020). Fuel treatment implementation will change depending on the goals (reducing high severity fire vs. improving forest health) and environmental context of the treatment (a shrub dominated riparian region vs. a high elevation conifer-dominated region) (Stephens et al., 2012). Underlying these treatment options though, is the total area treated. Decisions on area treated can depend on a variety of factors. In some cases treatment area is limited by design, either due to land ownership or other planning considerations, but often, area treated is dependent on physical limitations (slopes that are too steep, areas inaccessible due to distance from roads) or economic limitations (Anderson et al., 2020; U. S. GAO, 2019). Sometimes these factors coincide – forest thinning using heavy machinery is more efficient in time and cost, but physical limitations often require manual hand thinning which increases both time and cost. Factors influencing area treated are also changing along with climate change. Current economic priorities are likely to shift over the course of the next century as climate change increases in magnitude such that even ambitious goals for area treated today may become necessities in the future. Area treated is also a key variable of interest considering the large magnitude of effect, both on fire risk and beyond (Ager et al., 2010). Area treated is impactful due to the increased chance of the treatment to encounter and mitigate high

severity fire with increased treatment size (Barnett et al., 2016). Larger treatment area will also have a larger impact on basin-scale outputs such as streamflow which is the product of the contributing areas of the watershed.

This research uses modeling methods to better understand how the effects of fuel treatments may change under climate change. We are specifically interested in assessing the interactions between climate change and changes in area treated. Using a coupled ecohydrologic model, with novel model developments to better characterize and simulate fuel treatments and their effects, we model fuel treatment effects for a mid-elevation watershed in the California Sierra Nevada. The goals of this work are to explore:

1. How do fuel treatments of different areas affect fire risk, streamflow, and forest health? How do these changes vary in the short (< 5 years) and long term (20 years)?
2. How do climate change and treatment area, alone and in combination, interact to alter how fuel treatments effect fire risk, streamflow, and forest health?

2. Methods

2.1. *RHESSys & Multiscale Routing*

We use the Regional Hydro-Ecological Simulation System (RHESSys 7.4) along with the multiscale routing (MSR) method for RHESSys to simulate the effects of fuel treatments and climate change on hydrology and plant physiology. RHESSys is a mechanistic distributed watershed model that simulates hydrology, dynamic plant growth, radiation budget, and nutrient cycling (carbon and nitrogen) (Garcia et al., 2013; Tague and Band, 2004). Multiscale routing builds on the existing RHESSys architecture and the method is more fully

described by Chapter 1. RHESSys has been used previously to model forest thinning and thinning effects, along with the effects of climate change on plant growth and fire (Grant et al., 2013; Hanan et al., 2020; Tague et al., 2009; Tague and Moritz, 2019). Recent additions to RHESSys have incorporated both fire spread and fire effects models to simulate changing fire regimes and their impacts on vegetation structure (Bart et al., 2020a; Kennedy et al., 2017).

There are several key model components which make RHESSys well suited to assessing the effects of fuel treatments. RHESSys simulates vegetation ecophysiology using parameters that can be adjusted to simulate a different plant species, either relying on established parameters from the literature or those used in previous RHESSys implementations. Vegetation is simulated using up to two canopy strata (understory and overstory), with gross photosynthesis estimated using Farquhar Photosynthesis model (1980), and resulting net assimilation, once respiration has been accounted for, is allocated using Dickinson et al. (1998). Radiation is budgeted at the patch scale, adjusted for topography and horizon angle, and accounts for variable leaf scale fluxes owing to sunlit vs. shaded areas (Running et al., 1987). Water, along with nutrients (carbon and nitrogen) cycle vertically and can transfer laterally. Evapotranspiration is based on Penman-Monteith (1965), and is separately calculated for canopy interception and soil. Snowmelt processes are calculated based on radiation budget and are fed into the vertical profile drainage. A more complete description of RHESSys functionality and internal equations can be found in Tague & Band (2004) and Garcia et. al. (2013), with more recent additions and application-specific accounting can be found in Burke et al. (2020).

The MSR method is a key addition to RHESSys that facilitates modelling thinning and the subsequent effects of thinning (Burke et al., 2020; Tsamir et al., 2019). RHESSys-MSR routes water both topographically over the hillslope as well as non-topographically at a within-stand scale. The MSR method builds on the structure of RHESSys – the smallest spatial unit in RHESSys is a 'patch', MSR adds multiple 'aspatial patches' in the location where there was only a single spatial patch previously. These aspatial patches, collectively a 'patch family', are defined by percent coverages. Individual patches within a patch family can be used to account for small scale variations in vegetation, for example, to simultaneously account for conifer, shrub, and open spaces within stands. These same units can also be subjected to thinning, reducing carbon for a specific subset of the stand instead of applying an average effect over a larger unit to accomplish the same net reduction. MSR facilitates the routing of water and nutrients between the co-located aspatial patches, allowing for realistic post-thinning regrowth dynamics, which can be influence by the lack or presence of access to the storage of neighboring vegetation MSR also introduces shading associated with neighboring vegetation that occurs between patches in each patch family, accounting for the role that significantly taller neighboring vegetation can have in reducing incoming solar radiation of shorter stature neighbors. These changes all coincide with the existing functionality of RHESSys, which routes water topographically over the hillslope, calculates the energy budget, and dynamically grows vegetation. Full details on both the routing and shading components of multiscale routing are featured in Chapter 1.

2.2. *Site*

The study site for this research is the Big Creek watershed, located in the Southern California Sierra Nevada, encompassing the Providence Creek watersheds which are a part of

the Kings River Experimental Watersheds (KREW) and Southern Sierra Critical Zone Observatory (Hunsaker et al., 2012; O'Geen et al., 2018). While the entire ~66 square kilometer watershed is used for the main analysis, the smaller P301 subcatchment is used for soil parameter calibration. The meteorology station at the subcatchment outlet (Grant Grove, National Climate Data Center Station, Lat: 36.73603°N, Lon: 118.96122°W, elevation 2,005m) is used to drive baseline historic simulations. Historic climate at the site (1943 - 2015) features a mean annual temperature of 8ºC and mean annual precipitation of 1037 mm (highly variable from 635 mm to 2172 mm) (Bart et al., 2021). The watershed elevation spans from 957 m to 2344m, with areas of seasonal snowpack at high elevations and rain dominated at lower elevations. Dominant soils vary by subregion, but include Gerle-Cagwin and Shaver at depths of 76 to 203 cm (Bales et al., 2011). Vegetation is dominated by mixed conifer forest, with some areas of shrub and chaparral, as well as regions of bare earth. Vegetation species include white fir (*Abies concolor*), ponderosa pine (*Pinus ponderosa*), Jeffery pine (*Pinus jeffreyi*), California black oak (*Quercus kelloggii*), sugar pine (*Pinus lambertiana*), and incense cedar (*Calocedrus*), that transition to sclerophyll shrubs (greenleaf manzanita (*Arctostaphylos patula*), mountain whitehorn (*Ceanothus cordulatus*)) (Safeeq and Hunsaker, 2016). The Big Creek site has benefited from a variety of previous research, with multiple previous studies using RHESSys to model parts or all of the watershed (Bart et al., 2021, 2016; Son et al., 2016b; Tague and Moritz, 2019)

2.3. *Model Initialization and Calibration*

Initialization and calibration of RHESSys for the Big Creek watershed was done in a series of steps commonly used when setting up and running RHESSys: spin up of soil nutrient stores, calibration of soil and vegetation parameters based on observed streamflow

and vegetation data. The P301 subcatchment was set up and run for a period of 300 years to ensure soil nutrients reached steady states. The same subcatchment was then cleared of vegetation and regrown for 50 years to achieve vegetation ages and sizes more appropriate to the mixed conifer site. The initialized model was used to calibrate soil parameters using observed meteorological data and streamflow data from the Southern Sierra Critical Zone Observatory for the period from 2000 to 2015. Starting parameters and ranges were taken from Son et al. (2016b), which provides soil parameter values for the same basin, though significant changes to the model have occurred since those parameters were found. Eight soil parameters (including depth, pore size index, conductivity, saturated conductivity, and the decay of conductivity with depth) were included in the calibration, though this was complicated by the inclusion of the two sharing coefficients (sh_l and sh_g), which modulate the water transferred among a patch family in multiscale routing. A total of 1500 calibration runs were done, sampling uniform parameters, with the best performing parameter set having a Nash-Sutcliffe efficiency (NSE) of 0.61. Though the complexity of the vegetation dynamics as well as the spatial and temporal scales being run at may make RHESSys challenging to calibrate, this NSE value is still on the low end and may warrant further investigation. Additionally, new strategies may be needed to properly include MSR in soil parameter calibration. Following calibration using the P301 subcatchment, the full Big Creek watershed was initialized, based on a DEM using a 90-meter resolution, the watershed was again run for 300 years until the soil nutrient stores reached steady-state. After clearing and regrowing the vegetation to a more realistic age of 50 years, vegetation behavior and structure were assessed in the case additional parameter tuning was needed, but the existing vegetation parameters were sufficient (Burke et al., 2020; Son et al., 2016b).

2.4. *Model Scenarios*

Model scenarios in this research were defined by variations in climate and area treated. Fuel treatment scenarios were selected to capture a wide range of possible area treated, while keeping the type and intensity of that treatment constant. While varying the type and intensity of treatment would add additional information the computation cost where prohibitive for this study. Previous work has shown the importance of both treatment method and intensity but given the watershed scale of the outputs of interest in this work, treatment area is likely to play a powerful enough role without additional variation to method and intensity (Burke et al., 2020) With respect to the fuel treatment itself, we vary the area treated, while leaving the treatment itself as a moderately high intensity reduction of overstory biomass – a 40% removal from the conifer overstory, coupled with a 100% removal of the shrub understory. This treatment method and intensity, while not the most extreme fuel treatment scenario, is still a relatively intense treatment. Treatments are applied at the start of the simulation and compared with a control no treatment scenario. We include three treatment area options using the previously described method and intensity: no thinning, minimal thinning, and maximized thinning. Minimal thinning is a treatment of 20% of the total area, and for simplicity of implementation, is arranged based on a random sampling over the watershed. The maximized treatment scenario treats all area below a slope threshold of 40% slope rise (~22°). While there are a range of mechanical forest thinning machinery that can operate up to 50% slope, and in rarer cases even in steeper more extreme slopes over 50%, we use a threshold of 40% to account for the less than perfectly optimistic access to machinery, and the fact that many areas of shallower slopes are made inaccessible

due to barriers of steeper slopes. This area of the 'maximized thinning' scenario translates to ~90% coverage of the watershed.

We use three climate scenarios: observed, RCP 4.5, and RCP 8.5. Observed climate data from the Grant Grove meteorological station for the 20-year period of 1995-2015 serves as the 'historic', or more accurately 'early 21st century' period. Projected climate data using the localized constructed analogs (LOCA) method was retrieved via the Cal-Adapt data portal (Pierce et al., 2014). A single model, selected from the four priority models for California, the HadGEM2-ES was chosen. This is both to simplify the subsequent analysis, but was specifically selected due to the prevalence of drought in the modeled climate, as highlighted in Pierce et al. (2018) as a part of the analysis for California's Fourth Climate Change Assessment. Representative concentration pathways (RCPs) 4.5 and 8.5 from the HadGEM2-ES model, representing increases in net radiative forcing of 4.5 W/m^2 and 8.5 W/m^2 respectively, are used to simulate moderate and more severe climate change. To be comparable with the observed data, and to capture the more extreme end of climate change effects, the 20-year period from 2069-2099 is used for the projected data. Altogether these three climate scenarios and three treatment options combine to 9 total scenarios.

3. Results

Observed climate for the Big Creek watershed broadly aligns with the modeled and downscaled data (Figures 3 & 4). Comparing the HadGEM2-ES reanalysis product to the observed Grant Grove meteorological data, the observed data is lower by an average of ~1.8 °C. Though this is a substantial difference, even larger changes in temperature are seen when comparing the observed and projected temperature data for the model periods (1995-2015 and 2079-2099). The observed model period has a mean daily temperature of 8.1°C, while

RCP's 4.5 and 8.5, for the late 21st century model period, project mean daily temperatures of 13.6°C and 15.8°C respectively, increases of 4.9°C and 7.1°C over the course of the century. Observed baseline precipitation for Big Creek averages 1032 mm annually, slightly above the estimate from the HadGEM2-ES historical reanalysis of 943 mm. For only the model periods (1995-2015 and 2079-2099), the baseline period has an average annual precipitation of 1019 mm while the projected climate periods have average annual precipitation of 862 mm and 912 mm for RCP 4.5 and 8.5, respectively. Accounting only for days non-zero precipitation, the baseline and projected periods are compared in Figure 4. The baseline period has both greater variability as well as larger mean precipitation events of 16 mm, compared to RCP 4.5 at 7 mm and RCP 8.5 at 8 mm. These metrics are based only on days with non-zero precipitation, which for the observed period constitutes 17% of days, while for RCP's 4.5 and 8.5 are 32% and 33% of days. This together indicates that the projected periods anticipate more frequent but lower average intensity rainfall compared to observed data, though the difference is slight overall.

The direct effect on total forest carbon of the implemented fuel treatment – a 40% reduction in conifer overstory, and a 100% reduction in shrub understory, performed at the start of the model runs, is shown in Figure 5. Climate scenarios were spun up separately leading to differences in initial conditions, 8.9 and 7.3 kg of Carbon/m^2 for baseline and RCP 8.5 climate scenarios respectively. Short-term (2-year) effects of treatment on total carbon are shown in Figures 5 A & B, starting with the drop in carbon due to the fuel treatment itself. Changes to mean total carbon during the 20 years following treatment are generally minor, reductions of 3% and 11% in the baseline climate, and 1% and 2% in RCP 8.5 climate, for minimal and maximum treatments respectively.

Long term projections of carbon (Figure 5C) point to climate scenario as being a key predictor. Compared to the baseline climate, RCPs 4.5 and 8.5 lead to reductions in average carbon of 31% and 40% over the 20-year simulation period. The effects of treatment, though consistent across climate, are relatively small compared to climate differences. The reduction due to treatment comparing maximum treatment to no treatment only spans 6% for baseline climate or 3% for RCPs 4.5 or 8.5. The range of variability for each treatment and climate scenario is typically small, less than 0.5 kg Carbon for the projected climate scenarios and only slightly greater for the baseline climate.

GPP is gross photosynthesis, which can be used as an indicator of forest health (Figure 6). Short term differences in GPP show the effect of treatment, with noteworthy reductions in GPP resulting from the maximized treatment scenario, for both observed and projected RCP 8.5 climate scenarios. The effect of the minimal treatment scenarios is smaller, with small differences compared to the untreated scenarios. Though the maximum treatment scenarios show notable reductions in peak GPP, the differences are minor during the trough periods (typically January) and all treatment scenarios converge at the trough at the end of 2 years following treatment. Though Figures 6 A & B span only 2 years, the longer-term trajectory and behavior of GPP is noteworthy. For both the baseline and RCP 8.5 climates the effects of all treatment scenarios progressively diminish until 5 years following treatment when there is no discernable effect of the treatment. Crucially though, while there remains no differences from treatment for the RCP 8.5 climate, for the baseline climate the maximum treatment scenario leads in higher peak summer GPP compared to no treatment and minimal options, starting in year 5 and lasting until year 15.

Long term differences in GPP are dominated by the differences in the climate scenario (Figure 6). The baseline scenarios are on average 32 % greater than RCP 4.5 and 69% greater than RCP 8.5. For each climate scenario, treatment scenario has little impact on long term GPP, and minor decreases in GPP occur as treatment area increases. For each climate scenario, the range of variation from no treatment to maximum treatment only spans 4%, 8%, and 14% for baseline, RCP 4.5, and RCP 8.5 (absolute ranges of 0.00016, 0.00019, and 0.00016 kg Carbon/m^2 daily). Variability (range from 25^{th} to 75^{th} percentiles) within climate scenarios is substantial and eclipses differences in the median values.

We use height gap as an indicator of likely fire risk. Long term estimates of height gap, the distance from the shrub understory to the conifer overstory (in the patches which feature two canopy strata), is included in Figure 7. The effect of treatment on height gaps is consistent across climate scenarios, although maximum treatment scenarios lead to an initial increase in height gap (when averaged over the basin), the long-term effects show slightly smaller height. Climate is the larger driver of height gap, with baseline climate having substantially larger and more varied height gaps compared to RCP 4.5 and 8.5. Though there is some variation in shrub heights (3 m – 1 m), the greater control on height gap is the conifer heights, ranging from an average of 13 m in the baseline scenario to 10 m and 5 m in RCP 4.5 and 8.5. Dead trees and trees unable to successfully grow are a large component of the vegetation in RCP 8.5, with the 25^{th} percentile height falling at 1 m.

Figure 8 shows the effects of treatment and climate scenarios on streamflow. In the short-term (2 years following treatment), the maximized treatment stands out, leading to nontrivial increases in peak streamflow across climate scenarios (Figure 8 A). The largest relative differences in peak streamflow due to treatment occur in the RCP 4.5 scenario, maximum

treatment is 91% greater than no treatment, though RCP 8.5 has larger absolute differences between maximum and no treatment (5 mm peak average daily streamflow, 38% greater). Minimal treatment falls between maximum and no treatment scenarios, though for all climate scenarios it falls closer to no treatment than maximum treatment. Interestingly, despite both RCP 4.5 and 8.5 being over the same period, the streamflow behavior is markedly different between the two climate scenarios, with RCP 4.5 having nearly no winter streamflow peak in the first year following treatment. Total water yields in year one after treatment are 99 mm averaged across treatment scenarios for RCP 4.5 compared to 688 mm and 415 mm for RCP 8.5 and baseline climate respectively.

Long-term (20-year) seasonal streamflow, both monthly medians and 25th to 75th percentile boxplots, is shown across climate and treatment scenarios in Figure 8 B and C. Changes in climate scenario result in more substantial differences in the magnitudes of monthly flows whereas fuel treatment scenarios lead to similar distributions of seasonal flow. Compared to baseline, RCP 4.5 leads to a long-term average increase in mean daily streamflow of 22% and RCP 8.5 leads to an increase of 77%. Though peak flows follow a similar shift (increases of 5% and 73% for RCP 4.5 and 8.5 respectively), RCP 4.5 does have relatively less 25th to 75th percentile variability compared to baseline, particularly in peak months (March – May). There is also a 1-month shift in peak timing, moving from April in the baseline climate to March in both projected climate scenarios. Differences in fuel treatment have minor impacts on long-term streamflow (Figure 8C). Fuel treatments result in long-term average increases in streamflow of 1% and 22% for minimal and maximum treatment scenarios respectively. Though average flows change somewhat, peak flows are unaffected by fuel treatment scenarios, increasing less than 1% compared to no treatment.

Across both climate and fuel treatment scenarios, low flows are consistently unchanged, and the lowest flow months (September and October) feature no change in mean streamflow.

4. Discussion

Climate models broadly agree on projections of temperature but in many other respects there is a large degree of uncertainty as to how climate will impact our environment. Precipitation is emblematic of this – climate models are unclear as to the direction of change in the western U.S., though there is agreement as to the expected increase in variability (Garfin et al., 2018). As we trace the effects of climate change further from the more certain projections of temperature change, increased uncertainty is both expected and difficult to avoid. Projecting climate impacts on wildfire is such a challenge – fire, and specifically the risk of high severity wildfire, is linked to both temperature and precipitation, as well as a range of other difficult to predict variables such as wind, forest structure, and fuel loading. Recommendations in regards to managing wildfire in the context of climate change often point towards restoring forests, building resiliency, and anticipating change (Stephens et al., 2013). While these are excellent recommendations in general, watershed or forest-specific plans are nonetheless desirable when considering the long-term effects of climate change on fire.

Observed and projected climate data for Big Creek broadly align with the expected changes for California and the Western U.S. The offset of the observed temperature data as compared to the historic reanalysis or projected data (Figure 3) is somewhat notable but is likely a product of both model/downscaling inaccuracy as well as bias or microclimate present at the Grant Grove Meteorological station. The larger trend in temperature, in particular the expected changes from observed to late 21st century projected data directly

aligns with regional projections for climate warming (Garfin et al., 2018). Similarly, while precipitation projections, as compared to observed data, don't align perfectly with the regional prediction of increased variability and large storms, the mean rainfall is largely unchanged which does agree to wider expectations.

Modeling is a key means by which we can compensate for this uncertainty through simulation of a range of potential outcomes. Model simulations are only useful if they can paint a complete picture though, and any accounting of climate and climate change impacts on fire will be tightly linked and influenced by potential fuel treatments. Fuel treatments in the short term are a means of modifying forest structure in order to alter key biophysical variables like high severity fire risk, forest health, or streamflow. Our research supports this, with carbon, GPP, and streamflow effects responding clearly to treatment, particularly to the more intense 'maximized' treatment. Previous work has argued that fuel treatments have the potential to mitigate climate change (Hurteau et al., 2014a; Vernon et al., 2018). These papers highlight the effects on fire and on reductions in drought mortality losses. In this paper we focus only on the latter effect. When viewed through the lens of productivity, fuel treatment effects on carbon sequestration in Big Creek are either too short lived, or not achieved at all and are overwhelmed by the effect of climate change.

Across responses in total carbon, GPP, height gap, and streamflow, changes in climate scenario stand out by comparison to changes in treatment scenario. The treatment itself, as shown in Figure 5 A & B, has a direct but typically minor effect on total carbon in terms of percent change, at most an 11% reduction in carbon in the first two years. The relatively small effect of the fuel treatment is partially because of the limits of the treatment itself on total carbon, total carbon includes carbon stores not directly altered by fuel treatments,

including root carbon, coarse woody debris, and litter. Additionally rapid short-term recovery and the compensating growth of unthinned trees combine to quickly return the basin to pre-treatment levels of carbon. Long-term effects on carbon are most influenced by climate, with projected climate periods anticipating substantial decreases in total carbon regardless of treatment (31% and 40% for RCPs 4.5 and 8.5). Though the possibility of fuel treatments leading to increased carbon sequestration is often considered, we show no evidence for that being an option here. While the goal of carbon sequestration may be partially addressed with a different fuel treatment, and effects will change if the dynamic effects of fire and fire severity were included, it also seems likely that Big Creek as a mixed conifer Sierran watershed has limited capacity to substantially increase sequestered carbon (Stephens et al., 2012).

Changes in GPP (Figure 6) are varied between short and long-term perspectives, with fuel treatments having a substantial effect in the short term and climate scenario ultimately having a greater impact on long-term (20-year) productivity. This differences in GPP points towards less productive forests in the short-term as a repercussion of the maximum treatment option, with a more moderated effect from the minimal treatment. Long-term GPP instead looks to be limited by climate scenario and is not sensitive to differences in treatment scenarios. The projected lower GPP for RCP 8.5, and to a lesser extent RCP 4.5, likely originates in part from the differences in precipitation between observed and projected periods, a reduction of 157 mm average annual rainfall in the case of RCP 8.5. This is particularly relevant due to the tight linking in Mediterranean watersheds like Big Creek between seasonal precipitation and productivity. We also see the limits in terms of a longevity of a single treatment in the context of a 20-year period. We find noteworthy

differences in the longevity of impact on GPP due to climate, with the RCP 8.5 climate leading to more temporally limited effects due to treatment compared to baseline climate. Beyond the role of climate that we highlight, reductions in the effects of treatment over time can also be due to other factors such as soil water storage which can influence regrowth and recover following treatment (Tague and Moritz, 2019).

To assess potential fire risk, we use the height gap (Figure 7) between the conifer overstory and the shrub understory as an indicator of the chances that a low intensity fire could climb ladder fuels and make the jump to being a crown fire with potential for higher fire severity. Height gap provides one of the most compelling cases where the impact of climate is overshadowing the potential impact of fuel treatments. It is also important to note that the fuel treatment that was implemented, a 40% reduction in overstory and 100% reduction in understory, is not focused on creating a large height gap. The reduction of overstory results in small height gaps, further limited by the slower growth of the conifer overstory compared to the shrub understory in the post thinning period. Conifer heights for RCP 4.5 and 8.5 average 10 m and 5m, but the 25^{th} percentile for both is 1 m and medians are 2.7 m and 1.6 m, indicating a large amount of dead and unsuccessful vegetation. In the context of such a large coverage of short overstory vegetation, a different fuel treatment strategy, one targeting more of the overstory, would be much more effective at reducing potential for high severity fire(Stephens et al., 2012). By comparison, the baseline climate scenarios feature much more successful conifer overstories (median height of 6 m) and so maintained a larger height gap despite the treatment reducing it slightly.

Fuel treatments also can impact climate change indirectly by mitigating the effects of climate change. For instance, by encouraging forest stands with both lower risk of high

severity fire, but that also allow for greater streamflow to reach downstream where it can be used to meet the ever-increasing demands for freshwater. In this way it becomes critical that we have a complete picture of how fuel treatments impact the biophysical environment under a range of climate change scenarios. Streamflow (Figure 8), over the long term, mirrors the behaviour of total carbon and GPP where effects are dominated by climate scenario. Despite this, there are noteworthy short-term effects in the maximized treatment scenarios. Most notable are the short-term increases to peak flows from maximum treatment (38-91% increase), though simultaneously the minimal treatment has very little effect compared to the no treatment scenario. In the longer-term (Figure 8 B & C), fuel treatment scenario is of lesser impact, while climate scenario shifts streamflow more noticeably (1% and 22% for minimal and maximum treatments, 22% and 77% for RCP 4.5 and 8.5). Changes due to treatment, specifically in the case of the maximum treatment (22% increase in mean daily streamflow), are partially due to the treatment itself but also dependent on the broader impacts of the projected climate scenarios on plant growth, which when combined with the more prevalent maximum treatment, lead to more noticeable effects on streamflow compared to the minimal treatment. The largest mean changes due to treatment scenario are in February of the RCP 8.5 climate scenario, which has an average increase of 0.4 mm/day in comparing the no treatment to maximized treatment scenarios, but low flow months (September and October) remain unchanged across climate and treatment scenarios. Fuel treatments have substantial effects on streamflow in the short term across climate scenarios, and still notable effects in the case of maximum treatment in the long-term, but these increases to streamflow are occurring at or adjacent to the existing peak streamflow. Increases to streamflow like this are less beneficial as it is the low-flow months where the need for additional water is

greatest, and a tool like fuel treatments has the most potential. The longevity of treatment effects on streamflow varies by climate scenario. Both baseline and RCP 8.5 have no differences in daily streamflow after 5 years while RCP 4.5 features persistent differences in the maximum treatment scenario leading to increased peak flows, that last through the 20-year simulation.

5. Conclusions

Fuel treatments are both multi-faceted and multi-purposed, with the potential to interact with and affect a wide variety of biophysical variables. We highlight a handful of those here through total carbon, GPP, height gap, and streamflow. We show the consistent impact of high intensity treatments in the short-term, but in each case, long-term effects are diminished in the context of, or because of, climate change. While there is the potential for more frequent treatments or changes to the treatment implementation, the underlying issue we find here is that climate change is an often-overwhelming force across a range of variables and contexts. Though there is still room for fuel treatments to play a range of roles, particularly at shorter (<5 year) time scales, the context of that treatment matters, as differences between historic climate, and RCP's 4.5 and 8.5 can be noteworthy. There are ever-present financial limitations on repeat treatments, and that can often lead to infrequent or one-off treatments. Based on the longevity of effects on both GPP and streamflow, the most substantial impacts of fuel treatments are no longer evident after 5 years, and given this, fuel treatment repetition would need to occur within that 5-year window to maintain effects. This work further underscores the need to investigate the full context and effects of potential fuel treatments. We find that accounting for and including the long-term effects of climate change is an

integral part of assessing future treatments and planning forest management through the end of the 21st century.

6. Figures

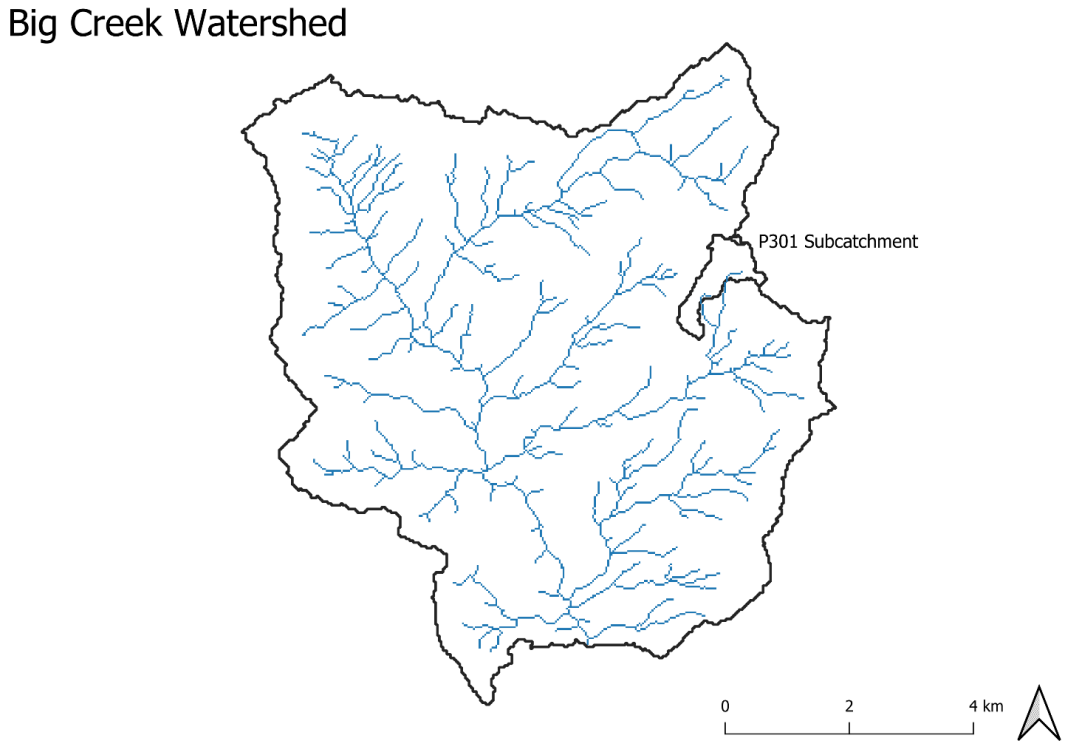

Figure 1. Study site of the Big Creek watershed and the p301 subwatershed.

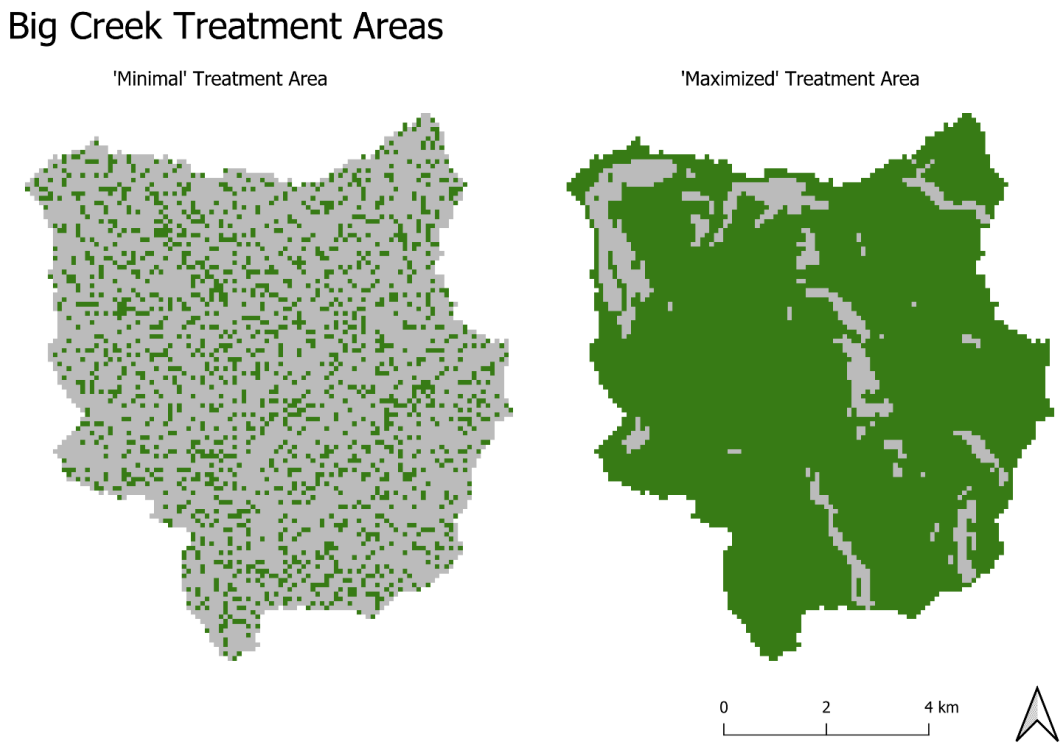

Figure 2. Big Creek watershed showing fuel treatment area coverages in green. Showing both ‘minimal’ and ‘maximized’ treatment scenarios in green. For both coverage options, the treatment implamemnted is a 40% removal of overstory canopy and complete clearing of the shrub understory.

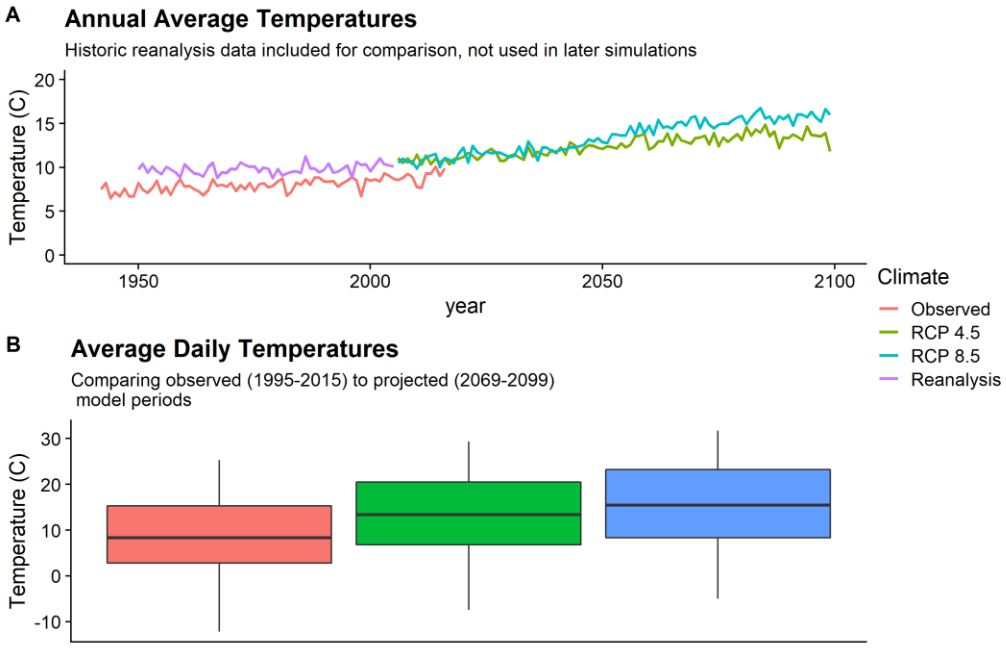

Figure 3. Temperature data for Big Creek watershed. Shows baseline observed data from the Grant Grove meteorological station and modeled data using the HadGEM2 model, downscaled using LOCA. Representative concentration pathways 4.5 and 8.5 from the projected period are used in the ecohydrologic modeling, while historic reanalysis data is used for comparison to observed data.

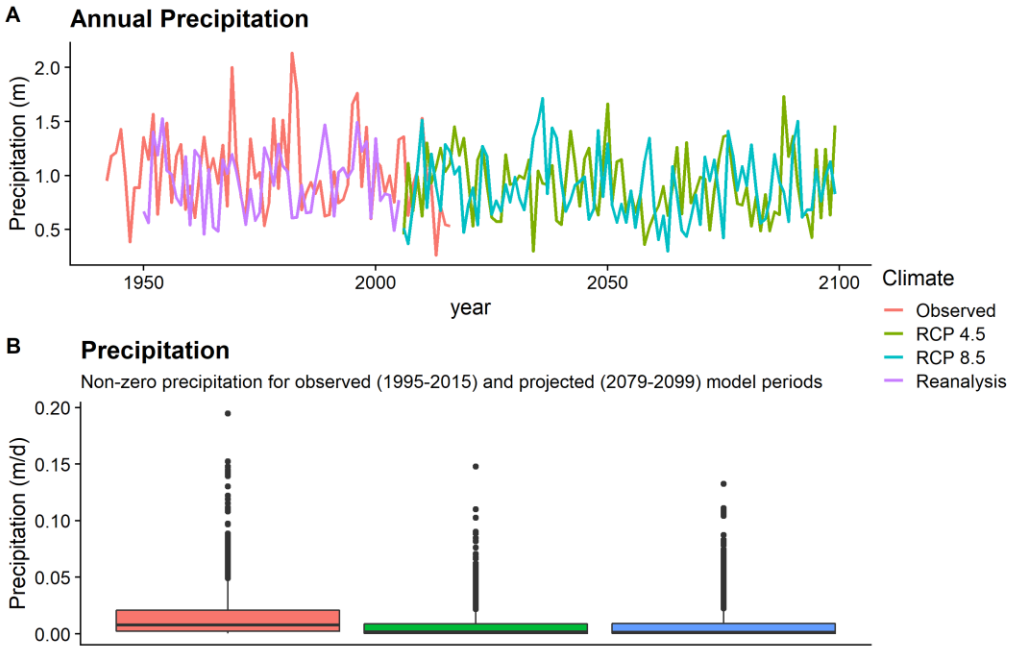

Figure 4. Precipitation data for Big Creek watershed. Shows observed data from the Grant Grove meteorological station and modeled data using the HadGEM2 model, downscaled using LOCA. Representative concentration pathways 4.5 and 8.5 from the projected period are used in the ecohydrologic modeling, while historic reanalysis data is used for comparison to observed data. Subplot A shows annual totals, while subplot B shows daily averages.

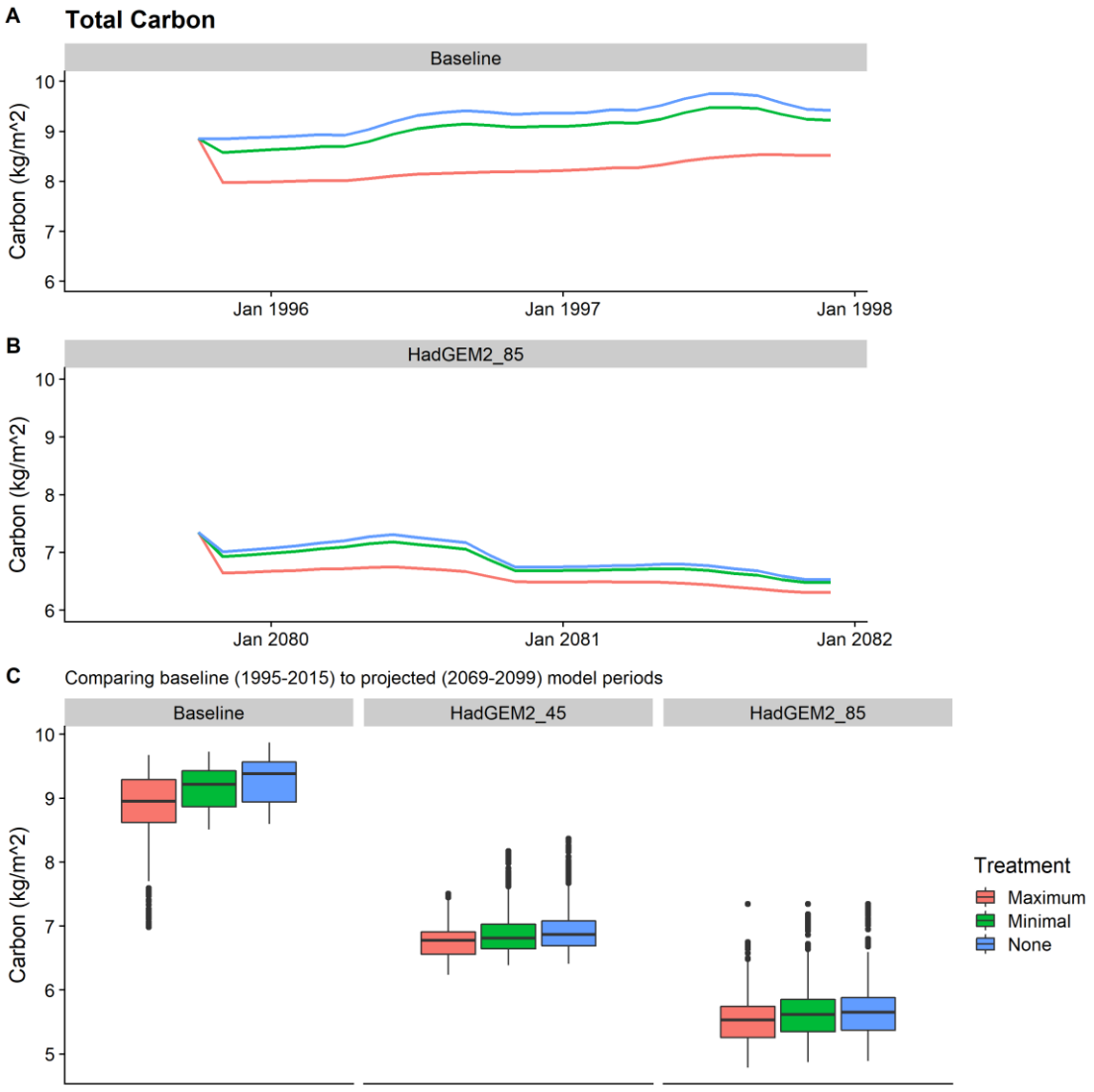

Figure 5. Total carbon following treatment. A, B, and C show total carbon short-term (2 years) following treatment, including the effect of the 40% reduction in conifer overstory and complete removal of shrub understory at the start of simulation. D shows long term (20 year) effects of treatment across climate projections. All plots are faceted by climate, boxplots span 25th to 75th percentile ranges of monthly carbon.

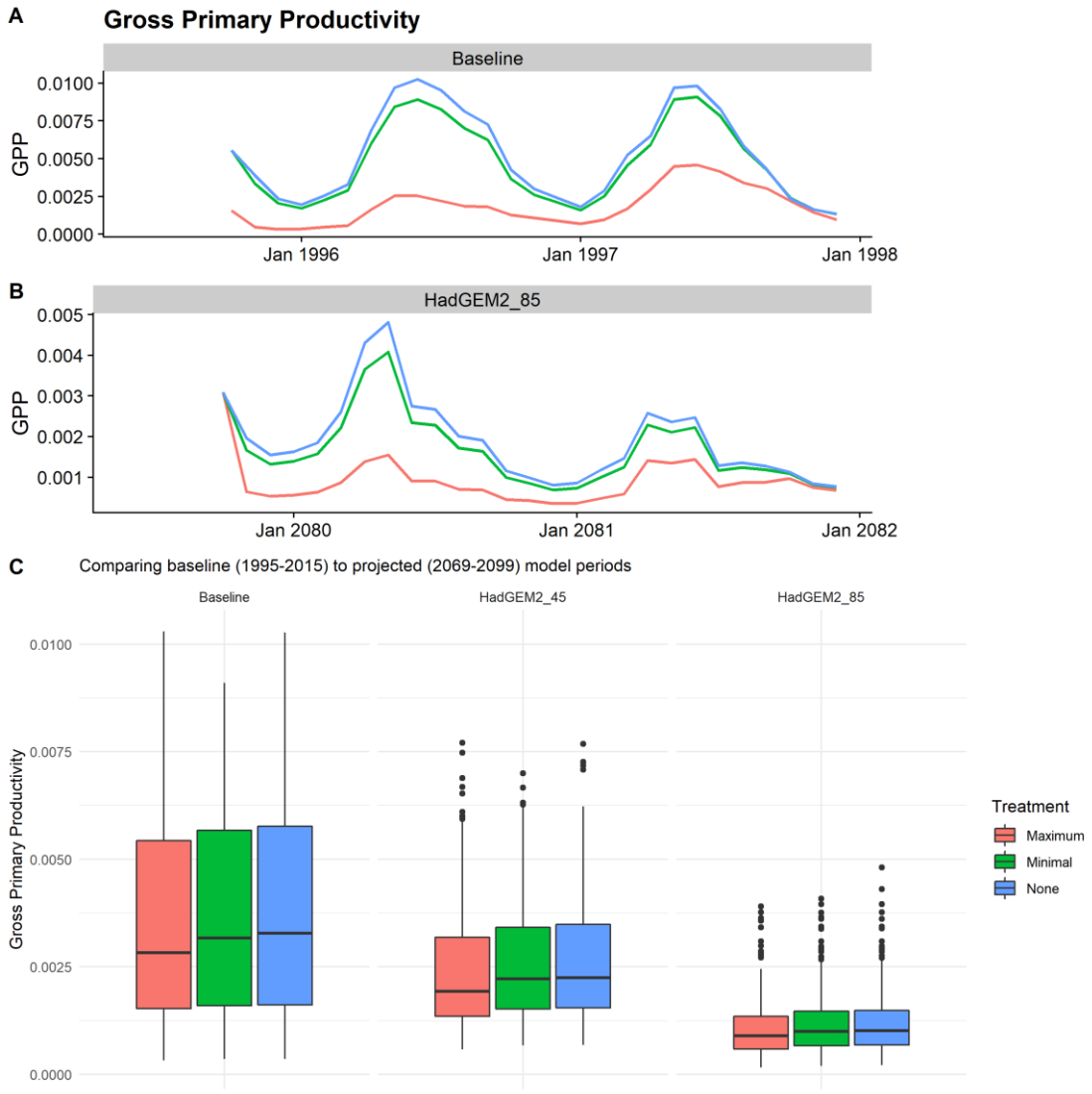

Figure 6. Gross primary productivity. A and B show GPP short-term (2 years) following treatment, including the effect of the 40% reduction in conifer overstory and complete removal of shrub understory. C shows long term (20 year) effects of treatment across climate projections. Showing boxplots spanning 25th to 75th percentile ranges.

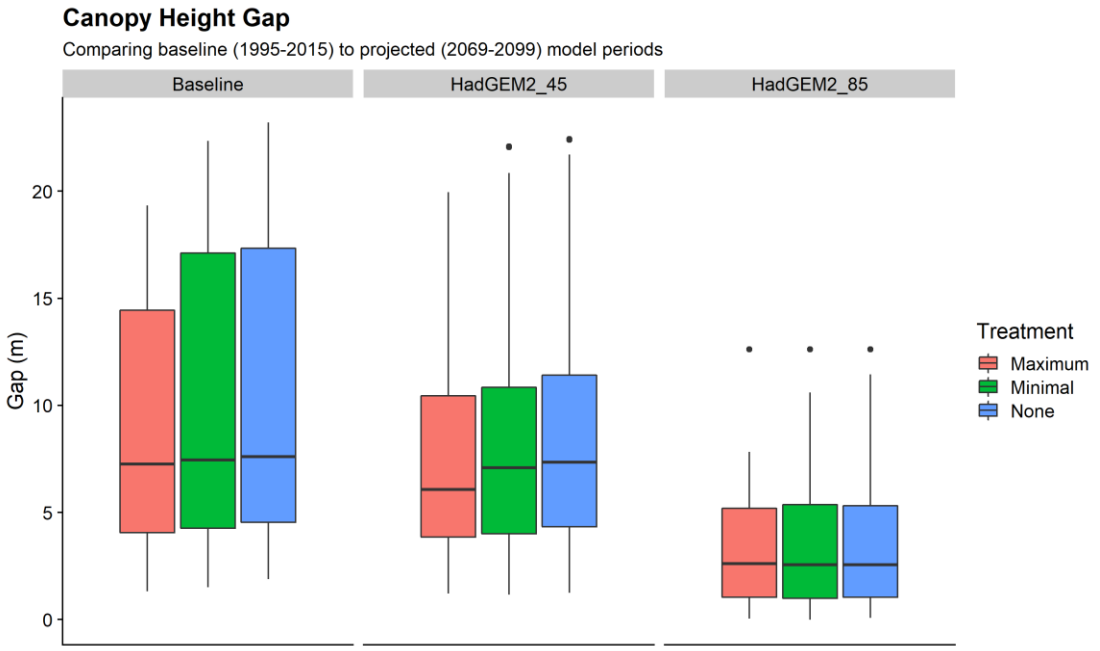

Figure 7. Height gap in meters between shrub understory and conifer overstory across climate and treatment scenarios. Showing boxplots spanning 25th to 75th percentile ranges.

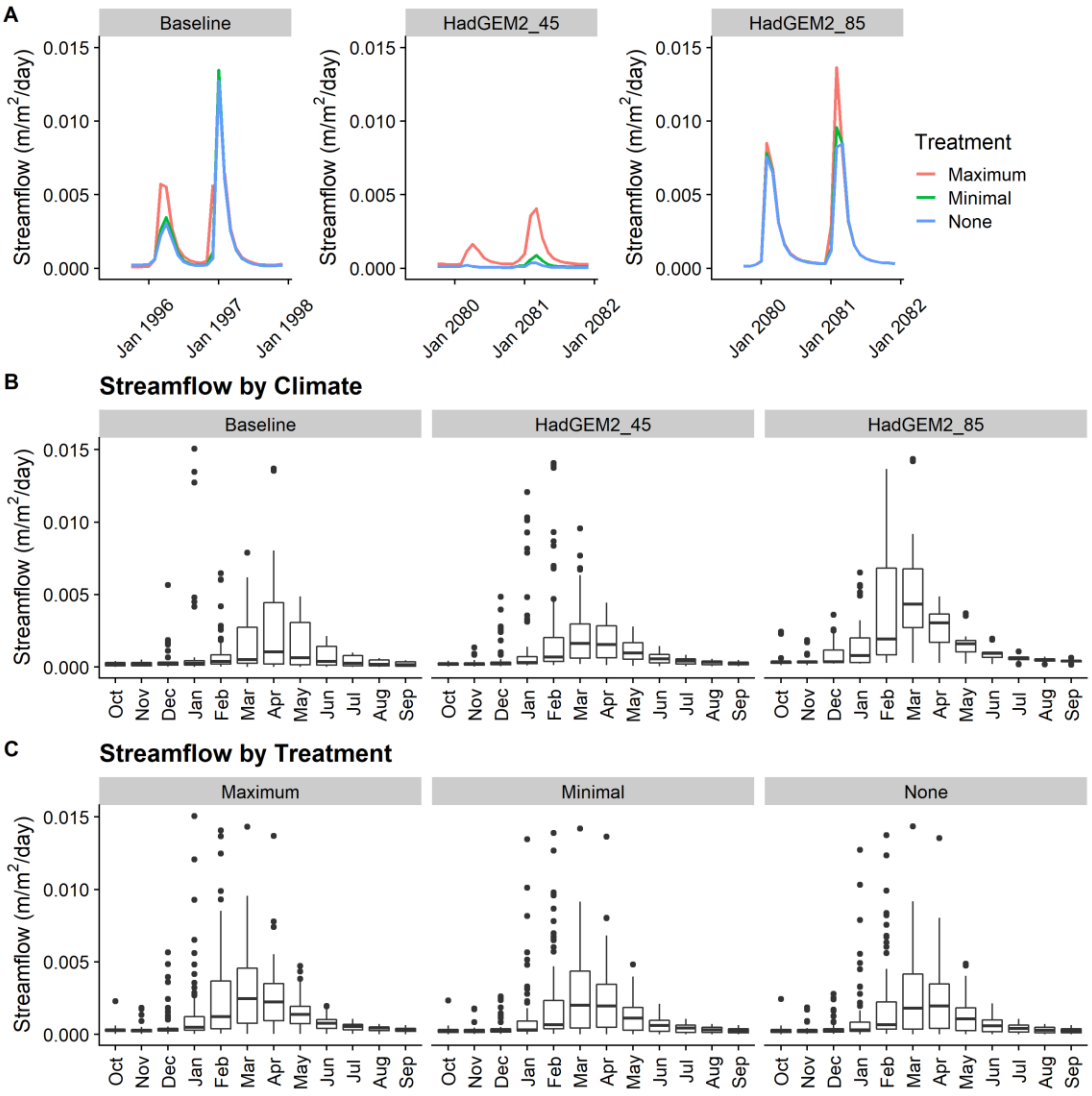

Figure 8. Daily streamflow per unit watershed area ($m/m^2/day$), shown at short (2-year) and long (20-year) time scales. A shows time series of streamflow for 2 years following treatment, across climate projections and treatment scenarios. B and C boxplots, spanning 25^{th} to 75^{th} percentiles, show distributions of daily streamflow across the 20-year simulation period for each month.

Conclusions

The chapters of this dissertation take important steps towards understanding the effects of fuel treatments. The development of RHESSys-MSR, and the functionality it enables are prime among these contributions. The RHESSys-MSR method developed in Chapter 1 is valuable in that it not only enables the research pursued in Chapters 2 & 3, but also a variety of applications beyond. RHESSys-MSR fills a niche in the domain of process-based ecohydrologic modeling; it enables characterization and simulation of fuel treatments at scales that were previously not possible or practical for RHESSys or comparable existing models. The key to this is the simulation of both within-forest stand ecohydrologic effects due to changes in forest structure and the watershed-scale simulation of ecohydrologic processes including hillslope hydrology and spatial variations in atmospheric forcing conditions (radiation, temperature, precipitation) among other factors. Results of Chapter 2 highlight the different roles that environmental and climatic variables can play in influencing fuel treatment effects. Notable among these influential environmental variables are vegetation type and plant accessible water storage capacity. Results further emphasize the year-to-year variability in fuel treatment effects coming from variation in climate and treatment type. In this context it becomes necessary to consider the outcomes of treatments as probabilities rather than more direct and certain responses to treatments. Chapter 3 focuses on the relative effects of projected climate change and fuel treatments. While projected climate impacts tend to be dominant in the long-term, fuel treatments have clear short-term effects on carbon, gross primary productivity, and streamflow. These results reflect the potential extreme magnitude of climate change at the end of the 21st century, as well as the

specific interaction of environmental conditions and climate in the Southern Sierran Big Creek watershed.

There is ample opportunity and directions for continuation of this dissertation research. Application of the fully coupled RHESSys-MSR and WMFire fire model are a priority which will facilitate further research into the dynamics among fuel treatments, fire severity, vegetation growth, and climate. The applied components of this thesis in Chapters 2 & 3 also present opportunities for replication, particularly in regions with differences in fire regime, vegetation, and climate type. Model applications of this type, using the RHESSys-MSR method, are key to building site-site specific understanding of fuel treatment effects. The variation in fuel treatments and the environments in which they are done is inherently linked to the distribution of likely fuel treatment effects – and this new method can provide estimates of this distribution. As we continue to gain understanding, through methods like RHESSys-MSR and many others, we can reduce uncertainty and make better informed decisions for future forest management.

References

Agee, J.K., Skinner, C.N., 2005. Basic principles of forest fuel reduction treatments. Forest Ecology and Management 211, 83–96. https://doi.org/10/fgpnjx

Ager, A.A., Vaillant, N.M., Finney, M.A., 2010. A comparison of landscape fuel treatment strategies to mitigate wildland fire risk in the urban interface and preserve old forest structure. Forest Ecology and Management 259, 1556–1570. https://doi.org/10.1016/j.foreco.2010.01.032

Allen, C.D., Macalady, A.K., Chenchouni, H., Bachelet, D., McDowell, N., Vennetier, M., Kitzberger, T., Rigling, A., Breshears, D.D., Hogg, E.T., 2010. A global overview of drought and heat-induced tree mortality reveals emerging climate change risks for forests. Forest ecology and management 259, 660–684. https://doi.org/10/c3s4s4

Anderson, S., Plantinga, A.J., Wibbenmeyer, M., 2020. Inequality in Agency Responsiveness: Evidence from Salient Wildfire Events.

Anderson, S.E., Bart, R.R., Kennedy, M.C., MacDonald, A.J., Moritz, M.A., Plantinga, A.J., Tague, C.L., Wibbenmeyer, M., 2018. The dangers of disaster-driven responses to climate change. Nature Climate Change 8, 651–653. https://doi.org/10/gdm4cf

Asner, G.P., Brodrick, P.G., Anderson, C.B., Vaughn, N., Knapp, D.E., Martin, R.E., 2016. Progressive forest canopy water loss during the 2012–2015 California drought. Proceedings of the National Academy of Sciences 113, E249–E255. https://doi.org/10/gft998

Bales, R.C., Hopmans, J.W., O'Geen, A.T., Meadows, M., Hartsough, P.C., Kirchner, P., Hunsaker, C.T., Beaudette, D., 2011. Soil moisture response to snowmelt and rainfall in a Sierra Nevada mixed-conifer forest. Vadose Zone Journal 10, 786–799. https://doi.org/10.2136/vzj2011.0001

Barnett, K., Parks, S.A., Miller, C., Naughton, H.T., 2016. Beyond fuel treatment effectiveness: characterizing interactions between fire and treatments in the US. Forests 7, 237.

Barros, A.M., Ager, A.A., Day, M.A., Palaiologou, P., 2019. Improving long-term fuel treatment effectiveness in the National Forest System through quantitative prioritization. Forest ecology and management 433, 514–527. https://doi.org/10/ggjnz7

Bart, R.R., Kennedy, M.C., Tague, C.L., McKenzie, D., 2020a. Integrating fire effects on vegetation carbon cycling within an ecohydrologic model. Ecological Modelling 416, 108880. https://doi.org/10/ggnht4

Bart, R.R., Kennedy, M.C., Tague, C.L., McKenzie, D., 2020b. Integrating fire effects on vegetation carbon cycling within an ecohydrologic model. Ecological Modelling 416, 108880. https://doi.org/10/ggnht4

Bart, R.R., Ray, R.L., Conklin, M.H., Safeeq, M., Saksa, P.C., Tague, C.L., Bales, R.C., 2021. Assessing the effects of forest biomass reductions on forest health and streamflow. Hydrological Processes 35, e14114. https://doi.org/10.1002/hyp.14114

Bart, R.R., Tague, C.L., Moritz, M.A., 2016. Effect of Tree-to-Shrub Type Conversion in Lower Montane Forests of the Sierra Nevada (USA) on Streamflow. PLOS ONE 11, e0161805. https://doi.org/10/f9rn4w

Blöschl, G., Sivapalan, M., 1995. Scale issues in hydrological modelling: A review. Hydrological Processes 9, 251–290. https://doi.org/10/dx685m

Boisramé, G.F., Thompson, S.E., Tague, C., Stephens, S.L., 2019. Restoring a Natural Fire Regime Alters the Water Balance of a Sierra Nevada Catchment. Water Resources Research 55, 5751–5769. https://doi.org/10/ggnhs9

Brown, A.E., Zhang, L., McMahon, T.A., Western, A.W., Vertessy, R.A., 2005. A review of paired catchment studies for determining changes in water yield resulting from alterations in vegetation. Journal of Hydrology 310, 28–61. https://doi.org/10/cbrm5q

Burke, W., Tague, C.N., Kennedy, M., Moritz, M., 2020. Understanding fuel treatments: how treatments interact with climate and biophysical setting to affect fire, water, and forest health. Frontiers in Forests and Global Change 3, 143. https://doi.org/10.3389/ffgc.2020.591162

Burke, W., Tague, N., 2019. Multiscale Routing-Integrating the Tree-scale Effects of Disturbance into a Watershed Ecohydrologic Model. AGUFM 2019, H53O-2022.

Cabon, A., Mouillot, F., Lempereur, M., Ourcival, J.-M., Simioni, G., Limousin, J.-M., 2018. Thinning increases tree growth by delaying drought-induced growth cessation in a Mediterranean evergreen oak coppice. Forest Ecology and Management 409, 333–342. https://doi.org/10/gc45k2

California Forest Observatory, 2019.

Calkin, D., Gebert, K., 2006. Modeling fuel treatment costs on Forest Service lands in the western United States. Western Journal of Applied Forestry 21, 217–221. https://doi.org/10/gg2bfh

Clark, J.S., Iverson, L., Woodall, C.W., Allen, C.D., Bell, D.M., Bragg, D.C., D'Amato, A.W., Davis, F.W., Hersh, M.H., Ibanez, I., Jackson, S.T., Matthews, S., Pederson, N., Peters, M., Schwartz, M.W., Waring, K.M., Zimmermann, N.E., 2016. The impacts of increasing drought on forest dynamics, structure, and biodiversity in the United States. Glob Change Biol 22, 2329–2352. https://doi.org/10/f8s8tz

Clark, M.P., Fan, Y., Lawrence, D.M., Adam, J.C., Bolster, D., Gochis, D.J., Hooper, R.P., Kumar, M., Leung, L.R., Mackay, D.S., Maxwell, R.M., Shen, C., Swenson, S.C., Zeng, X., 2015. Improving the representation of hydrologic processes in Earth System Models: REPRESENTING HYDROLOGIC PROCESSES IN EARTH SYSTEM MODELS. Water Resources Research 51, 5929–5956. https://doi.org/10/f7wc44

Dickinson, R.E., Shaikh, M., Bryant, R., Graumlich, L., 1998. Interactive canopies for a climate model. Journal of Climate 11, 2823–2836. https://doi.org/10/dsjktb

Ellison, D., Futter, M.N., Bishop, K., 2012. On the forest cover–water yield debate: from demand- to supply-side thinking. Global Change Biology 18, 806–820. https://doi.org/10/b5t4vg

Evans, A.M., Everett, R.G., Stephens, S.L., Youlz, J.A., 2011. Comprehensive Fuels Treatment Practices Guide for Mixed Conifer Forests: California, Central and Southern Rockies, and the Southwest. JFSP Synthesis Report 12, 113.

Evaristo, J., McDonnell, J.J., 2019. RETRACTED ARTICLE: Global analysis of streamflow response to forest management. Nature 570, 455–461. https://doi.org/10/gf478c

Fan, Y., Clark, M., Lawrence, D.M., Swenson, S., Band, L.E., Brantley, S.L., Brooks, P.D., Dietrich, W.E., Flores, A., Grant, G., Kirchner, J.W., Mackay, D.S., McDonnell, J.J., Milly, P.C.D., Sullivan, P.L., Tague, C., Ajami, H., Chaney, N., Hartmann, A., Hazenberg, P., McNamara, J., Pelletier, J., Perket, J., Rouholahnejad-Freund, E., Wagener, T., Zeng, X., Beighley, E., Buzan, J., Huang, M., Livneh, B., Mohanty, B.P., Nijssen, B., Safeeq, M., Shen, C., van Verseveld, W., Volk, J., Yamazaki, D., 2019. Hillslope Hydrology in Global Change Research and Earth System Modeling. Water Resources Research. https://doi.org/10/gfv8bz

Fan, Y., Miguez-Macho, G., Jobbágy, E.G., Jackson, R.B., Otero-Casal, C., 2017. Hydrologic regulation of plant rooting depth. Proceedings of the National Academy of Sciences 114, 10572–10577. https://doi.org/10/gb26pv

Farquhar, G.D., von Caemmerer, S. von, Berry, J.A., 1980. A biochemical model of photosynthetic CO 2 assimilation in leaves of C 3 species. Planta 149, 78–90. https://doi.org/10/fs9dpz

Fatichi, S., Vivoni, E.R., Ogden, F.L., Ivanov, V.Y., Mirus, B., Gochis, D., Downer, C.W., Camporese, M., Davison, J.H., Ebel, B., 2016. An overview of current applications, challenges, and future trends in distributed process-based models in hydrology. Journal of Hydrology 537, 45–60. https://doi.org/10/f8m6vj

Fernandes, P.M., 2015. Empirical support for the use of prescribed burning as a fuel treatment. Current Forestry Reports 1, 118–127. https://doi.org/10/ggq38k

Filoso, S., Bezerra, M.O., Weiss, K.C.B., Palmer, M.A., 2017. Impacts of forest restoration on water yield: A systematic review. PLoS ONE 12, e0183210. https://doi.org/10/gbshvj

Finney, M.A., 2001. Design of regular landscape fuel treatment patterns for modifying fire growth and behavior. Forest Science 47, 219–228.

Finney, M.A., Seli, R.C., McHugh, C.W., Ager, A.A., Bahro, B., Agee, J.K., 2007. Simulation of long-term landscape-level fuel treatment effects on large wildfires. International Journal of Wildland Fire 16, 712. https://doi.org/10/bg96jc

Garcia, E.S., Tague, C.L., Choate, J.S., 2016. Uncertainty in carbon allocation strategy and ecophysiological parameterization influences on carbon and streamflow estimates for two western US forested watersheds. Ecological Modelling 342, 19–33. https://doi.org/10/f9ctkn

Garcia, E.S., Tague, C.L., Choate, J.S., 2013. Influence of spatial temperature estimation method in ecohydrologic modeling in the Western Oregon Cascades: TEMPERATURE INTERPOLATION INFLUENCES ECOHYDROLOGIC MODELING. Water Resources Research 49, 1611–1624. https://doi.org/10/gfdb8z

Garfin, G., Gonzalez, P., Breshears, D., Brooks, K., Brown, H., Elias, E., Gunasekara, A., Huntly, N., Maldonado, J., Mantua, N., 2018. The Fourth National Climate Assessment, Chapter 25: Southwest.

Giorgi, F., Avissar, R., 1997. Representation of heterogeneity effects in earth system modeling: Experience from land surface modeling. Reviews of Geophysics 35, 413–437. https://doi.org/10/fwgj7k

Gould, D., 2019a. Revised Draft Land Management Plan for the Sequoia National Forest (No. R5- MB-320). USDA.

Gould, D., 2019b. Revised Draft Land Management Plan for the Sierra National Forest (No. R5- MB-319). USDA.

Grant, G.E., Tague, C.L., Allen, C.D., 2013. Watering the forest for the trees: an emerging priority for managing water in forest landscapes. Frontiers in Ecology and the Environment 11, 314–321. https://doi.org/10/f47v5x

Hanan, E.J., Ren, J., Tague, C.L., Kolden, C.A., Abatzoglou, J.T., Bart, R.R., KENNEDY, M.C., Liu, M., Adam, J., 2020. How climate change and fire exclusion drive wildfire regimes at actionable scales. Environ. Res. Lett. https://doi.org/10/ghr52k

Hanan, E.J., Tague, C., Choate, J., Liu, M., Kolden, C., Adam, J., 2018. Accounting for disturbance history in models: using remote sensing to constrain carbon and nitrogen pool spin-up. Ecological Applications 28, 1197–1214. https://doi.org/10/gdgd68

Hayhoe, K., Wuebbles, D.J., Easterling, D.R., Fahey, D.W., Doherty, S., Kossin, J., Sweet, W., Vose, R., Wehner, M., 2018. 2018: Our Changing Climate. In Impacts, Risks, and Adaptation in the United States: Fourth National Climate Assessment, Volume II. U.S. Global Change Research Program, Washington, DC, 72–144. https://doi.org/10/gf2x7k

Hessburg, P.F., Spies, T.A., Perry, D.A., Skinner, C.N., Taylor, A.H., Brown, P.M., Stephens, S.L., Larson, A.J., Churchill, D.J., Povak, N.A., 2016. Tamm review: management of mixed-severity fire regime forests in Oregon, Washington, and Northern California. Forest Ecology and Management 366, 221–250. https://doi.org/10/f8k6xk

Hewlett, J.D., Hibbert, A.R., 1967. Factors affecting the response of small watersheds to precipitation in humid areas. Forest hydrology 1, 275–290.

Hunsaker, C.T., Whitaker, T.W., Bales, R.C., 2012. Snowmelt Runoff and Water Yield Along Elevation and Temperature Gradients in California's Southern Sierra Nevada 1. JAWRA Journal of the American Water Resources Association 48, 667–678. https://doi.org/10/ggq6nc

Hurteau, M.D., Bradford, J.B., Fulé, P.Z., Taylor, A.H., Martin, K.L., 2014a. Climate change, fire management, and ecological services in the southwestern US. Forest Ecology and Management 327, 280–289. https://doi.org/10.1016/j.foreco.2013.08.007

Hurteau, M.D., Robards, T.A., Stevens, D., Saah, D., North, M., Koch, G.W., 2014b. Modeling climate and fuel reduction impacts on mixed-conifer forest carbon stocks in

the Sierra Nevada, California. Forest Ecology and Management 315, 30–42. https://doi.org/10/f5tksf

Kennedy, M.C., McKenzie, D., Tague, C., Dugger, A.L., 2017. Balancing uncertainty and complexity to incorporate fire spread in an eco-hydrological model. International Journal of Wildland Fire 26, 706. https://doi.org/10/gbswwc

Kirchner, J.W., Berghuijs, W.R., Allen, S.T., Hrachowitz, M., Hut, R., Rizzo, D.M., 2020. Streamflow response to forest management. Nature 578, E12–E15. https://doi.org/10/ggxx5x

Klein, T., Siegwolf, R.T., Körner, C., 2016. Belowground carbon trade among tall trees in a temperate forest. Science 352, 342–344. https://doi.org/10/gnz72t

Klos, P.Z., Goulden, M.L., Riebe, C.S., Tague, C.L., O'Geen, A.T., Flinchum, B.A., Safeeq, M., Conklin, M.H., Hart, S.C., Berhe, A.A., Hartsough, P.C., Holbrook, W.S., Bales, R.C., 2018. Subsurface plant-accessible water in mountain ecosystems with a Mediterranean climate. Wiley Interdisciplinary Reviews: Water 5, e1277. https://doi.org/10/gfdb86

Krogh, S.A., Broxton, P.D., Manley, P.N., Harpold, A.A., 2020. Using Process Based Snow Modeling and Lidar to Predict the Effects of Forest Thinning on the Northern Sierra Nevada Snowpack. Frontiers in Forests and Global Change 3. https://doi.org/10.3389/ffgc.2020.00021

Liang, S., Hurteau, M.D., Westerling, A.L., 2018. Large-scale restoration increases carbon stability under projected climate and wildfire regimes. Frontiers in Ecology and the Environment 16, 207–212. https://doi.org/10/gdb8xg

Liaw, A., Wiener, M., 2002. Classification and regression by randomForest. R news 2, 18–22.

McDowell, N.G., Adams, H.D., Bailey, J.D., Kolb, T.E., 2007. The role of stand density on growth efficiency, leaf area index, and resin flow in southwestern ponderosa pine forests. Canadian Journal of Forest Research 37, 343–355. https://doi.org/10/cxf8hg

Monteith, J.L., 1965. Evaporation and environment. Symposia of the Society for Experimental Biology 19, 205–234.

Moritz, M.A., Batllori, E., Bradstock, R.A., Gill, A.M., Handmer, J., Hessburg, P.F., Leonard, J., McCaffrey, S., Odion, D.C., Schoennagel, T., Syphard, A.D., 2014. Learning to coexist with wildfire. Nature 515, 58–66. https://doi.org/10/f6n4hc

Moritz, M.A., Parisien, M.-A., Batllori, E., Krawchuk, M.A., Dorn, J.V., Ganz, D.J., Hayhoe, K., 2012. Climate change and disruptions to global fire activity. Ecosphere 3, art49. https://doi.org/10/gdm786

North, M., Brough, A., Long, J., Collins, B., Bowden, P., Yasuda, D., Miller, J., Sugihara, N., 2015. Constraints on mechanized treatment significantly limit mechanical fuels reduction extent in the Sierra Nevada. Journal of Forestry 113, 40–48. https://doi.org/10/gg2bfg

North, M., Hurteau, M., Innes, J., 2009. Fire suppression and fuels treatment effects on mixed-conifer carbon stocks and emissions. Ecological applications 19, 1385–1396. https://doi.org/10/dfrnt9

O'Geen, A.T., Safeeq, M., Wagenbrenner, J., Stacy, E., Hartsough, P., Devine, S., Tian, Z., Ferrell, R., Goulden, M., Hopmans, J.W., 2018. Southern Sierra Critical Zone Observatory and Kings River Experimental Watersheds: A synthesis of measurements, new insights, and future directions. Vadose Zone Journal 17. https://doi.org/10/gf27k3

Omi, P.N., Martinson, E.J., 2002. Effects of Fuels Treatment on Wildfire Severity. Joint Fire Science Program Governing Board, Western Forest Fire Research Center, Fort Collins: Colorado State University.

Paluszynska, A., Biecek, P., Jiang, Y., 2019. randomForestExplainer: Explaining and Visualizing Random Forests in Terms of Variable Importance.

Parks, S.A., Abatzoglou, J.T., 2020. Warmer and drier fire seasons contribute to increases in area burned at high severity in western US forests from 1985 to 2017. Geophysical Research Letters 47, e2020GL089858. https://doi.org/10.1029/2020GL089858

Pierce, D.W., Cayan, D.R., Thrasher, B.L., 2014. Statistical downscaling using localized constructed analogs (LOCA). Journal of Hydrometeorology 15, 2558–2585. https://doi.org/10.1175/JHM-D-14-0082.1

Pierce, D.W., Kalansky, J.F., Cayan, D.R., 2018. Climate, drought, and sea level rise scenarios for California's fourth climate change assessment. California Energy Commission and California Natural Resources Agency.

Prichard, S.J., Povak, N.A., Kennedy, M.C., Peterson, D.W., 2020. Fuel treatment effectiveness in the context of landform, vegetation, and large, wind-driven wildfires. Ecological Applications 30, e02104. https://doi.org/10.1002/eap.2104

Roche, J.W., Goulden, M.L., Bales, R.C., 2018. Estimating evapotranspiration change due to forest treatment and fire at the basin scale in the Sierra Nevada, California. Ecohydrology 11, e1978. https://doi.org/10.1002/eco.1978

Running, S.W., Nemani, R.R., Hungerford, R.D., 1987. Extrapolation of synoptic meteorological data in mountainous terrain and its use for simulating forest evapotranspiration and photosynthesis. Canadian Journal of Forest Research 17, 472–483. https://doi.org/10/c6rfrs

Ryan, M.G., 1991. Effects of climate change on plant respiration. Ecological Applications 1, 157–167. https://doi.org/10/d4pcn4

Safeeq, M., Hunsaker, C.T., 2016. Characterizing Runoff and Water Yield for Headwater Catchments in the Southern Sierra Nevada. J Am Water Resour Assoc 52, 1327–1346. https://doi.org/10/f9gb6w

Safford, H.D., Stevens, J.T., Merriam, K., Meyer, M.D., Latimer, A.M., 2012. Fuel treatment effectiveness in California yellow pine and mixed conifer forests. Forest Ecology and Management 274, 17–28. https://doi.org/10/f32d6h

Saksa, P.C., Conklin, M.H., Battles, J.J., Tague, C.L., Bales, R.C., 2017. Forest thinning impacts on the water balance of S ierra N evada mixed-conifer headwater basins. Water Resources Research 53, 5364–5381. https://doi.org/10/gbvj8g

Schenk, H.J., Jackson, R.B., 2002. Rooting depths, lateral root spreads and below-ground/above-ground allometries of plants in water-limited ecosystems. Journal of Ecology 90, 480–494. https://doi.org/10/csvk9r

Sohn, J.A., Saha, S., Bauhus, J., 2016. Potential of forest thinning to mitigate drought stress: A meta-analysis. Forest Ecology and Management 380, 261–273. https://doi.org/10/f8765j

Son, K., Tague, C., Hunsaker, C., 2016a. Effects of model spatial resolution on ecohydrologic predictions and their sensitivity to inter-annual climate variability. Water 8, 321. https://doi.org/10/f8xwh4

Son, K., Tague, C., Hunsaker, C., 2016b. Effects of Model Spatial Resolution on Ecohydrologic Predictions and Their Sensitivity to Inter-Annual Climate Variability. Water 8, 321. https://doi.org/10/f8xwh4

Spittlehouse, D.L., Stewart, R.B., 2003. Adaptation to climate change in forest management. Adaptation to climate change 4, 12.

Stephens, S.L., Agee, J.K., Fulé, P.Z., North, M.P., Romme, W.H., Swetnam, T.W., Turner, M.G., 2013. Managing Forests and Fire in Changing Climates. Science 342, 41–42. https://doi.org/10/gcpnqj

Stephens, S.L., McIver, J.D., Boerner, R.E., Fettig, C.J., Fontaine, J.B., Hartsough, B.R., Kennedy, P.L., Schwilk, D.W., 2012. The effects of forest fuel-reduction treatments in the United States. BioScience 62, 549–560. https://doi.org/10/gdm8f2

Swain, D.L., Langenbrunner, B., Neelin, J.D., Hall, A., 2018. Increasing precipitation volatility in twenty-first-century California. Nature Climate Change 8, 427–433. https://doi.org/10.1038/s41558-018-0140-y

Tague, C., 2009. Modeling hydrologic controls on denitrification: sensitivity to parameter uncertainty and landscape representation. Biogeochemistry 93, 79–90. https://doi.org/10/bkzcnx

Tague, C., Seaby, L., Hope, A., 2009. Modeling the eco-hydrologic response of a Mediterranean type ecosystem to the combined impacts of projected climate change and altered fire frequencies. Climatic Change 93, 137–155. https://doi.org/10.1007/s10584-008-9497-7

Tague, C.L., Band, L.E., 2004. RHESSys: Regional Hydro-Ecologic Simulation System—An Object-Oriented Approach to Spatially Distributed Modeling of Carbon, Water, and Nutrient Cycling. Earth Interactions 8, 1–42. https://doi.org/10/d6j278

Tague, C.L., Moritz, M., Hanan, E., 2019. The changing water cycle: The eco-hydrologic impacts of forest density reduction in Mediterranean (seasonally dry) regions. Wiley Interdisciplinary Reviews: Water 0, e1350. https://doi.org/10/gf2w7c

Tague, C.L., Moritz, M.A., 2019. Plant Accessible Water Storage Capacity and Tree-Scale Root Interactions Determine How Forest Density Reductions Alter Forest Water Use and Productivity. Front. For. Glob. Change 2. https://doi.org/10/gf4nbt

Thompson, M.P., Bowden, P., Brough, A., Scott, J.H., Gilbertson-Day, J., Taylor, A., Anderson, J., Haas, J.R., 2016. Application of wildfire risk assessment results to wildfire response planning in the southern Sierra Nevada, California, USA. Forests 7, 64.

Tsamir, M., Gottlieb, S., Preisler, Y., Rotenberg, E., Tatarinov, F., Yakir, D., Tague, C., Klein, T., 2019. Stand density effects on carbon and water fluxes in a semi-arid forest, from leaf to stand-scale. Forest Ecology and Management 453, 117573. https://doi.org/10/ggqnm2

U. S. GAO, 2019. Wildland Fire: Federal Agencies' Efforts to Reduce Wildland Fuels and Lower Risk to Communities and Ecosystems.

Vernon, M.J., Sherriff, R.L., van Mantgem, P., Kane, J.M., 2018. Thinning, tree-growth, and resistance to multi-year drought in a mixed-conifer forest of northern California. Forest Ecology and Management 422, 190–198. https://doi.org/10.1016/j.foreco.2018.03.043

Vose, J.M., Peterson, D.L., Domke, G.M., Fettig, C.J., Joyce, L., Keane, R.E., Luce, C.H., Prestemon, J.P., 2018. Chapter 6 : Forests. Impacts, Risks, and Adaptation in the United States: The Fourth National Climate Assessment, Volume II. U.S. Global Change Research Program. https://doi.org/10.7930/NCA4.2018.CH6

Vose, R.S., Easterling, D.R., Kunkel, K.E., LeGrande, A.N., Wehner, M.F., 2017. Temperature changes in the United States. Climate science special report: fourth national climate assessment 1.

Westerling, A.L., Hidalgo, H.G., Cayan, D.R., Swetnam, T.W., 2006. Warming and earlier spring increase western US forest wildfire activity. science 313, 940–943. https://doi.org/10/frgg6p

Wibbenmeyer, M., Anderson, S., Plantinga, A.J., 2016. Risk Salience, Public Pressure, and Agency Action: Wildfire and the Management of Public Lands. mimeo (http://www. bren. ucsb. edu/events/seri_fireaward. htm).

Wigmosta, M.S., Vail, L.W., Lettenmaier, D.P., 1994. A distributed hydrology-vegetation model for complex terrain. Water resources research 30, 1665–1679. https://doi.org/10.1029/94WR00436